

ACTIVE VIBRATION CONTROL OF STRUCTURE USING PIEZOELECTRIC PATCHES

A DISSERTATION

*Submitted in partial fulfilment of the
requirements for the award of the degree*

of

MASTER OF TECHNOLOGY

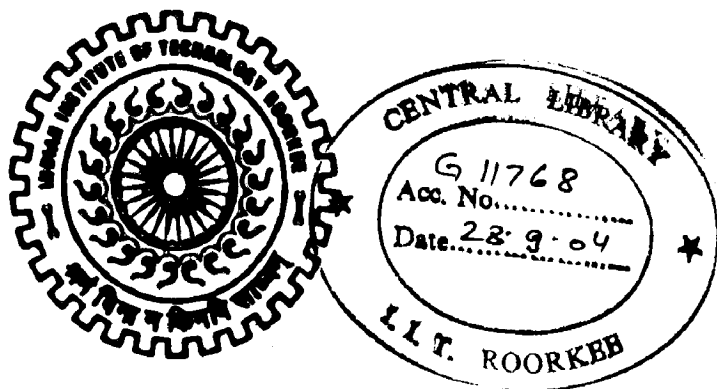
in

MECHANICAL ENGINEERING

(With Specialization in Machine Design Engineering)

By

MAHESH PRABHAKAR YEOLA



**DEPARTMENT OF MECHANICAL AND INDUSTRIAL ENGINEERING
INDIAN INSTITUTE OF TECHNOLOGY ROORKEE
ROORKEE-247 667 (INDIA)**

MAY, 2004

CANDIDATE'S DECLARATION

I hereby declare that the work is being presented in the Dissertation entitled **"ACTIVE VIBRATION CONTROL OF STRUCTURE USING PIEZOELECTRIC PATCHES"** towards partial fulfillment of the requirements for the award of the degree of **Master of Technology in Mechanical Engineering** with specialization in **Machine Design Engineering**, submitted to the Department of Mechanical and Industrial Engineering, Indian Institute of technology, Roorkee, is an authentic record of my own work carried out from July 2003 to April 2004, under the guidance of **Dr. Ashish K. Darpe**, Assistant Professor, Department of Mechanical and Industrial Engineering.

I have not submitted the matter embodied in this dissertation for the award of any other degree or diploma.

Date: 29.04.2004

Place: Roorkee


(MAHESH P. YEOLA)

CERTIFICATE

This is to certify that the above statement made by the candidate is correct to the best of my knowledge.

Date: 29.04.2004

Place: Roorkee


(Dr. ASHISH K. DARPE)

Assistant Professor
Mech. & Ind. Engg. Department
IIT Roorkee
Roorkee – 247 667
INDIA

ACKNOWLEDGEMENT

"If brain is the nucleus of thoughts, teacher is the source of energy to run the operation of solving puzzles of doubts that often poise the mind of student."


I like to express my most sincere appreciation, deep sense of gratitude and sincere thanks to **Dr. Ashish K. Darpe**, Assistant Professor, Mechanical and Industrial Engineering Department, Indian Institute of Technology, Roorkee, for his invaluable guidance, continuous encouragement and painstaking supervision for this Dissertation Work. Without his guidance & timely suggestions the dissertation would never have reached its completion. I wish to express my sincere thanks to him for providing necessary help and co-operation at all stages of this dissertation work.

I am also thankful to Dr. B. K. Mishra, Associate Professor, Mechanical and Industrial Engineering Department, Indian Institute of Technology, Roorkee, for providing necessary facilities to complete this work.

At the last but not the list I express heartfelt regards to my family members and friends for their inspirational impetus and moral support during the course of this work.

Date: 29.04.2004

Place: Roorkee


(MAHESH P. YEOLA)

ABSTRACT

The work presented here deals with Active Vibration Control (AVC) of a Cantilever Beam with Piezoelectric Patches using Finite Element Method (FEM). One patch is used as a sensor, sending the signal in terms of voltage to the control system; while other is used as an actuator, which applies moments based on the signal (voltage) received from the control system. Newmark method of direct numerical integration has been used in the programmes coded in Matlab 5.3 to analyse transient responses. Negative velocity feedback control (NVFBC), Independent Modal Space Control (IMSC) and Modified Independent Modal Space Control (MIMSC) are used to control both free and forced vibrations.

In case of free vibration, it is found that with the increase in the value of Gain in Negative Velocity FBC, the damping gets increased, while settling time reduces till some value of gain, after which response gets unstable. MIMSC gives better performance than IMSC, and in both, IMSC as well as MIMSC, damping and settling time increases with weighting factor (R); while the peak voltage i.e. control effort decreases with increasing R.

In case of forced vibration with harmonic force input, steady state amplitude as well as maximum amplitude decreases with increasing gain in Negative Velocity FBC, till some value of gain after which response becomes unstable; while steady state amplitude and maximum amplitude increases with weighting factor R in MIMSC and IMSC. Control voltage decreases with increase in R in IMSC, MIMSC. In the case of forced vibration, IMSC gives better performance than MIMSC.

The study of forced vibration with ramp input is carried out to achieve vibration control by varying axial stiffness of beam by applying same polarity voltage on both actuators bonded to the beam in collocated fashion. Control of vibration using variable axial stiffness during sweeping excitation has been investigated. When patches are activated from beginning and deactivated at about 50% of average of first natural frequencies with and without the axial stiffness variation, maximum amplitude of the vibration has found to be reduced substantially. Though cantilever beam has been considered, merely ^{by} changing boundary conditions (B.C.) the developed software can be used to analyse other types of beams.

CONTENTS

Candidate's Declaration	I
Acknowledgement	II
Abstract	III
Contents	IV
Nomenclature	VII
List of Figures	X
List of Tables	XII
Chapter 1 INTRODUCTION	1
1.1 Smart Materials	3
1.2 Classification of Smart Materials	3
1.3 Introduction to Smart Materials	4
1.4 Smart Structures	5
1.5 Smart Materials and Vibration Control	6
1.6 Piezoelectric Materials	7
1.6.1 Piezoelectric Effect	7
1.6.2 Polarisation (Polling)	9
1.6.3 Piezoelectric Materials	10
1.6.4 Classification of Piezoelectrics	10
1.6.5 Constitutive Equations	11
1.6.6 Piezoelectric Material in Vibration Control	13
Chapter 2 LITERATURE REVIEW	14
2.1 Conclusions and Scope for Proposed Work	23
Chapter 3 FEM OF A BEAM WITH PIEZOELECTRIC PATCHES	24
3.1 Assumptions in the Modelling	24
3.2 Statement of the Problem	25
3.3 Finite Element Model of Beam with Patches	26

3.3.1	Beam Finite Element with Piezoelectric Patch	27
3.4	Natural Frequencies of Beam	29
3.4.1	Formation of Global Mass and Stiffness Matrix	30
3.5	Formation of Global Damping Matrix	32
3.6	Newmark Method	33
3.6.1	Selection of Time Step, Δt	34
3.6.2	Determination of Constants	34
3.7	Mass Normalised Mode Shape Vector	35
3.8	Modal Displacements and Modal Velocity	35
3.9	Axial Force due to Patch Actuation	36
3.9.1	Calculation of Change in Stiffness due to Axial Force	37
3.10	Summary	37
Chapter 4	FREE AND FORCED VIBRATION: WITH AND WITHOUT CONTROL	38
4.1	Negative Velocity Feedback Control	38
4.1.1	Negative Velocity Feedback Control (Simple)	39
4.1.2	Negative Velocity Feedback Control (Sensor & Actuator)	39
4.2	Independent Modal Space Control (IMSC)	40
4.2.1	Weighting Factor, R	41
4.3	Modified Independent Modal Space Control (MIMSC)	42
4.3.1	Time Sharing Strategies	42
4.4	Free Vibration Response	43
4.4.1	Free Damped Vibration: Negative Velocity FBC (Simple)	43
4.4.2	Free Damped Vibration: Negative Velocity FBC (Sensor)	44
4.4.3	Free Damped Vibration: IMSC	44
4.4.4	Free Damped Vibration: MIMSC	44
4.5	Forced Vibration Response	45
4.5.1	Forced Damped Vibration: Negative Velocity FBC (Simple)	45
4.5.2	Forced Damped Vibration: Negative Velocity FBC (Sensor)	45
4.5.3	Forced Damped Vibration: IMSC	46
4.5.4	Forced Damped Vibration: MIMSC	46
4.6	Vibration Control using controlled Axial Stiffness Variation	46

Chapter 5	RESULTS AND DISCUSSION	48
5.1	Free Damped Vibration	49
5.1.1	Free Damped Vibration: NVFBC (First Approach)	50
5.1.2	Free Damped Vibration: NVFBC (Second Approach)	53
5.1.3	Free Damped Vibration with IMSC	58
5.1.4	Free Damped Vibration with MIMSC	59
5.1.5	Comparison of controlled Vibration using IMSC, MIMSC	61
5.2	Forced Damped Vibration	67
5.2.1	Forced Damped Vibration with NVFBC (First Approach)	68
5.2.2	Forced Damped Vibration with NVFBC (Second Approach)	70
5.2.3	Forced Damped Vibration with IMSC	73
5.2.4	Forced Damped Vibration: MIMSC	75
5.2.5	Forced Damped Vibration: IMSC Vs MIMSC	77
5.3	Vibration Control: Axial Stiffness Variation	81
Chapter 6	CONCLUSION AND SCOPE FOR FUTURE WORK	84
6.1	Scope for Future Work	87
	REFERENCES	88
	APPENDIX A	92

NOMENCLATURE

ABBREVIATIONS

AVC	Active Vibration Control
DOF	Degrees of Freedom
ER	Electro - Rheological
FBC	Feedback Control
FEM	Finite Element Method
FFC	Feed Forward Control
FOS	Fiber Optic Sensor
FSMA	Ferromagnetic Shape Memory Alloys
HVC	Hybrid Vibration Control
IMSC	Independent Modal Space Control
LQR	Linear Quadratic Regulator
LQG	Linear Quadratic Gaussian
MIMSC	Modified Independent Modal Space Control
MR	Magneto - Rheological
MSM	Magnetic Shape Memory Alloys
NVFC	Negative Velocity Feedback Control
PVC	Passive Vibration Control
PVDF, PVF ₂	Polyvinylidene Fluoride
PZT	Lead Zirconate Titanate
SMA	Shape Memory Alloys

SYMBOLS

A	Area of Cross-section
a_0 to a_7	Constants used in Newmark Method
b	Width
$[C]$	Global Damping Matrix
$[C_G]$	Generalised Damping Matrix
D	Charge Density
$[d]$	Matrix of Piezoelectric Coupling Terms
d_{31}	Piezoelectric Strain Constant

E	Electric Field, Young's Modulus or Modulus of Elasticity
$\{F\}$	Force Vector
$\{F_{Control}\}$	Control Force Vector
$\{F_{Modal}\}$	Modal Force Vector
F_s	Axial Force in beam, due to piezo-patch actuation
G	Gain in Negative Velocity Feedback Control
g_{31}	Piezoelectric Stress Constant
I	Moment of Inertia
L	Length
$[K], [k_g]$	Global Stiffness Matrix
$[K_G]$	Generalised Stiffness Matrix
$[k], [k_e]$	Element Stiffness Matrix
$[k_P]$	Axial Stiffness Matrix
$[\hat{K}]$	Effective Stiffness Matrix
$[M], [m_g]$	Global Mass Matrix
M_A	Moment applied by Actuator
$[M_G]$	Generalised Mass Matrix
$[m], [m_e]$	Element Mass Matrix
R	Weighting Factor in IMSC, MIMSC
$\{S\}$	Strain Vector
$[s]$	Compliance Matrix
$\{T\}$	Stress Vector
t	Thickness
$[U]$	Eigenvector Matrix
u	Displacements at each node, Global Displacement Vector
$[U_n]$	Mass Normalised Eigenvector Matrix
V	Voltage, Volume Ratio
x	Global Displacement, Global Displacement Vector
\dot{x}	Global Velocity, Global Velocity Vector
\ddot{x}	Global Acceleration, Global Acceleration Vector

GREEK AND LATIN LETTERS

α	Thermal Coefficient of Expansion, Constant in Newmark Method
$\{\delta\}$	Modal Displacement Vector, Logarithmic Displacement, Constant in Newmark Method
$\{\dot{\delta}\}$	Modal Velocity Vector
ε	Permittivity, strain
ε_p	Free Strain in the Actuator
ε_s	Strain in the beam, due to actuation of Piezo-Patch
ε_x	Linear Strain in x-direction
Δt	Time Step for Newmark Method
ρ	Mass Density
σ	Axial Stress
τ	Shear Stress
θ	Temperature Difference
θ_y	Rotational (Angular) Displacement at node y
γ_{xy}	Shear Strain in XY plane
ω	Frequency of Vibrating Force, Excitation Frequency
ω_n	Natural frequency in (rad/s)
ω_r	Natural Frequency corresponding to the mode to be controlled
$\{\phi_i\}$	Eigenvector corresponding to i^{th} Natural Frequency (Eigenvalue)
$[\phi]$	Mass Normalised Eigenvector Matrix
ξ	Damping Ratio

SUBSCRIPTS

a	Actuator, Patch
beam	Host Beam
c	Composite
PZT	Lead Zirconate Titanate
patch	Piezoelectric Patch
s	Structure, Beam

LIST OF FIGURES

Figure 1.1	Block Diagram of AVC: Smart Materials as Sensors and Actuator	6
Figure 1.2	Piezoelectric Effect and Reverse Piezoelectric Effect	8
Figure 1.3	Piezo effect on the crystal structure (example of the quartz)	8
Figure 1.4	Mono-Crystal Vs Poly-Crystal	8
Figure 1.5	Example of Piezoelectric Effect	9
Figure 1.6	Polarisation of Ceramic Material to Generate Piezoelectric Effect	9
Figure 1.7	Classification of Piezoelectric Materials	11
Figure 1.8	Convention of piezoelectric Materials	12
Figure 3.1	Uniform Strain Model and Euler – Bernoulli Model	25
Figure 3.2	Cantilever Beam with Piezoelectric Patches	26
Figure 3.3	Beam under bending deformation	27
Figure 3.4	Transformation Section Method	28
Figure 3.5	Transformed Section of Beam with Piezo-Patches	29
Figure 3.6	Global matrix assembly from element matrices	30
Figure 4.1	Effect of Axial Stiffness Variation on Vibration Response	47
Figure 5.1	Variation of displacement with time (uncontrolled Free Vibration)	49
Figure 5.2	Variation of displacement with time (NVFBC) (Gain = 0.1)	50
Figure 5.3	Variation of amplitude (at the end of 5 sec) with Gain (NVFBC)	51
Figure 5.4	Variation of damping ratio with gain (Negative Velocity FBC)	52
Figure 5.5	Variation of settling time with gain (Negative Velocity FBC)	52
Figure 5.6	Variation of displacement with time (NVFBC) (Unstable Response)	53
Figure 5.7	Variation of displacement with time (Negative Velocity FBC)	54
Figure 5.8	Variation of actuator voltage with time (Negative Velocity FBC)	54
Figure 5.9	Variation of amplitude (at the end of 5 sec) with gain (NVFBC)	56
Figure 5.10	Variation of damping ratio with gain (Negative Velocity FBC)	56
Figure 5.11	Variation of settling time with gain (Negative Velocity FBC)	57
Figure 5.12	Variation of actuator voltage with gain (Negative Velocity FBC)	57
Figure 5.13	Variation of displacement with time (IMSC)	58
Figure 5.14	Variation of voltage with time (IMSC)	59
Figure 5.15	Variation of displacement with time (MIMSC)	60

Figure 5.16	Variation of voltage with time (MIMSC)	60
Figure 5.17	Comparison of Free Vibration response with IMSC and MIMSC (Variation of amplitude with R)	62
Figure 5.18	Comparison of Free Vibration response with IMSC and MIMSC (variation damping ratio with R)	62
Figure 5.19	Comparison of Free Vibration response with IMSC and MIMSC (variation of Settling Time with R)	63
Figure 5.20	Comparison of Free Vibration response with IMSC and MIMSC (Variation of Voltage with R)	63
Figure 5.21	Variation of displacement with time (uncontrolled forced vibration)	67
Figure 5.22	Variation of displacement with time (NVFBC) (Gain = 0.1)	69
Figure 5.23	Variation of Maximum and Steady state amplitude with gain	69
Figure 5.24	Variation of displacement with time (NVFBC) (Gain = 0.1)	70
Figure 5.25	Variation of actuator voltage with time (NVFBC) (Gain = 0.1)	70
Figure 5.26	Variation of maximum and steady state amplitude with gain	72
Figure 5.27	Variation of actuator voltage with gain (NVFBC)	72
Figure 5.28	Variation of displacement with time (IMSC) (R = 1.0)	74
Figure 5.29	Variation of voltage with time (IMSC) (R = 1.0)	74
Figure 5.30	Variation of displacement with time (MIMSC) (R = 1.0)	76
Figure 5.31	Variation of voltage with time (MIMSC) (R = 1.0)	76
Figure 5.32	Comparison of Forced Vibration response with IMSC and MIMSC (variation of amplitude at end of 2.5 seconds with R)	77
Figure 5.33	Comparison of Forced Vibration response with IMSC and MIMSC (variation of Maximum Amplitude with R)	78
Figure 5.34	Comparison of Forced Vibration response with IMSC and MIMSC (variation of Steady State Amplitude with R)	78
Figure 5.35	Comparison of Forced Vibration response with IMSC and MIMSC (variation of voltage with R)	79
Figure 5.36	Time domain response of the beam (patches in deactivated state)	81
Figure 5.37	Time domain response of the beam (patches in activated state)	82
Figure 5.38	Comparison of time domain response of the beam (Patches in activated state, deactivated state and controlled switching cases)	83

LIST OF TABLES

Table 1.1	Actuator Candidates for Smart Materials	6
Table 1.2	Sensor Candidates for Smart Materials	7
Table 1.3	Piezoelectric Materials	10
Table 3.1	Description of Beam and Piezoelectric Patches	26
Table 3.2	Properties of Finite Element with and without Patches	29
Table 3.3	Natural Frequencies of Beam with and without patches	31
Table 3.4	Natural Frequencies comparison with Empirical Results	32
Table 4.1	Properties of Beam and Patches	47
Table 5.1	Free Damped Vibration with Negative Velocity FBC (Simple)	51
Table 5.2	Free Damped Vibration with Negative Velocity FBC (Sensor)	55
Table 5.3	Free Damped Vibration with IMSC	64
Table 5.4	Free Damped Vibration with MIMSC	65
Table 5.5	Free Vibration IMSC Vs. MIMSC	66
Table 5.6	Forced Damped Vibration with Negative Velocity FBC (Simple)	68
Table 5.7	Forced Vibration Negative Velocity Control (Sensor)	71
Table 5.8	Forced Vibration with IMSC	73
Table 5.9	Forced Vibration with IMSC	75
Table 5.10	Forced Vibration IMSC vs. Modified IMSC	80

CHAPTER 1

INTRODUCTION

Vibration control is a wide and important area of interest in all sections of industry. Before controlling vibrations it is necessary to check various causes of vibrations as well as effect of various parameters on the vibration. Elasticity, inertia and damping are the main constituents of the vibrating system. Unwanted vibration can have a detrimental and some times catastrophic effect on the serviceability or structural integrity of the structure. The effects of uncontrolled vibration can be seen on a large scale, such as the collapse of the bridges, big structures, etc. e.g. the collapse of the Takoma Narrows suspension bridge in 1940 as well as to a much smaller scale e.g. blurring of photographs taken by space telescopes, error in readings taken by precision measuring devices, etc.

In general, from buildings to airplanes, space trusses and satellites, cars, electric transformers and large bridges, all can be disturbed in their normal function by vibration and noise. The control of vibration and noise can be considered as one of the most relevant technological challenges in this century. Vibration control is aimed at reducing or modifying the vibration level in a mechanical structure.

Most systems cope up with these problems with conventional passive methods. These systems reduce vibrations by simply dissipating energy as heat. Unfortunately their damping performance is generally quite poor as they are unable to adapt or retune to changing disturbances or structural characteristics, over time. Use of lightweight and flexible structures are becoming important in space and aerospace activities, either to reduce the high cost of lifting the mass into the orbit or transportation cost. Due to flexibility and low internal damping, vibrations once introduced in such systems grow to large amplitudes. The conventional form of external passive damping is not preferred as addition of a damper adds to overall system weight, which is undesirable.

Though Passive Vibration Control (PVC) has advantages like low cost, stability, robustness, reliability, and simple systems but due to recent technological advancements such as the availability of high speed computing devices, smart materials and advanced control techniques have led to growing use of Active Vibration Control (AVC). AVC has disadvantages like high cost, complexity and

somewhat unreliable systems but these can be compensated by the control achieved by them.

Smart Materials has been emerged as a very important component in AVC of structures. A smart structure has the capability to respond to the changing external environment (load, temperature and shape) as well as to internal environment (damage or failure). Smart materials have numerous applications like AVC, Active Noise Control, Active Buckling Control, Shape Control, Damage Assessment and Health Monitoring.

A variety of smart materials already exists, and is being researched extensively. These include Piezoelectric Materials, Shape Memory Alloys (SMA), Magnetostrictive Materials, Electrostrictive Materials, Fiber Optic Sensors (FOS), Electro-rheological (ER) and Magneto-rheological (MR) fluids. Each individual type of smart material has a different property, which can be significantly altered, such as viscosity, volume, conductivity, etc.

Coupled mechanical properties of piezoelectric materials and their availability in the form of thin sheets make them well suited for use as sensors and actuators. Direct and converse piezoelectric effect governs the interaction between these types of materials and structures. Integration of piezoelectric sensors, actuators and advanced composites make it possible the formation of high-strength, high-stiffness, lightweight structures capable of self-monitoring and self-controlling. Piezoelectric materials have another advantage that they do not affect, significantly, mass and stiffness properties of original structure. So original dynamic response characteristics of structure remain almost unchanged when piezoelectric materials are not activated.

Next part of this chapter gives information regarding Smart Materials and Structures, and Piezoelectricity. Chapter 2 contains literature survey. Chapter 3 contains finite element formulation of piezo-laminated beam and information regarding Newmark Method. Chapter 4 contains information regarding control methods used, free and forced vibration response with and without control and effect of axial stiffness variation due to actuation of patches and their use in vibration control. Chapter 5 details about result and discussion followed by conclusion and suggestions for future work in chapter 6. References and appendix containing flowcharts are given at the end of the report

Reference!

1.1 SMART MATERIALS

Smart Materials can be defined as the materials, which have one or more properties that can be dramatically altered by external driving forces (stimuli) and returns to original state when stimuli is removed.

Such materials have the ability to change their physical properties like shape or size simply by application of heat, electric or magnetic field or to change instantly from a liquid to a solid. Most everyday materials have physical properties, which cannot be significantly altered; for example if oil is heated it will become a little thinner, whereas a smart material with variable viscosity may turn from a liquid to a solid within a millisecond duration.

As stated earlier, a variety of smart materials already exist, and are being researched extensively. These include Piezoelectric Materials, Shape Memory Alloys (SMA), Magnetostrictive Materials, Electrostrictive Materials, Fiber Optic Sensors (FOS), Electro-rheological (ER) and Magneto-rheological (MR) fluids. Each individual type of smart material has a different property, which can be significantly altered, such as viscosity, volume and conductivity. Some everyday items are already incorporating smart materials (coffeepots, cars, International Space Station, eyeglasses, etc).

The following terms can be used interchangeably:

- Smart materials
- Intelligent Materials
- Active Materials
- Adaptive Materials

Smart materials will be probably only option for next generation of products that must operate under varying service conditions in constrained environment.

1.2 CLASSIFICATION OF SMART MATERIALS

Depending upon the applied driving forces smart materials can be broadly classified into three categories

- Electrical fields - Common materials include Electrostrictive, Piezoelectric (Ceramic and Polymers) and Electro-Rheological (ER) fluids.
- Thermal fields - Common materials include Shape Memory Alloys (SMA).
- Magnetic field - Common materials include Magnetostrictive Materials, Magnetic Shape Memory Alloys (MSM), Ferromagnetic Shape Memory Alloys (FSMA), and Magneto-Rheological (MR) fluids.

1.3 INTRODUCTION TO SMART MATERIALS

- **Shape Memory Alloys (SMA):** The term Shape Memory Alloys (SMA) is applied to a group of metallic materials that can return to a previously defined shape when subjected to an appropriate thermal procedure. Generally, these materials can be plastically deformed at some relatively low temperature, and upon exposure to some higher temperature will return to their shape prior to the deformation. SMAs allow one to recover up to 5% strain from the phase change induced by temperature. SMAs are best suited for one-way tasks such as deployment. SMAs are little used in vibration control. Examples are Ni-Ti alloys, Cu-Zn-Al, Cu-Al-Ni, Fe-Mn, and Fe-Mn-Si, etc.
- **Piezoelectric Materials:** Piezoelectricity is the ability of a material to develop an electrical charge when subjected to a mechanical strain and conversely. They have a recoverable strain of 0.1% under electric field; they can be used as actuators as well as sensors. Detailed information is given in Section 1.6. Examples are PZT, PVDF, etc.
- **Magnetostrictive Materials:** As a magnetostrictive material is magnetized, there is a change in length. Conversely if an external force produces a strain in magnetostrictive materials, its magnetic state will change. Magnetostrictive materials have a recoverable strain of 0.15% under magnetic field; the maximum response is obtained when the material is subjected to compressive loads. They can be used in high precision applications. Example is Terfenol-D.
- **Electrostrictors (Electrostrictive Materials):** These are quite similar to piezoelectric materials with slightly better strain capability, but very sensitive to temperature. The conceptual difference between piezoceramics and electrostrictors is their response upon reversing of the electric field. Piezoceramics can be elongated and compressed, while electrostrictors only exhibit an elongation, independent of the direction of the applied electric field. This effect is found in all materials though in very small quantity 10^{-5} to 10^{-7} %.

- **Ferromagnetic Shape Memory Alloy (FSMA):** Ferromagnetic shape memory alloys (FSMA) are a recently discovered class of actuator materials, whose salient features are magnetically driven actuation and large strains (around 6%) e.g. Ni-Mn-Ga ternary alloy. As the name suggests FSMA are ferromagnetic alloys that also support the shape memory effect.
- **Electro-Rheological (ER) and Magneto- Rheological (MR) Fluids:**
When an external electric field is applied to an ER fluid, the viscosity of the fluid increases remarkably. And when the electric field is taken away, the viscosity of the fluid goes back to the original state. The phenomenon is so called ER effect. These fluids can change from a thick fluid (similar to motor oil) to nearly a solid substance within a span of a millisecond when exposed to an electric field; the effect can be completely reversed just as quickly when the field is removed. MR fluids experience a viscosity change when exposed to magnetic field. Examples of MR fluid is tiny iron particles suspended in oil and that of ER fluid are milk chocolate or cornstarch and oil.
- **Fiber Optics:** Fiber optics is becoming popular as sensors because they can be easily embedded in composite structures with little effect on the structural integrity. They are widely used in Structural Health Monitoring equipments.

1.4 SMART STRUCTURES

Anything that is designed to take a mechanical load is called as a structure. Within this definition we have everything ranging from overhead power cables to bridges to aircraft to mechanical gearboxes to highways. A smart structure is therefore one that monitors itself and / or its environment in order to respond to changes in its condition. Spillman and his colleagues attempted to develop a formal definition of smart structure in their survey as:

“A Smart Structure is a non-biological physical structure having the following attributes:

1. A definite purpose
2. A means and imperative to achieve that purpose, and
3. A biological pattern of functioning ”

Smart structure has the capability to respond to changing external environment (such as change in load or shape change) as well as to changing internal environment (such as damage or failure) for desired performance. An active structure or smart structure consists of a structure provided with a set of actuators and sensors coupled by a controller. Figure 1.1 shows the block diagram of AVC using smart materials as sensors and actuators.

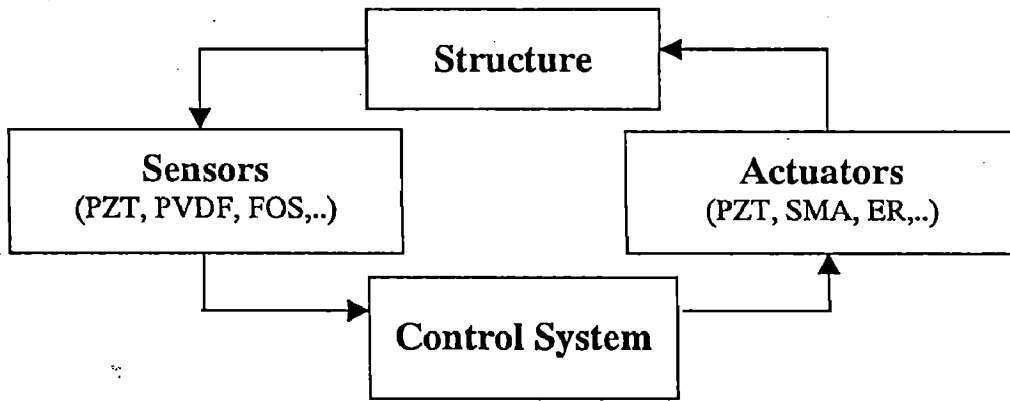


Figure 1.1 Block Diagram of AVC: Smart Materials as Sensors and Actuators

reference

1.5 SMART MATERIALS AND VIBRATION CONTROL

Depending on the application, a wide range of actuators (Piezoceramics, Electrostrictive, Magnetostrictive, MR fluid and SMA) and sensors (PVDF, PZT, FOS) has been successfully implemented. Tables 1.1 and 1.2 summarises performance of smart materials as actuators and sensors.

Table 1.1 Actuator Candidates for Smart Materials

Characteristics	Electro- strictive Materials	ER Fluids	Magneto- strictive Materials	Nitinol SMA	Piezoelectric Ceramics
Cost	Moderate	Moderate	Moderate	Low	Moderate
Networkable	Yes	Yes	Yes	Yes	Yes
Embedability	Good	Fair	Good	Excellent	Excellent
Linearity	Fair	Fair	Good	Good	Good
Response (Hz)	1-20000	0-12000	1-20000	0-5	1-20000
Maximum Microstrain	200	-	200	5000	200
Max Temp ($^{\circ}$ C)	300	300	400	300	300

Table 1.2 Sensor Candidates for Smart Materials

Characteristics	FOS	Nitinol SMA	Piezo-Ceramic	Strain Gauge
Cost	Moderate	Low	Moderate	Low
Networkable	Yes	Yes	Yes	Yes
Embedability	Excellent	Excellent	Excellent	Good
Linearity	Good	Good	Good	Good
Response (Hz)	1-10000	0-10000	1-20000	0-500000
Sensitivity (Microstrain)	0.11 per fiber	0.1-1.0	0.001-0.01	2
Maximum Microstrain	3000	5000	550	10000
Max Temp ($^{\circ}$ C)	300	300	200	300

1.6 PIEZOELECTRIC MATERIALS

Piezoelectric materials are the materials, which have coupled electro-mechanical properties, when stressed they produce voltage and when applied voltage, they deform. A large number of natural and synthetic materials possess piezoelectric properties. Following this is a detailed description about piezoelectricity and piezoelectric materials.

1.6.1 Piezoelectric Effect

The piezoelectric effect was first discovered in 1880 when Pierre and Currie demonstrated that certain crystalline material produces an electrical charge on its surface when it is subject to a stress field. It was subsequently demonstrated that the converse effect is also true; when an electric field is applied to the piezoelectric material, its shape and size change. In the former case, the material works like a sensor while in the latter case, the material can be used as an actuator if it is constrained against deformation.

In the single crystal of a piezoelectric material, if a force is applied, a strain and hence a change in dimensions occurs, this produces a charge build up on one face of the crystal and hence a potential difference across the crystal. This is the piezoelectric effect shown in Figures 1.2 and 1.3.

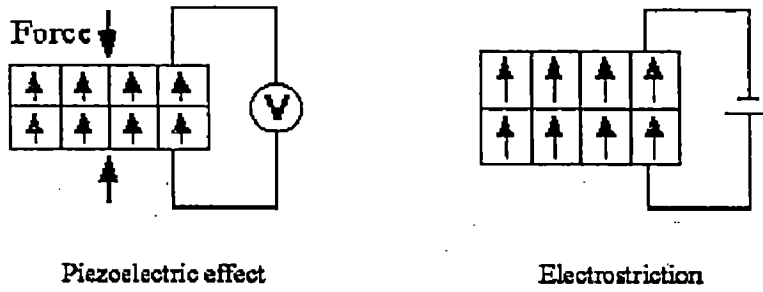


Figure 1.2 Piezoelectric Effect and Reverse Piezoelectric Effect

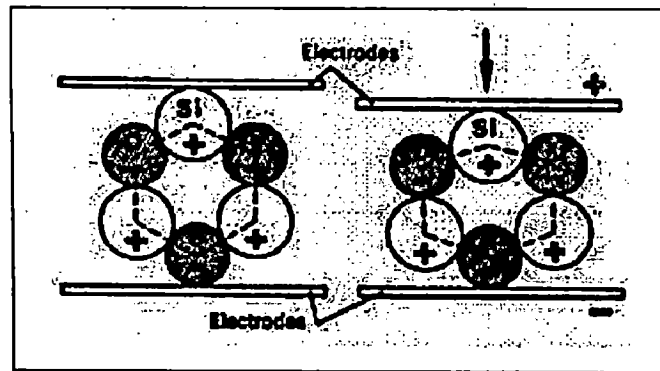


Figure 1.3 Piezo effect on the crystal structure (example of the quartz)

In contrast, when a voltage is applied across these crystals a dimension change is observed and this is known as electrostriction or the reverse piezoelectric effect as shown in Figure 1.2.

Polycrystalline materials such as PZT are a little different. They need to be subjected to an electric field to align the dipoles of each crystal cell before their piezoelectric properties are realized and this process is called as **Polling** or **Polarisation**. These polycrystalline ceramics (Figure 1.4) are more versatile than single crystal natural compounds because controlling the material combination can optimise their properties for specific application.

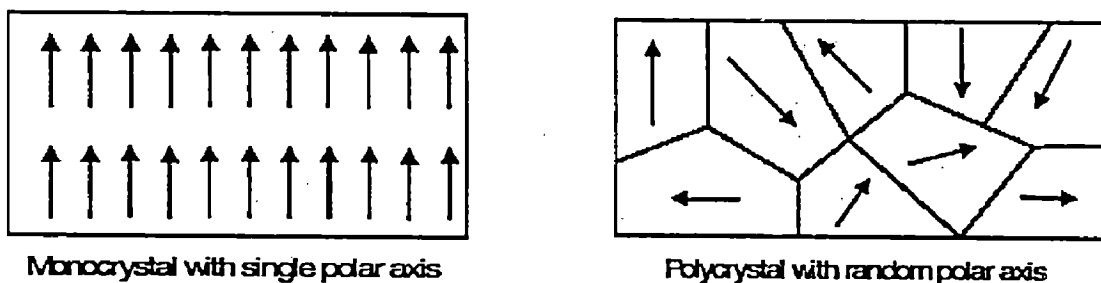


Figure 1.4 Mono-Crystal Vs Poly-Crystal

If an AC voltage is applied to these materials, alternating expansion - compression will take place as shown in Figure 1.5.

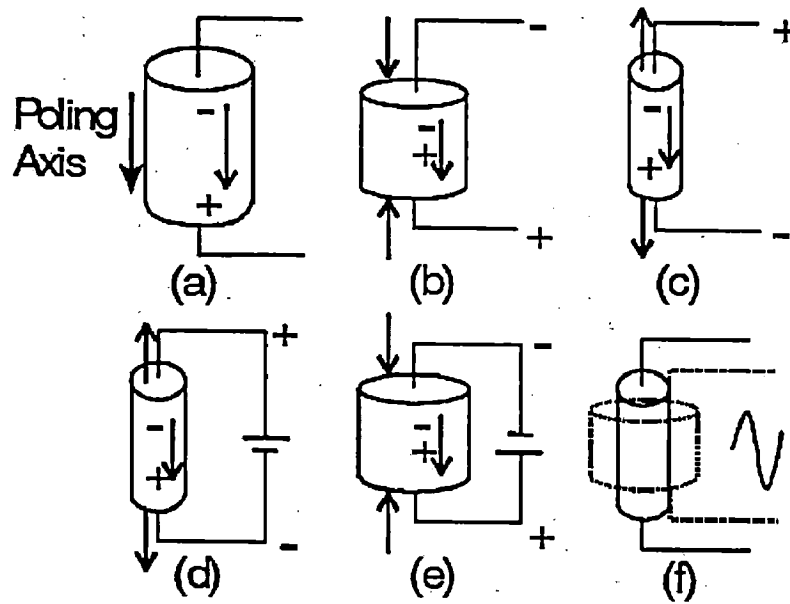


Figure 1.5 Example of Piezoelectric Effect

1.6.2 Polarisation (Polling)

The polycrystal is heated above its **Curie Temperature** and strong electric field is applied so that the molecules, free to rotate, align themselves in the direction of the field (Figure 1.6). During operation, an electric field applied in the direction of the polarisation induces compression of the crystal in this (Polarisation) direction. Reversing the field reverses the direction of the strain (Figure 1.5). Polarisation is the amount of charge associated with the dipolar or free charge in a dielectric

Handwritten note: } sentence is incomplete.

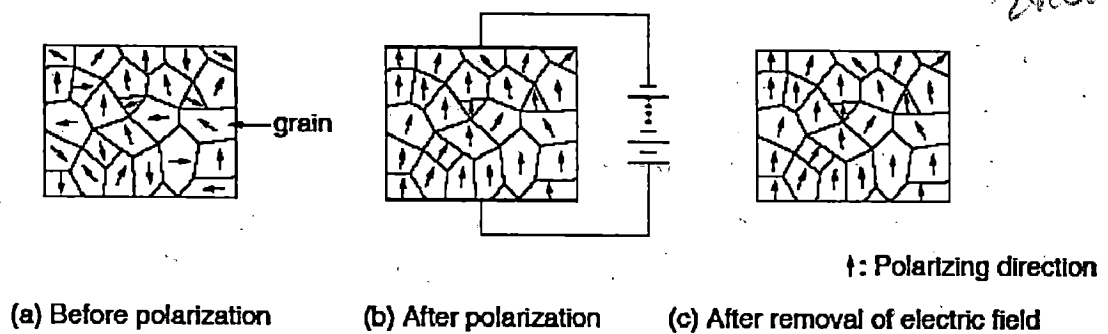


Figure 1.6 Polarisation of Ceramic Material to generate Piezoelectric Effect

1.6.3 Piezoelectric Materials

~~There~~ (They) are two broad classes of piezoelectric materials used in vibration control: ceramics and polymers. The piezopolymers are used mostly as sensors; because they require high voltages as well as they are lightweight and flexible so they are not effective as actuators on stiff structures. The best known is the polyvinylidene fluoride (PVDF) (PVF₂). Piezoceramics are used extensively as actuators and sensors, for a wide range of frequency including ultrasonic applications. The best-known piezoceramic is Lead Zirconate Titanate (PZT) [Pb (Zr, Ti) O₃].

Piezoelectric materials offer a number of advantages over conventional actuators like low energy consumption, fast response, high efficiency and compactness. But they have some limitations also like voltage that can be applied is limited in the range of -500 V to 1500 V, the piezo materials cannot be used above their curie temperature, which is 200 °C to 300 °C due to possibility of depolarisation. Table 1.3 summarises piezoelectric materials.

Table 1.3 Piezoelectric Materials

Type	Material
Single Crystal	Quartz Lead Magnesium Niobate (PMN – PT & PZN - PT)
Ceramics	Lead Zirconate Titanate (PZT) [Pb (Zr, Ti) O ₃] Lead Metaniobate (LMN) Lead Titanate (LT) Lead Magnesium Niobate (PMN)
Polymers	Polyvinyledene Fluoride
Composites	Ceramic Polymer Ceramic Glass
Natural	Quartz, Tourmaline
Synthetic	PZT, PVDF, Barium Titanate, LMN, LT, PN, etc

1.6.4 Classification Of Piezoelectrics

Pyroelectrics: materials in which electric field generates as a result of application of heat and degree of polarisation depends on the temperature.

Ferroelectrics: materials in which spontaneous polarisation can be induced by an electric field. Reversing external electric field can change their polarisation direction. Examples are PZT and PVDF.

Ferroelastics: materials in which spontaneous polarisation can be induced due to a mechanical load.

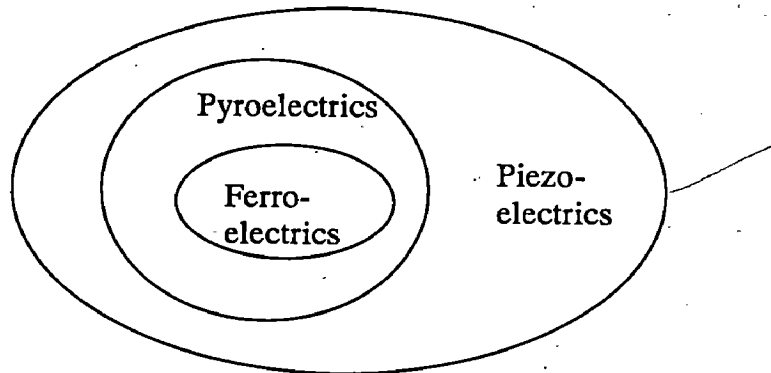


Figure 1.7 Classification of Piezoelectric Materials

1.6.5 Constitutive Equations

Piezoelectric materials are considered from both points of views: Mechanical and Electrical.

Mechanical: Relation between stress and strain (Hook's Law).

$$\text{Strain} = \text{Compliance} \times \text{Stress} \quad (S = s T) \quad (1.1)$$

Electrical: How charge moves in a dielectric material when it is subjected to a voltage and vice versa.

$$\text{Charge Density} = \text{Permittivity} \times \text{Electric Field} \quad (D = \epsilon E) \quad (1.2)$$

Constitutive Equations: Relate different Mechanical and Electrical quantities.

$$S = s_E T + d' E \quad \text{and} \quad D = \epsilon_T E + d T \quad (1.3)$$

Where,

Term	Meaning	SI Unit
S	Strain	mm/mm
s	Compliance	mm ² /N
T	Stress	N/mm ²
D	Charge Density (Dielectric Displacement) (Charge/ area)	C/m ²
ϵ	Permittivity	F/m
E	Electric Field	V/m
d	Matrix of Piezo Coupling Terms	m/V
s_E	Compliance at <u>constant/zero</u> electric field	mm ² /N
ϵ_T	Permittivity at <u>constant/zero</u> stress field	F/m

The convention used to formulate the constitutive equations in three dimensions is as shown in Figure 1.8. Poling is generally done in direction 3, while direction 1 is aligned with length of beam, plate, etc and direction 2 for width.

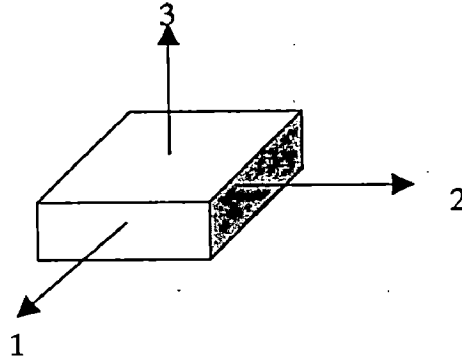


Figure 1.8 Convention of Piezoelectric Materials

Constitutive Equations considering thermal effect is in Equation 1.4 as

$$\begin{bmatrix} \varepsilon_1 \\ \varepsilon_2 \\ \varepsilon_3 \\ \gamma_{23} \\ \gamma_{31} \\ \gamma_{12} \end{bmatrix} = \begin{bmatrix} S_{11} & S_{12} & S_{13} & 0 & 0 & 0 \\ S_{21} & S_{22} & S_{23} & 0 & 0 & 0 \\ S_{31} & S_{32} & S_{33} & 0 & 0 & 0 \\ 0 & 0 & 0 & S_{44} & 0 & 0 \\ 0 & 0 & 0 & 0 & S_{55} & 0 \\ 0 & 0 & 0 & 0 & 0 & S_{66} \end{bmatrix} \begin{bmatrix} \sigma_1 \\ \sigma_2 \\ \sigma_3 \\ \tau_{23} \\ \tau_{31} \\ \tau_{12} \end{bmatrix} + \begin{bmatrix} 0 & 0 & d_{31} \\ 0 & 0 & d_{32} \\ 0 & 0 & d_{33} \\ 0 & d_{15} & 0 \\ d_{15} & 0 & 0 \\ 0 & 0 & 0 \end{bmatrix} \begin{bmatrix} E_1 \\ E_2 \\ E_3 \end{bmatrix} + \begin{bmatrix} \alpha_1 \\ \alpha_2 \\ \alpha_3 \\ 0 \\ 0 \\ 0 \end{bmatrix} \theta \quad (1.4)$$

Where,

ε_1 = Linear Strain in direction 1

γ_{23} = Shear Strain in direction 23

S_{ij} = Elements of Compliance Matrix

σ_1 = Axial Stress in direction 1

τ_{23} = Shear Stress in direction 23

α_1 = Thermal Coefficient of Expansion for direction 1

θ = Temperature difference

$$d = \begin{bmatrix} 0 & 0 & 0 & 0 & d_{15} & 0 \\ 0 & 0 & 0 & d_{15} & 0 & 0 \\ d_{31} & d_{32} & d_{33} & 0 & 0 & 0 \end{bmatrix} = \text{Matrix of Piezo-Coupling Terms} \quad (1.5)$$

In matrix 'd' for any term d_{ij} , i stand for applied electric field direction while j is the axis of induced mechanical deformation.

1.6.6 Piezoelectric Material In Vibration Control

Coupled electro-mechanical properties of piezoelectric ceramics and polymers and their availability in thin sheets make them well suited for the use as sensors and actuators. Piezoelectric materials are widely used in vibration control due to their competitive performance characteristics as listed in Tables 1.1 and 1.2. Besides these, the lightweight actuators don't affect significantly the mass and stiffness properties of the original structure, so the original dynamic characteristics of the structure remain unchanged when the piezoelectric patches are not activated.

Piezoelectric patches apply two types of effects on structures:

Passive – Change in mass and stiffness characteristics (this effect is negligible for stiff structures), and

Active – Generation of charge and strain due to applied stress and voltage respectively.

Resonance is said to occur when the excitation frequency matches any of the natural frequencies of the system, so one should know the natural frequencies of the system, hence the eigenvalues of beam with and without patches have been calculated. The contribution of patches in mass and stiffness matrices has been considered. The change in mass and stiffness of beam and patches due to application of voltage has been considered. Control is achieved by using Negative Velocity Feedback Control, IMSC and MIMSC. Comparison has ^{been} made among them. The study of forced vibration with ramp input is done to achieve vibration control by varying axial stiffness of beam by applying same polarity voltage on both actuators. Though cantilever beam has been considered, merely by changing boundary conditions one can switch to other types of beam.

CHAPTER 2

LITERATURE REVIEW

A lot of work has been done in the fields of Vibration Control, Smart Materials as well as Vibration Control using Smart Materials. Various researchers have used different concepts and structural elements as their focus of research. A brief review of the existing available literature is attempted here. The review is arranged with work dealing with smart materials and their use in vibration control followed by literature dealing with finite element modeling of piezo-laminated beam, basic piezoelectric equations, location and size of sensors and actuators. After this work describing various control methods like Negative Velocity Feedback Control, IMSC and MIMSC and other control methods have been reviewed and in the last research work on special problems in this area have been mentioned.

Richard Lane and Benjamin Craig [1] have given description of smart materials and their applications. A description regarding piezoelectricity, its subclasses, electrostriction, ER, MR fluids and SMA has been given. Flatau A.B. and Chong K.P. [2] have mentioned the importance of basic research in smart materials and structural systems and their development as a great potential for enhancing the functionality, serviceability and durability of civil and mechanical infrastructure systems and, as a result, offer the potential for significant contributions to the improvement of every nation's productivity, efficiency and quality of life. In support of this they have quoted some examples of NSF-funded projects and research needs as well as some initiatives.

Kevin Poulin and Rimas Vaicaitis [3] used ER Fluids and PZT actuators to control structural vibrations of stiffened composite panels subjected to random inputs. A collocated velocity feedback control mechanism is integrated using piezoelectric materials as sensors and actuators. They have used transfer matrix method and optimal control theory to determine the vibration response of the system.

Working with synthesis of intelligent structures with shape memory alloys Choi, S.B. and Hwang J.H. [4] worked on the sliding mode control for vibration control of a flexible structure with the dynamics of SMA. They have considered actuator dynamics for the first time in this kind of work. They experimentally

identified the dynamic behavior of SMA and employed in the equation of motion of a flexible structure.

New control algorithms that combine spillover suppression with semi-active modal vibration control via the use of magnetorheological (MR) dampers have been studied by Whalen *et al.* [5]. The advantages of this approach include the traditional positive attributes of MR dampers as well as more efficient use of the dampers obtained by targeting control effort at high-energy modes and preventing spillover. Strategies for this combined approach are compared with the existing algorithms that concentrate solely upon vibration control. Performance measure improvements have been found and discussed.

As stated earlier ER fluids have electrically controllable stiffness, viscosity and heat transfer properties. Since 1940s researchers are trying to model these properties for use in hydraulic valves, soft clutches and active suspension systems. Radcliffe *et al.* [6] presented a new approach to the control of ER fluids that overcome the problems of imprecise, slow, nonlinear response and high electric fields.

In their paper Cox and Lindner [7] have discussed the use of a modal domain optical fiber sensor (MD Sensor) as a component in an active control system to suppress vibrations in a flexible beam. An MD Sensor consists of a laser source, an optical fiber, and detection electronics. They have shown that the output of the MD Sensor is proportional to the integral of the axial strain along the optical fiber.

Jinsong *et al.* [8] used a FOS and ER fluid actuator for vibration monitoring of smart composite structures. They found same sensitivity in FOS as piezoelectric materials with lower cost. They found change in structural damping and natural frequencies with varying electric field and hence vibrations can be monitored by using FOS and ER fluid.

Nakra [9] proposed use of viscoelastic damping in vibration control over wide frequency band, but they observed dependence of viscoelastic materials on various factors like type of dynamic excitation, temperature and strain, etc. Some of the high polymers are known to exhibit viscoelastic behavior. Lio and Wang [10] used active constrained layer damping (ACLD) with active part of vibration control is supported by piezoelectric patches and passive part by viscoelastic materials. Galerkin - GHM (Golla - Hughes - McTavish) method is used to discretize and analyze the model in time domain. Similar kind of work has been done by Balamurugan and Narayanan

[11] with smart constrained layer damping (SCLD), in which a viscoelastic layer is sandwiched between two layers of piezoelectric actuators and sensors. This composite SCLD when bonded to a vibrating structure acts as a smart treatment. The sensor piezoelectric layer measures the vibration response of the structure and a feedback controller is provided which regulates the axial deformation of the piezoelectric actuator (constraining layer), thereby providing adjustable and significant damping in the structure. The damping offered by SCLD treatment has two components, active action and passive action. The active action is transmitted from the piezoelectric actuator to the host structure through the viscoelastic layer. The passive action is through the shear deformation in the viscoelastic layer.

The foregoing literature dealt with general work related to vibration control and smart materials. The literature based on finite element modeling of piezolaminated beam and its vibration control follows next.

Colla [12] presented work describing the basic knowledge required for AVC using Piezo-patches and description of actuators and sensors and smart materials has mentioned. Various control strategies like feedback control (FBC), feed forward control (FFC), has been mentioned in details. Piezoelectric constitutive equations, related terms and the limitations of piezoelectric materials have been mentioned.

Crawley and Luis [13] derived static and dynamic analytical models for segmented piezoelectric actuators that are either bonded to an elastic substructure or embedded in a laminated composite. They used various piezoelectric materials to find their effectiveness in transmitting strain to the substructure. They experimented with three types of beams – aluminum beam with surface bonded actuators, glass/epoxy beam with embedded actuators and a graphite/epoxy beam with embedded actuators. They found the piezoelectric materials either bonded or embedded are highly effective. They derived models of piezoelectric patches in this work.

Sze and Yao [14] prepared a number of finite element models for modelling of smart structures with segmented piezoelectric patches. These included eight-node solid shell element for modelling homogeneous and laminated host structures as well as an eight-node solid shell and a four-node piezoelectric membrane element for modelling surface bonded piezoelectric sensing and actuating patches. They studied number of problems with these models and found results agreeing with experimental results.

The location and dimensions of piezoelectric patches and their size make a lot of impact on the dynamic characteristics of the structure besides other factors like cost, control system complexity, etc. For simple structures it is easy to address these problems but as the elements and complexity of structure increases this problem also grows. Many researchers have been working on this issue. They used different analytical and experimental techniques to solve this problem.

Aldrainhem *et al.* [15] stated the optimal location of the actuator for a particular structure as the position at which the strain energy of the structure is the highest. They found one point of maximum strain energy in shape control while as the response in combination of several modes in vibration control, the highest strain energy locations at different points for different modes. They experimented with beams using various boundary conditions. They used double as well as single pair of actuators for comparing performances. Mota Silva *et al.* [16] addressed the problem of shape control and correction of small displacements in composite structures using piezoelectric actuators glued or embedded. They gave equal importance to formulation of an accurate mathematical model able to deal with shape control applications, and the determination of the optimal location of the piezoelectric actuators together with the optimal actuation voltages. They used Genetic Algorithms (GAs) as the optimisation technique and the optimisation function was defined, in terms of the surface error, by the square root of the deviation between the predefined shape and the achieved shape obtained when applying the optimum actuation voltages. Maximum errors of 15% were obtained between simulation/experimental results and the pre-defined curve.

Devasia *et al.* [17] considered the problem of simultaneous placement and sizing of distributed piezoelectric actuators to achieve the control objective of damping vibrations in a beam. They found the position and length of piezoelectric actuators to maximize modal damping with FBC. Beam considered was simply supported beam.

Schwinn and Janocha [18] built a very different aspect of Self-Configurable Actuator Sensor Array for Active Vibration Suppression. The usually applied method for the design of an active vibration control is to describe first the modal behavior of the structure and then to place the actuators and sensors according to an optimisation criterion. The new concept presented in this paper is to apply a number of piezoelectric ceramic patches onto a structure, without necessarily knowing the

structural behavior in advance. This system is able to identify itself with the help of the ceramic patches and the specific functionality of a patch as an actuator, a sensor or as inactive, is determined according to a performance index. Different actuator/sensor configurations for varying boundary conditions were studied, and the results are presented in this paper. Number of authors worked on this subject of optimisation with number of concepts, Frecker [19] done excellent work of summarizing all these concepts. He classified these concepts as Actuator Placement, Actuator Placement-Controller, Electronics, and Actuator-Structure.

A lot of works dealing with different control strategies like Negative Velocity FBC, IMSC, MIMSC, etc., have been carried out in the past. Trindade *et al.* [20] presented the design and analysis of the piezoelectric active control of damped sandwich beams. This was done using a specific finite element, able to handle sandwich beams with piezoelectric laminated surface layers and viscoelastic core. The control design and performance were then evaluated using three control algorithms applied to the reduced-order model, namely, Linear Quadratic Regulator (LQR), Linear Quadratic Gaussian (LQG) and Derivative Feedback. Derivative feedback controllers found less effective than an LQR one, but their well-known spillover destabilizing effects were attenuated by the increase of stability margins provided by the viscoelastic damping, while LQG controllers performed well as LQR ones.

Balamurugan and Narayanan [21] prepared finite element model based on Euler-Bernoulli beam theory to study AVC of beam with distributed sensor and actuator layers. They used three types of control strategies, namely direct proportional feedback, constant-gain negative velocity feedback and Lyapunov feedback and an optimal control strategy LQR to study control effectiveness. They used different types of loadings, such as impulse, step, harmonic and random. They developed sensor and actuator equations for the case of distributed sensor and actuator on cantilever beam, which were quoted later in this report. Narayanan and Balamurugan [22] used Timoshenko Beam Theory to model Plate and Shell and used Constant-gain Negative Velocity Feedback, Lyapunov feedback as well as a LQR approach, subjected to impact, harmonic and random excitations. They also considered influence of the pyroelectric effects on the vibration control performance. They found the LQR approach to be more effective in vibration control with lesser peak voltages applied in the piezo actuator layers. They highlighted the application of these elements in high performance, lightweight structural systems. Chen *et al.* [23] presented a finite

element formulation for vibration control and suppression of intelligent structures with a new piezoelectric plate element. On the basis of a negative velocity feedback control law, a general method of active vibration control and suppression for intelligent structures was put forth. Dynamic stability and the effect of vibration control for intelligent structures were investigated by introducing the state space equations of intelligent structures. The damped frequencies as well as the damping ratio were derived by state space analysis.

9 | There has been a lot of work on very effective control techniques like Independent Modal Space Control (IMSC) and Modified Independent Modal Space Control (MIMSC).

9 | Nguyen [24] quoted that IMSC method avoids control spillover generated by conventional control schemes such as Coupled Model Control (CMC) by decoupling the large flexible space structure into independent subsystems of second order and controlling each mode independently. The IMSC implementation requires the number of actuators be equal to modelled modes, which in general is very huge. He proposed two methods for the implementation of IMSC with reduced number of actuators. In the first method, first m modes are optimised, leaving last $(n-m)$ modes unchanged. In the second method, generalised inverse matrices are employed to design the feedback controller so that the control scheme is suboptimal with respect to IMSC. He simulated on Simply Supported Beam.

PI
9 | Baz, Poh and Fedor [25] studied on Independent Modal Space Control whose modal forces were generated by Positive Position Feedback (PPF) strategy, which is in contrast with negative velocity and position FBC. They found the model maintained the simplicity of IMSC and at the same time it utilises only the modal position signal to provide a damping action to undamped modes. The results were compared with those obtained from IMSC, PPF with second order filters, the Psuedo-Inverse (PI) and MIMSC. The proposed method found to be useful for VC of large flexible structures.

Wang and Huang [26] introduced a vibration control method for a flexible beam subjected to arbitrary, unmeasurable disturbance forces with IMSC. They chose the modal filters as the state estimator to obtain the modal coordinates and modal velocities for the modal space control. Because of the existence of the disturbance forces, applying only the state feedback to suppress the vibration usually cannot achieve the desired control performance hence they introduced modal space

feedforward control to cancel out the disturbance forces. The disturbance force observer as established to observe the disturbance modal forces for the feedforward control. The control gains were derived from the extended optimal control algorithm, where the disturbance modal forces were treated as exogenous state variables. By combining the feedback, feedforward control laws and the disturbance force observer together, the vibration control performances were discussed.

Kamath [27] gave a description of IMSC and the equations required for that purpose. He also has given the summary of actuators, sensors, FBC, Velocity FBC, Collocated vs. Non-Collocated, IMSC, LQR. He compared the results obtained by IMSC with Velocity FBC and Impedance Control. Singh *et al.* [28] presented general equations required for the problem formulation on IMSC as well as MIMSC. They recommended this method to be useful in flexible structures that were mostly useful in space activities. They described some efficient strategies for AVC of a beam structure using piezoelectric materials. The essence of the method proposed is that a feedback force in different modes be applied according to the vibration amplitude in the respective modes i.e., modes having lesser vibration may receive lesser feedback. This weighting may be done on the basis of either displacement or energy present in different modes. The method proposed is in fact an extension of the MIMSC with the addition that it proposes to use the sum of weighted multiple modal forces for control. They found from the analytical results that the maximum feedback control voltage required in the proposed method is further reduced as compared to existing methods of IMSC and MIMSC for similar vibration control. They also discussed limitations of the proposed method.

Baz, Poh and Studer [29] developed MIMSC method for designing AVC systems for large flexible structures. The method accounts for the interaction between controlled and residual modes. The MIMSC relies on an important feature that is based on 'time-sharing' of a small number of actuators, in the modal space, to control effectively a large number of modes. Generally flexible structures are controlled by their dominating modes, but these modes get controlled after some time, and residual modes get excited due to these control forces. IMSC method relies only on dominant modes but neglect effect of control forces on residual modes. MIMSC modifies IMSC to account for the spillover from the controlled modes into the uncontrolled modes. Working on MIMSC onwards Baz and Poh [30] used a beam with piezo-patches and compared the results obtained by MIMSC with IMSC and PI method. They found

MIMSC to be more useful for AVC of large flexible structures with small number of actuators.

Other control methods apart from the above mentioned ones have also been tried by the researchers. Kashani [31] worked on active damping of a flexible plate using LOR and LQG methods. He previously used collocated controllers i.e. actuation and sensing required at same location(s) which is not possible so then he used these methods to achieve better control. Clark and Bernstein [32] worked on LQG with FBC as well as FFC. They found hybrid control to be more advantageous due to advantages from both methods. They worked on TITO (two input – two output) system. In many contemporary engineering works traditional control methods can not be used either because the required actuators become too heavy for the application at hand or because the method itself can not cope with the circumstances of the applications, like space structures such as satellites. Salemi and Golnaraghi [33] worked on beam using Linear Coupling Control (LCC), by coupling a second order linear system to an oscillatory plant to create an energy exchange between the two components of the system.

The last phase of this literature survey contains the papers with some special work related to this topic. Generally the actuators are unimorph; that is, single piezoelectric layer is bonded to single elastic layer and bimorph, where one piezo-layer is attached at top and other at the bottom.

Sitti *et al.* [34] focused on the design, fabrication and characterisation of unimorph actuators for a microaerial flapping mechanism. PZT-5H and PZN-PT were investigated as piezoelectric layers in the unimorph actuators. Design issues for microaerial flapping actuators were discussed, and criteria for the optimal dimensions of actuators were determined. For low power consumption actuation, a square wave based electronic driving circuit was proposed. Yunfeng Li *et al.* [35] worked on Vibration Control of a PZT Actuated Suspension Dual-Stage Servo System using a PZT Sensor. They utilised as a vibration sensor to control both the voice coil motor (VCM) actuator butterfly mode and the suspension sway mode.

The important assumption, usually made by most of authors is the bonding between piezoelectric material and beam is perfect. But during operation as well as due to applied large voltages/ forces this assumption ceases after some time and debonding may take place during service life. Sun, Tong and Atluri [36] discussed effects of piezoelectric sensor/actuator debonding on vibration control of smart

beams. They took into account, both flexural and longitudinal displacements of the host beam and piezoelectric layer as well as the peel and shear strains of the adhesive layer. They used both, collocated and non-collocated control schemes to study effects of sensor and actuator debonding on AVC of smart beams. They found high peel stresses might be created around the periphery of an actuator layer causing debonding. They created a model of debonding on a beam and found the governing equations.

One of the most popular methods of modelling piezoelectric laminates, is via the modal analysis technique. In this approach the solution of the PDE, that governs the dynamics of the laminate, is assumed to consist of an infinite number of terms. In control design problems, one is often interested only in designing a controller for a particular frequency range. In these situations, it is common practice to remove the modes that correspond to frequencies that lie out of the bandwidth of interest and only keep the modes that directly contribute to the low-frequency dynamics of the system. Reza Moheimani [37] suggested a method of minimizing the effect of the removed higher order modes on the low-frequency dynamics of the truncated model of a piezoelectric laminate beam by adding a zero frequency term to the low-order model of the structure. He presented simulations and experimental results to support his ides.

Hybrid Vibration Control has advantages of both, AVC and PVC. Kang *et al.* [38] worked on interaction of active and passive vibration control of laminated composite beams with piezoceramic sensors/actuators. They used FEM for the analysis of laminated composite beams, and also considered damping and stiffness of adhesive and piezoceramic layers. They used velocity feedback control to carry out experiments. The finite element analysis was verified by comparing the experimental results in terms of active and passive damping ratios (ξ) and modal dampings ($2\xi\omega$) as well as fundamental frequency. They found, when the gain in velocity feedback control is small, the active control followed the trend of the passive control, but provided additional effects due to the active control; but for a large feedback gain, the active control is dominant over the passive control. Garga and Anderson [39] briefly reported the advances made in the area of vibration suppression via recently developed innovative techniques (for example, constrained layer damping (CLD) treatments) applied to civilian and military structures. They quoted some research projects related to themes such as developing and evaluating the performance of novel

active-passive hybrid smart structures for real-time vibration control; developing theoretical equations that govern the vibration of smart structural systems treated with piezomagnetic constrained layer damping (PMCLD) treatments; and developing innovative surface damping treatments using micro-cellular foams and active standoff constrained layer (ASCL) treatments.

2.1 CONCLUSIONS AND SCOPE FOR PROPOSED WORK

A critical study of literature reveals that Smart/Intelligent System often incorporate beam, plate or shell like flexible structures. A beam or beam like structure is very common in large flexible structures like, aircraft wings, helicopter blades and antenna. Many researchers have worked on beam, plate and shells as structural elements to study and control vibrations. They have used different models to model the beam like Euler-Bernoulli Model, Timoshenko beam theory, etc. It has found that location and size of piezoelectric patches matter a lot in dynamic characteristics of the beam. Various types of loadings have been used, viz. Impulse, Harmonic, Step and Random. Control techniques used by them are Negative Velocity Feedback Control, Independent Modal Space Control (IMSC), Modified Independent Modal Space Control (MIMSC), Positive Position Feedback (PPF) and Pseudo Inverse (PI) to control either vibrations or shape. Some authors worked only on Active Vibration Control (AVC) or Passive Vibration Control (PVC), while others highlighted the effectiveness of Hybrid Vibration Control (HVC) to take advantages of both techniques.

Work presented here deals with active vibration control (AVC) of a cantilever beam with piezoelectric patches used as both actuators and sensors. Finite element method (FEM) has been used to model the beam and Newmark method of direct numerical integration has been used to find transient responses by developing programmes using Matlab. When same polarity voltage is applied to piezo-patches, bonded on both sides of beam there is increase in stiffness of beam due to tensile force generated by patches. A new concept of using an increased axial stiffness of the beam due to applied voltage on patches has been attempted to control vibrations. Due to increase in stiffness, the natural frequencies of the beam increases, so one can actuate patches till the beam passes through original natural frequency resonance and later the patches can be de-activated so the beam can pass from increased natural frequency resonance.

CHAPTER 3

FEM OF A BEAM WITH PIEZOELECTRIC PATCHES

This chapter contains statement of the problem, description of Finite Element Model of a beam with piezo-patches, Transformation-Section Method necessary to calculate Young's Modulus and Moment of Inertia of a composite (sandwiched) beam, an introduction to Newmark Method to get transient responses, formation of global damping matrix using Rayleigh's (Proportional) Damping, concepts of modal displacement, modal velocity and mass normalised eigenvectors and their use in estimating vibration response.

The method used to formulate the problem is finite element method due to its ability to take into account effect of dimensions, material properties and the forces exerted by actuators or external forces in active vibration control of structure easier than analytical methods, as well as changes in the parameters can be made easily.

3.1 ASSUMPTIONS IN THE MODELLING

Following assumptions are made while formulating the finite element model of the beam.

- A. Bonding between patches and beam is assumed to be perfect. Validation of results largely depends on this assumption of the perfect bond. If the patches are rigid (like PZT), its length should be minimum for perfect bond.
- B. Bonding is assumed to be thin enough, not to alter the dynamic characteristics of the beam, significantly.
- C. Effect of temperature on Electrical and Mechanical properties of patches as well as beam is assumed to be negligible.
- D. The strain distribution is assumed to be linearly varying, across the thickness of the patches, though in real case it is uniform. Euler - Bernoulli beam model is considered (Figure 3.1).
- ✓ E. Moments are uniform throughout patch, but they are assumed to be applied at nodes (end points) only, this model is called as Pin-Force Model. *if load is applied at the patch what may happen?*
- F. Piezoelectric patch is assumed to be of pure uniaxial actuation case, i.e. $d_{31} \neq 0$, $d_{32} = 0$. The effective axis of piezo-layer is aligned with the length direction of the beam to ensure maximum piezoelectric force. *hollow beam
Circular x n beam }?*

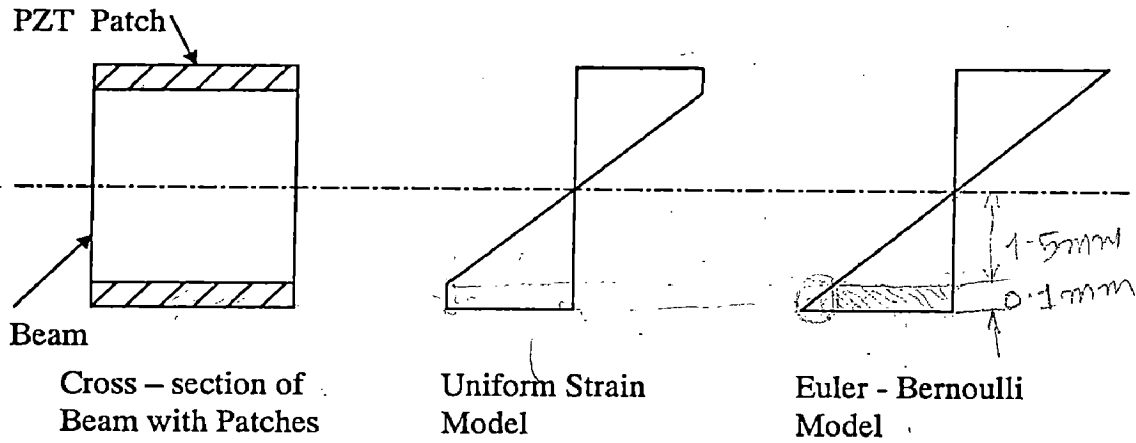


Figure 3.1 Uniform Strain Model and Euler – Bernoulli Model

3.2 STATEMENT OF THE PROBLEM

The sequence used to analyse the vibration response of beam with and without control is as given below:

1. Assembly of Global Matrices from Element Matrices and formation of Global Damping Matrix.
2. Eigenvalue and Eigenvector determination to calculate Natural Frequencies.
3. Free vibration response without control.
4. Free vibration response with negative velocity feedback control (Simple)
5. Free vibration response with negative velocity feedback control (Sensor and Actuator)
6. Free vibration response with Independent Modal Space Control (IMSC).
7. Free vibration response with Modified Independent Modal Space Control (MIMSC).
8. Forced vibration response without control.
9. Forced vibration response with negative velocity feedback control (simple).
10. Forced vibration response with negative velocity feedback control (Sensor and Actuator)
11. Forced vibration response with Independent Modal Space Control (IMSC).
12. Forced vibration response with Modified Independent Modal Space Control (MIMSC).
13. Vibration control using axial stiffness variation due to patch actuation.

3.3 FINITE ELEMENT MODEL OF BEAM WITH PATCHES

The dimension and material details of the cantilever beam and piezoelectric patches considered are as shown in Table 3.1 and model is shown in Figure 3.2.

Table 3.1 Descriptions of Beam and Piezoelectric Patches

Property	Beam	Piezoelectric Patches
Material	Steel C 35	PZT
Young's Modulus (GPa)	206	63
Mass Density (Kg / m ³)	8000	7600
Length (mm)	350	40
Width (mm)	30	20
Thickness (mm)	3.0	0.1
d_{31} (m/V)	-	200×10^{-12}
g_{31} (Vm/N)	-	0.01

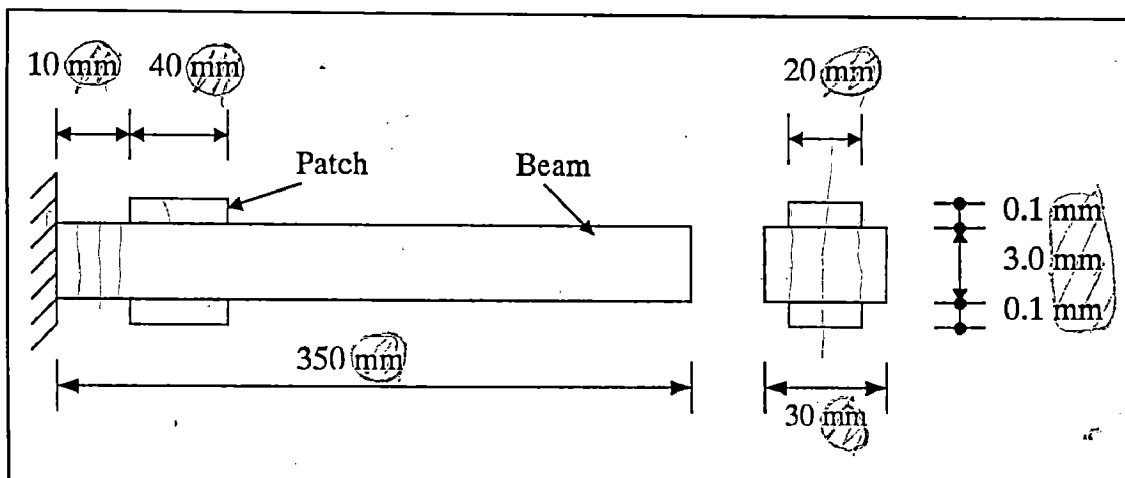


Figure 3.2 Cantilever Beam with Piezoelectric Patches

The number of Finite Elements considered in this problem is 12. For the case of beam considered here, one-dimensional element with two degree of freedom (DOF) system, that means, slope (u_2, u_4) and deflection (u_1, u_3) are taken into account at every node as shown in Figure 3.3.

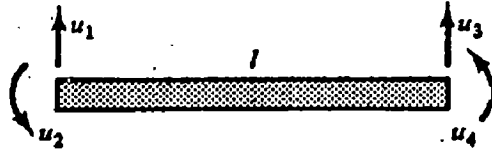


Figure 3.3 Beam under bending deformation

The element stiffness and element mass matrix for the beam with bending deformation [40] are given in Equations 3.1 and 3.2.

Element Stiffness Matrix

$$k_e = \frac{EI}{l^3} \begin{bmatrix} 12 & 6l & -12 & 6l \\ 6l & 4l^2 & -6l & 2l^2 \\ -12 & -6l & 12 & -6l \\ 6l & 2l^2 & -6l & 4l^2 \end{bmatrix} \quad (3.1)$$

Element Mass Matrix

$$m_e = \frac{\rho Al}{420} \begin{bmatrix} 156 & 22l & 54 & -13l \\ 22l & 4l^2 & 13l & -3l^2 \\ 54 & 13l & 156 & -22l \\ -13l & -3l^2 & -22l & 4l^2 \end{bmatrix} \quad (3.2)$$

The patches are applied on top and bottom of the beam at second element (Figure 3.2), starting the numbering of elements from root (fixed end). The details required in this element stiffness and element mass are length (l), Young's modulus (E), moment of inertia (I), mass density (ρ) and cross-sectional area (A) (Equations 3.1 and 3.2).

3.3.1 Beam Finite Element With Piezoelectric Patch

A beam with piezoelectric patches is a case of composite (sandwiched) beam, in which beam is sandwiched between two piezoelectric patches. The effective Young's Modulus is calculated by Transformation - Section Method [41]. The description of this method is as bellow:

Transformation - Section Method

In this method, the sandwiched or composite beam, made of two or more, different materials is virtually transformed into an equivalent beam made of single material for the purpose of bending and similar type of analysis. Figure 3.4 shows the original and transformed cross section of the beam.

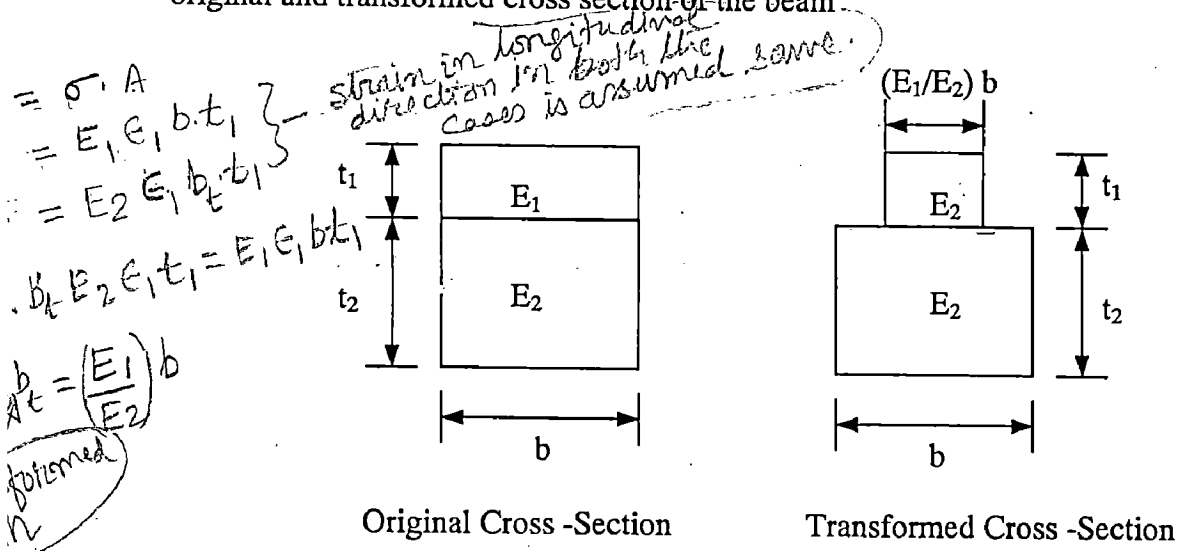


Figure 3.4 Transformation Section Method

The original beam is made of two different materials having modulus of elasticity E_1 and E_2 . The thickness of these materials is shown in Figure 3.4. Here the width of both is same, but it may be different.

In transformed section, the beam is virtually transformed to be made of only one material, either of first (E_1) or second (E_2). The Modular Ratio is getting multiplied to the width of the material to be transformed. When the transformed beam is to be made of first material, Modular Ratio (E_2/E_1) is multiplied to width of second material, and when the transformed beam is to be made of second material, Modular Ratio (E_1/E_2) is multiplied to width of first material. The Young's modulus to be taken into account is of transformed materials' Young's modulus, M.I. is of transformed section and cross-sectional area is of original cross-section. To calculate the mass density of patches element, original dimensions need to be taken into account.

Summarising,

$E = E$ of Transformed Section,

$A = A$ of Original Cross Section,

$I = I$ of Transformed Section,

$\rho = \rho$ of Original Cross Section.

For the model of the beam considered in this problem, the transformed section is as shown in Figure 3.5

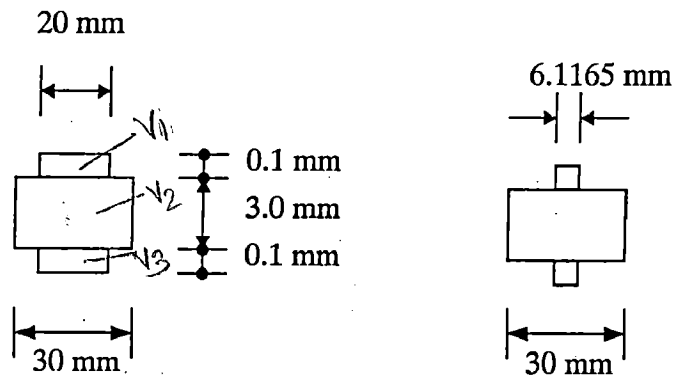


Figure 3.5 Transformed Section of Beam with Piezo-Patches

The mass density of the patched element is calculated by Equation 3.3.

$$\rho_c = \rho_{PZT} V_{PZT} + \rho_{Beam} V_{Beam} \quad (3.3)$$

Where, V_{PZT} = Volume Ratio of PZT material

= Volume of Patches / Total Volume of Patched Element

$$\frac{(V_1 + V_3)}{(V_1 + V_2 + V_3)}$$

The required properties of elements are tabulated in Table 3.2

Table 3.2 Properties of Beam Finite Elements

Property	First Element	Patched Element	Other Elements
Quantity	1	1	10
Length (mm)	10	40	30
A (mm ²)	90	94	90
E (GPa)	206	206	206
I (mm ⁴)	67.5×10^{-12}	70.4399×10^{-12}	67.5×10^{-12}
ρ (kg/m ³)	8000	7982.9787	8000

3.4 NATURAL FREQUENCIES OF BEAM

Resonance is said to occur when the excitation frequency matches any of the natural frequencies of the structure, so one should know the natural frequencies of the structure. Before determination of natural frequencies, one needs to form Global (Mass and Stiffness) Matrices from Element (Mass and Stiffness) Matrices, and then these Global Matrices are modified by putting boundary conditions of particular beam (structure). Boundary conditions for cantilever beam are the values of slope and deflection ^{which} are zero at fixed end. Corresponding rows and columns are deleted from

Global Stiffness Matrix and Global Mass Matrix, as well as Force Vector, Displacement Vector and others in Newmark Method. → 9

Then by using Matlab 5.3 Software the eigenvalues and eigenvectors are determined. Natural frequencies for the beam are calculated by taking square root of eigenvalues. Analytical formula [42] used to calculate first five natural frequencies of beam is given in Equation 3.4.

$$\omega_n = (r_i l)^2 \sqrt{\frac{EI}{mL^4}} \quad (3.4)$$

where,

m = mass per unit length

ω_n = Natural frequency in (rad/s)

L = Length of the beam

$r_i l$ = Constant

For cantilever beam $r_i l$ has values for first to fifth natural frequencies respectively as 1.875, 4.694, 7.855, 10.996, and 14.137 [42].

3.4.1 Formation Of Global Mass And Stiffness Matrix

The global matrices are formed by placing corresponding components of element matrices at the corresponding nodes. If m^{th} element is to be assembled, then it has 4×4 size element matrix, and nodes are m and $m+1$. The components of this matrix are placed from $2m-1$ to $2m+2$ places of global matrices, as each node has 2 DOF (Refer Figure 3.6).

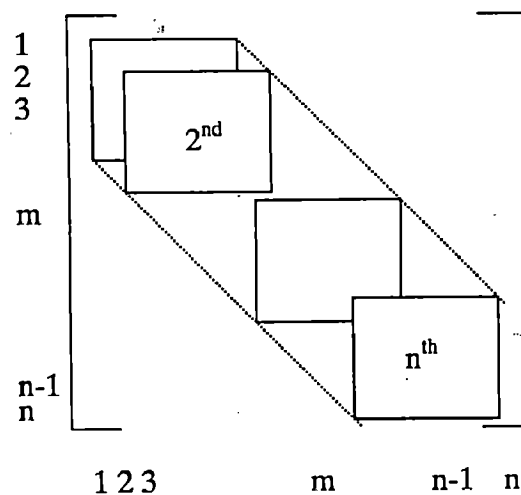


Figure 3.6 Global matrix assembly from element matrices

The results obtained from Matlab 5.3 and from Equation 3.4 are tabulated in Tables 3.3 and 3.4. For the problem considered here,

- Number of Finite Elements = 12
- Number of nodes = 13
- Degrees of Freedom (DOF) = 2 / Node
- Total Number of DOF = 26 (without B.C.)
- = 24 (with B.C.)

As number of DOF is 24, hence the beam has 24 natural frequencies. Size of global matrices is 24 x 24.

Table 3.3 Natural Frequencies of Beam with and without patches

Sr No	Natural Frequency (Hz) Matlab		Difference (%)
	with Patch	without Patch	
1	20.226	(1.051 + 18.975)	6.5929
2	126.260	(7.340) + 118.920	6.1722
3	352.760	19.750 + 333.010	5.9308
4	690.600	652.790	5.7921
5	1142.100	1079.900	5.7598
6	1709.600	1615.600	5.8183
7	2397.700	2262.000	5.9991
8	3213.600	3022.300	6.3296
9	4165.700	3901.100	6.7827
10	5261.400	4902.100	7.3295
11	6498.700	6020.700	7.9393
12	7820.700	7173.900	9.0160
13	9636.500	9208.500	4.6479
14	11367.000	10765.000	5.5922
15	13349.000	12653.000	5.5007
16	15652.000	14829.000	5.5499
17	18365.000	17321.000	6.0274
18	21555.000	20168.000	6.8772
19	25257.000	23401.000	7.9313
20	29413.000	27015.000	8.8766
21	33731.000	30897.000	9.1724
22	37426.000	34719.000	7.7969
23	46533.000	37778.000	23.1749
24	55055.000	46533.000	18.3139

0.226
8.975
1.051

define

?

Table 3.4 Natural Frequencies as ^{compared to} ~~comparison with~~ Analytical Results ^{define}

Sr No	Natural Frequency with Patch (Hz)		Difference (%)	Natural Frequency without Patch (Hz)		Difference (%)
	Matlab	Analytical		Matlab	Analytical	
1	20.226	20.024	0.9987	18.975	19.073	0.5138
2	126.260	125.500	0.6019	118.920	119.800	0.7346
3	352.760	351.440	0.3742	333.010	335.290	0.2962
4	690.600	688.700	0.2751	652.790	658.360	0.8460
5	1142.100	1138.300	0.3327	1079.900	1090.120	0.9375

As the number of finite elements increased, the results obtained by Matlab get closer to experimental/analytical results, but computational time increases a little bit. The difference is very less with analytical result (< 1 %), so FEM and Matlab ^{are} used for subsequent analysis.

3.5 FORMATION OF GLOBAL DAMPING MATRIX

Estimating the damping matrix for the physical system is not an easy task. There is no Element Damping Matrix concept, and damping needs to be considered in the global matrix form only. ^{many} ~~A lot of types~~ of models are available to model the damping, but most favored are proportional damping models in which damping is assumed to be some percent of either global stiffness matrix or global mass matrix or both (Rayleigh's Proportional Damping).

Rayleigh's (Proportional) damping matrix has an advantage of possessing the same characteristics as mass and stiffness matrix.

In this method, the values of first two natural frequencies and damping ratios are put in Equation 3.5 (where, $i = 1, 2$) and the global damping matrix will ^{be obtained} get from Equation 3.6. [40]

$$p + q\omega_i^2 = 2\xi_i\omega_i \quad (3.5)$$

$$[C] = p[M] + q[K] \quad (3.6)$$

From results,

$$\omega_1 = 127.083 \text{ rad/s}$$

$$\omega_2 = 793.304 \text{ rad/s} \quad \text{0 to 5\%} \quad (3.7)$$

The damping ratios are 0.01 to 0.03 for Mechanical Engineering structures. It is

^{taken here} $\xi_1 = 0.01$ and $\xi_2 = 0.03$ (3.8)

Why only 1st and 2nd lateral displacement are considered?

Putting corresponding values from Equations (3.7) and (3.8) in Equation (3.5)

$$\begin{aligned} p &= 1.3550 \\ q &= 7.3480 \times 10^{-5} \end{aligned} \quad (3.9)$$

By putting these values in Equation 3.6, global damping matrix is

$$[C] = 1.3550 [M] + 7.3480 \times 10^{-5} [K] \quad (3.10)$$

3.6 NEWMARK METHOD

Newmark method has been preferred to determine the transient free/forced vibration response of a structure (beam), which falls under the category of direct numerical integration method and has the advantage of definite stability [43]. This is also called as Newmark- β or β -Newmark method.

The procedure for this method is as below, before going for actual iterations, some initial calculations are necessary which are constant for particular application, and does not change for every iteration step.

A. Initial Calculations

1. Form Global Stiffness Matrix (K), Global Mass Matrix (M) and Global Damping Matrix (C).
2. Initialize \ddot{u} , \dot{u} , u at time $t = 0$ (generally the acceleration, and velocity are taken as zero and some displacement is given to the beam).
3. Select time step Δt and parameters α and δ and calculate integration constants,

$$\delta \geq 0.50 \quad \text{and} \quad \alpha \geq 0.25(0.5 + \delta)^2 \quad (3.11)$$

$$a_0 = \frac{1}{\alpha \Delta t^2}$$

$$a_1 = \frac{\delta}{\alpha \Delta t}$$

$$a_2 = \frac{1}{\alpha \Delta t}$$

$$a_3 = \frac{1}{2\alpha} - 1$$

$$a_4 = \frac{\delta}{\alpha} - 1$$

$$a_5 = \frac{\Delta t}{2} \left(\frac{\delta}{\alpha} - 2 \right)$$

$$a_6 = \Delta t (1 - \delta)$$

$$a_7 = \delta \Delta t \quad (3.12)$$

4. Form Effective Stiffness Matrix \hat{K}

$$\hat{K} = K + a_0 M + a_1 C \quad (3.13)$$

Now following equations 3.14 to 3.16 need for each iteration step.

B. For Each Time Step

1. Calculate effective loads at time $t + \Delta t$ as

$$\hat{R}_{t+\Delta t} = R_{t+\Delta t} + M(a_0 u_t + a_2 \dot{u}_t + a_3 \ddot{u}_t) + C(a_1 u_t + a_4 \dot{u}_t + a_5 \ddot{u}_t) \quad (3.14)$$

2. Solve for displacement at time $t + \Delta t$

$$\hat{K} u_{t+\Delta t} = \hat{R}_{t+\Delta t} \quad (3.15)$$

3. Calculate accelerations and velocities at time $t + \Delta t$ as

$$\begin{aligned} \ddot{u}_{t+\Delta t} &= a_0 (u_{t+\Delta t} - u_t) - a_2 (\dot{u}_t) - a_3 (\ddot{u}_t) \\ \dot{u}_{t+\Delta t} &= \dot{u}_t + a_6 (\ddot{u}_t) + a_7 (\ddot{u}_{t+\Delta t}) \end{aligned} \quad (3.16)$$

3.6.1 Selection Of Time Step, Δt

Lowest Natural Frequency = 20.226 Hz

Time Period = $1/20.226 = 0.049$ sec

Thus, the actual free vibration completes one cycle in 0.049 sec, so the time period of sampling wave should be at least 10 times smaller than this, i.e. 0.005 sec. For the case of Modified Independent Modal Space Control, the aim is to control at least first 6 modes. Time step used here is less than 50% of time period of sixth natural frequency.

Sixth natural frequency = 1709.6 Hz

Time period = $1/1709.6 = 0.000585$ sec

Time Step = Time Period / 2 = 0.0002925 sec

Let $\delta = 0.50$, $\alpha = 0.25$ (stability requirement of the integration scheme) and calculate constants a_0 to a_7 from Equation 3.12.

$$\begin{aligned} \Delta t &= 0.005 \text{ sec (For Vibration analysis, except MIMSC)} \\ &= 0.00025 \text{ sec (for MIMSC)} \end{aligned} \quad (3.17)$$

3.6.2 Determination Of Constants

For Vibration Analysis (Except MIMSC)

$\Delta t = 0.005$ sec, hence from equations 3.12,

$$\begin{aligned} a_0 &= 1.6 \times 10^5 & a_1 &= 400 & a_2 &= 800 \\ a_3 &= 1 & a_4 &= 1 & a_5 &= 0 \\ a_6 &= 2.5 \times 10^{-3} & a_7 &= 2.5 \times 10^{-3} \end{aligned} \quad (3.18)$$

For MIMSC

$\Delta t = 0.00025$, hence from equations 3.12,

$$\begin{aligned} a_0 &= 6.4 \times 10^7 & a_1 &= 8000 & a_2 &= 16000 \\ a_3 &= 1 & a_4 &= 1 & a_5 &= 0 \\ a_6 &= 1.25 \times 10^{-4} & a_7 &= 1.25 \times 10^{-4} & & \end{aligned} \quad (3.19)$$

3.7 MASS NORMALISED MODE SHAPE VECTOR

U = Matrix of Eigenvectors = Mode Shape Matrix

$$= [\phi_1 \quad \phi_2 \quad \dots \quad \dots \quad \dots \quad \dots \quad \phi_n] \quad (3.20)$$

ϕ_i = Eigenvector corresponding to i^{th} Natural Frequency (Eigenvalue)

$M_G = U^T M U$ = Generalised Mass Matrix = Diagonal ($M_{11} \ M_{22} \dots \ M_{nn}$)

$K_G = U^T K U$ = Generalised Stiffness Matrix

$C_G = U^T C U$ = Generalised Damping Matrix

When each column of eigenvector matrix is divided by corresponding generalised mass matrix element's square root, it is called as Mass Normalised Eigenvector Matrix.

$$\phi = \left[\frac{\phi_1}{\sqrt{M_{11}}} \quad \frac{\phi_2}{\sqrt{M_{22}}} \quad \dots \quad \dots \quad \dots \quad \frac{\phi_n}{\sqrt{M_{nn}}} \right] \quad (3.21)$$

3.8 MODAL DISPLACEMENT AND MODAL VELOCITY

Modal displacement and velocity are hypothetical quantities, useful to analyse the vibration behavior of a Multi-DOF system in easier manner. Let us assume the physical displacements of various nodes are arranged in a vector 'x' for any system, then,

$$x = \phi \delta \quad (3.22)$$

Where,

x = Global Displacement Vector

ϕ = Mass Normalised Eigenvector Matrix

δ = Modal Displacement Vector

In this similar manner differentiation of above equation with time gives Modal Velocity.

3.9 AXIAL FORCE DUE TO PATCH ACTUATION

Consider a beam with piezoelectric patches applied on both sides of the beam. When same polarity voltage is applied to patches, there is change in length of the beam due to axial forces (either tensile or compressive), but if opposite polarity voltage applied to both patches the beam bends in the similar manner as bimetallic strip. When axial tensile force is applied to the beam, its stiffness increases, and for axial compressive forces its stiffness decreases.

Explain

The formulae [44] useful for calculation of axial forces are as below:

Free strain in actuator due to application of voltage (Figure 3.2) is

$$\varepsilon_p = d_{31} \frac{V}{t_a} \quad (3.23)$$

The strain in the structure (beam), when piezo-patch is bonded to the beam and only voltage is applied to patch and no external loading.

$$\varepsilon_s = \frac{2E_a \varepsilon_p t_a}{2E_a t_a + E_s t_s} \quad (3.24)$$

Stress in the beam,

$$\sigma_s = \varepsilon_s E_s \quad (3.25)$$

Force (Axial) in the beam, due to piezoelectric patch actuation

$$F_s = \sigma_s A_s \quad (3.26)$$

Stress in the actuator

$$\sigma_a = -E_a (\varepsilon_s - \varepsilon_p) \quad (3.27)$$

Where,

ε_p = Free Strain in Piezo-Patch (without Constrain)

ε_s = Strain in beam (Host Structure)

E_a = Actuator (Piezo-Patch Modulus of Elasticity)

E_s = Beam (Host Structure Modulus of Elasticity)

t_a = Thickness of Actuator

t_s = Thickness of Beam (Host Structure)

σ_s = Stress in Beam

σ_a = Stress in Actuator

F_s = Force in Beam

A_s = Cross-section of beam

3.9.1 Calculation Of Change In Stiffness Due To Axial Force

The axial force is induced on account of same polarity voltage to two collocated piezoelectric patches, one on either side of the beam (Figure 3.1). The stiffness matrix due to external axial force [45], to be added to the corresponding Element Stiffness Matrix (where Piezoelectric patch is present) can be ^{obtained} getting from Equation 3.28.

$$k_P = \frac{F_s}{30l} \begin{bmatrix} 36 & 3l & -36 & 3l \\ 3l & 4l^2 & -3l & -l^2 \\ -36 & -3l & 36 & -3l \\ 3l & l^2 & -3l & 4l^2 \end{bmatrix} \quad (3.28)$$

This matrix is to be added at the corresponding element stiffness matrix of the element on which patches are applied.

3.10 SUMMARY

This chapter introduced all the formulae and finite element method concepts, necessary for the work of active vibration control of a piezo beam.

The element considered for this case of a beam is of two-dof element, among three types [40], viz. one-dof (only axial deflection), two-dof (slope and vertical deflection) and three-dof (slope, vertical and axial deflection). The Newmark- β method is very useful method to analyse and get the vibration response while other method is Wilson- θ method [43]. Transformation section method becomes useful to convert composite beam element in simple beam element. From results of natural frequency, it is clear that the error is very less (< 1%) between analytical and FEM results, and the error reduces with increased number of elements, so FEM is used for subsequent transient analysis.

CHAPTER 4

FREE AND FORCED VIBRATION: WITH AND WITHOUT CONTROL

This chapter is divided into three major topics

1. Free vibration response with and without active control,
2. Forced vibration response with and without active control,
3. Vibration control during sweeping excitation using controlled axial stiffness variation.

Before discussing the actual work, some description of the three control methods used is necessary, which is briefed in the coming sections.

4.1 NEGATIVE VELOCITY FEEDBACK CONTROL

When a voltage is applied to a piezoelectric patch, there is change in the dimensions of the patch and if only one side patch is used as actuator then this patch as well as beam bends. The moments applied by patch are directly co-related with voltage applied to it. These moments are assumed to be applied at the ends of patch (nodes) (Pin Force Model). This report contains two approaches for negative velocity feedback control method; in the first one, piezoelectric patches are not modelled in Newmark Method in terms of voltages, moments. Instead, a simple mathematical modelling of control process is attempted, while in the second approach, patches are modelled to sense rotational displacement of the beam, voltage corresponding to these is multiplied by some gain, and the resultant voltage is applied to actuators. The actuators apply opposite types of moments on the beam to control/reduce vibrations.

The mathematical model behind this is given by Equation 4.1.

The governing equation for a forced damped vibration response is

$$m\ddot{x} + kx + c\dot{x} = F \quad (4.1)$$

In forced damped vibration equation with Negative Velocity FBC, term $-G\dot{x}$ is added as an additional forcing term. When this term is transferred to LHS, then it can be seen that the damping of the system increases by G as in Equations 4.2 and 4.3.

↑
define

in where you will get the defined force the system?

define:

$$m\ddot{x} + kx + c\dot{x} = F - G\dot{x} \quad (4.2)$$

$$m\ddot{x} + kx + (c + G)\dot{x} = F \quad (4.3)$$

The approach here used is **Negative Velocity, Constant Gain FBC**. In which,

$$\text{Feedback Force} = -G\dot{x} \quad (4.4)$$

Where, **Gain, G is constant** and only velocity term varies.

Another approach is **Negative Velocity, Constant Amplitude FBC**. In this approach, feedback force is constant in magnitude only its direction changes.

$$\text{Feedback Force} = -G \text{sign}(\dot{x}) \quad (4.5)$$

Where, function $\text{sign}(\dot{x})$ works as,

$$\text{sign}(A) = \begin{cases} -1 & \text{if } A < 0 \\ 0 & \text{if } A = 0 \\ 1 & \text{if } A > 0 \end{cases} \quad (4.6)$$

4.1.1 Negative Velocity Feedback Control (Simple)

As stated earlier, in this method only simple mathematical modelling of the control process is done assuming that, the patches are doing their work of sensor and actuator as designed. The effective force term in Newmark Method (Equation 3.14) is modified accordingly.

At every iteration step, a feedback force $-G\dot{x}$ is added to the effective force. Hence the effective force is reduced so as the displacement.

4.1.2 Negative Velocity Feedback Control (Sensor And Actuator)

In this approach, the sensors are modelled to sense rotational (angular) displacements, while some gain is applied by control systems, producing resultant voltage to be applied to the actuators, which in turn applies moments on the beam [21,22].

The sensor voltage is given by Equation 4.7 [21,22].

$$V_s = -\frac{t_{patch}}{l_{patch}} g_{31} E_{patch} \left[\frac{1}{2} (t_{beam} + t_{patch}) \right] (\theta_y - \theta_{y-1}) \quad (4.7)$$

The actuator voltage is obtained by differentiating the sensor voltage and multiplying it by appropriate gain as in Equation 4.8 [21,22].

$$V_A = -G\dot{V}_s \quad (4.8)$$

which is $f(\dot{x})$ in (4.7)?

The moment applied by actuator are given by Equation 4.9 [21,22].

$$M_A = \left[\frac{1}{2} (t_{beam} + t_{patch}) \right] E_{patch} d_{31} b_{patch} V_A \quad (4.9)$$

Where,

V_S = Sensor Voltage (V)

V_A = Actuator Voltage (V)

θ_y = Rotational (Angular) Displacement at node y

M_A = Moment applied by the Actuator

4.2 INDEPENDENT MODAL SPACE CONTROL (IMSC)

Literature review reveals that Meirovitch and Baruh first put forth this concept in a well-planned manner [28], while Baz and Poh [25,29,30] put forth concept of MIMSC. Meirovitch and Baruh developed the IMSC method for controlling vibrations of a distributed mass body. They showed that, IMSC has advantages over traditional coupled mode technique in that it offers a larger choice of control techniques, including non-linear control, requires less computer storage, and needs far less computational effort, etc. In this method feedback control parameters, which are displacement and velocity gains, are selected as modal gains.

The formulae and steps for IMSC are as below [24,25,27,28].

Optimal Positional Gain and Optimal Velocity Gain are given by Equations

A.10 ~~4.11~~ and ~~4.12~~^{A.11}, respectively.

$$g_p = -\omega_r R + \sqrt{(\omega_r R)^2 + \omega_r^2 R} \quad (4.10)$$

$$g_v = \sqrt{2\omega_r R(-\omega_r R + \sqrt{(\omega_r R)^2 + \omega_r^2 R}) + \omega_r^2 R} \quad (4.11)$$

The piezo-location vector (D), which is necessary to give the location of the piezo-forces, is given by Equation 4.12. If the patch is bonded at the element having DOF as m to m+3, then only that elements in piezo-location vector need to be modified, so m:m+3 used in following equation.

$$D(m:m+3) = \frac{1}{2} b d_{31} E_{Patch} (t_{Beam} + t_{Patch}) \begin{bmatrix} 0 \\ 1 \\ 0 \\ -1 \end{bmatrix} \quad (4.12)$$

Modal force, voltage and control force are given by Equations 4.13 to 4.15, respectively.

$$F_{Modal} = \frac{-(g_p \omega_r \delta + g_v \dot{\delta})}{R} \quad (4.13)$$

at is F_m ?

$$Voltage = \frac{F_m}{U_N D} \quad (4.14)$$

plain?

$$F_{Control} = Voltage * D \quad (4.15)$$

Where where,

ω_r = Natural Frequency corresponding to the mode to be controlled.

R = Weighting Factor

g_p = Optimum Positional Gain

g_v = Optimum Velocity Gain

explain

δ = Modal Displacement

$\dot{\delta}$ = Modal Velocity

D = Piezo-location Vector

U = Matrix of Eigenvector

U_N = Matrix of Mass Normalised Eigenvector

F_{Modal} = Modal Force Vector

Voltage = Voltage to be applied at patch

$F_{Control}$ = Control Force Vector

b = width of the patch

→

4.2.1 Weighting Factor, R

← How do you get R?

R is the Weighting Factor that balances the reduction of the vibrational energy with respect to the control voltage required. The value of 'R' ranges from 1 to 1000.

From the above definition it is clear that R is actually a factor that balances vibrational energy and control energy during active vibration control of the structure. As value of 'R' increased, control force gets reduced, causing reduced damping and increased vibrations.

4.3 MODIFIED INDEPENDENT MODAL SPACE CONTROL (MIMSC)

Baz and Poh [25,29,30] modified the IMSC method to MIMSC to control different modes of vibrations of distributed structures separately depending on the energy in each mode given by $\omega^2\delta^2 + \dot{\delta}^2$.

In IMSC it is assumed that control forces will not excite residual higher order modes i.e. there is no control spillover from controlled modes to uncontrolled modes. But in practical situation, the spillover is present causing uncontrolled modes to get excited due to controlling forces.

MIMSC incorporates an extremely important feature, based on time-sharing of a small number of actuators in modal space to control a large number of modes. In practice there are two types of time-sharing strategies applied, description is given in Section 4.3.1.

4.3.1 Time Sharing Strategies

A. Sequential time sharing strategy

In this method, control forces are computed, at the first time interval, to control 1st to cth modes using C actuators. Then at the second time interval 2nd to (c+1)th modes controlled, and so on. Once all modes received their share of control this cycle is repeated again.

This strategy is useful in Vibration Control of large structures with relatively less number of actuators, when IMSC fails to do so.

B. Modal energy strategy

Better vibration control can be achieved when the time-sharing is based on modal energy strategy, particularly when the number of controlled modes is very small as compared to the number of uncontrolled modes. In this strategy, energy present in each mode ($\omega^2\delta^2 + \dot{\delta}^2$) is checked at specific intervals of time and the mode with the highest energy is controlled.

Time-sharing concept should be considered carefully in conjunction with the dynamic characteristics of actuators. If one actuator is used to control several modes of vibrations then its frequency band should be wide enough to cover desired controlled modes. In general practice, one actuator is dedicated to control low-frequency modes, another medium-frequency modes, while high-frequency modes can be damped quite easily and more effectively with passive damping methods.

4.4 FREE VIBRATION RESPONSE

What are these in Eq. 3.14

34 For free vibration, the external force term is absent in Newmark Method in Equation 3.14. The vibration is induced by an initial displacement excitation (preferably applied at the free end of the beam). To achieve this, a force of some value is applied at the tip, the displacement values got from this are taken as initial displacement vector and the force is removed and let the beam to vibrate freely.

The flowchart for this is given in Appendix A (Refer Flowchart 1).

The external force term as well as control force term is obviously not accounted for the free vibration response using Newmark Method. The values of displacement, velocity and acceleration as well as effective force are extracted at the end of each iteration step and stored in separate variables to plot corresponding graphs.

First calculating logarithmic decrement from the vibration response and then using the relation between logarithmic decrement and damping ratio, the damping ratio can be calculated (Equation 4.16).

$$\delta = \frac{2\pi\xi}{\sqrt{1-\xi^2}} = \frac{1}{(n-1)} \log_e \left(\frac{x_1}{x_n} \right) \quad (4.16)$$

Where,

x_1 = Amplitude at first cycle

x_n = Amplitude at n^{th} cycle

δ = Logarithmic Decrement

ξ = Damping Ratio

n = Number of Cycles considered to calculate Damping Ratio.

The vibration response by various control techniques can be compared based on the damping ratio or based on settling time, which is the time required for the vibration response to fall within a prescribed band (0.05 to 0.1 % of the maximum amplitude of free vibration without control). This band is also called Threshold Value.

4.4.1 Free Damped Vibration: Negative Velocity Feedback Control (Simple)

As stated earlier in this method, only mathematical force term is added as a control force. In Newmark Method, at the end of each iteration step, one will get values of displacement, velocity and acceleration at the tip of the beam. The rotational velocity values will be taken for the element corresponding to piezo-patch and these

values multiplied by Gain will give the control force (moments) that need to be applied on the beam. These control force term is getting added to the effective force term in Newmark Method and the cycle goes on.

The values of displacement, velocity, acceleration, effective force as well as control force at patch are extracted at the end of each iteration step and stored in separate variables to plot corresponding graphs (Refer Flowchart 2).

4.4.2 Free Damped Vibration: Negative Velocity FBC (Sensor And Actuator)

In this method the piezo-patches actually modelled to sense the rotational velocities and then these values are multiplied with Gain to give the voltage to be applied to piezo-actuator, which in turn applies moments on the beam.

The values of displacement, velocity, acceleration, effective force as well as control force at the patch, sensor voltage and actuator voltage are extracted at the end of each iteration step and stored in separate variables to plot corresponding graphs (Refer Flowchart 3).

4.4.3 Free Damped Vibration: IMSC

In this problem first mode (corresponding to lowest natural frequency) has been controlled. Values of optimal positional gain and optimal velocity gain are calculated based on this lowest natural frequency and Weighting Factor (R). Mass Normalised Eigenvector is also calculated using standard functions available in Matlab 5.3 to calculate eigenvectors and using Equations 3.20 and 3.21.

In Newmark Method, at each iteration step, the modal displacement and modal velocity are calculated and then modal force, voltage, control force is calculated from equations 4.13 to 4.15. This control force term is added to the effective force term in the Newmark Method (Equation 3.14). The values of displacement, velocity, acceleration, effective force, control force at patch and voltage are extracted at the end of each iteration step and stored in separate variables to plot corresponding graphs (Refer Flowchart 4).

4.4.4 Free Damped Vibration: MIMSC

Modal Energy Strategy has been used as a time-sharing strategy to find the mode with highest modal energy, at specific intervals (20 iterations = 5×10^{-3} sec) and to control that mode with highest modal energy. The IMSC method is modified as the

values of optimal positional gain and optimal velocity gain has to be calculated based on the natural frequency corresponding to the dominating mode and Weighting Factor (R) at each iteration of Newmark Method. Other procedure is similar to IMSC. So equations 4.10 to 4.15 needed at each iteration step. The values of displacement, velocity, acceleration, effective force, control force at patch and voltage are extracted at the end of each iteration step and stored in separate variables to plot graphs (Refer Flowchart 5).

4.5 FORCED VIBRATION RESPONSE

For Free Vibration the external force term is absent in Newmark Method (Equation 3.14) while for forced vibration term, this term is present. Depending on the type of the force to be applied this term can be modelled in the Newmark Method. For harmonic input, $f_0 \sin(\omega t)$ is used, while this term is modified for the case of sweeping excitation as $\omega = \omega_0 + \alpha \Delta t$. The impulse force input is given by a force for very short duration e.g. 1 ms, while for Step input this term is modified by applying force for some considerable time duration. The flowchart for harmonic input is given in Appendix A (Refer Flowchart 6).

The values of displacement, velocity and acceleration as well as effective force are extracted at the end of each iteration step and stored in separate variables to plot graphs. Comparison among results by various control techniques cannot be done by settling time, damping ratio as in case of free vibration, but steady state amplitude, maximum amplitude are used to compare results.

4.5.1 Forced Damped Vibration: Negative Velocity Feedback Control (Simple)

The difference between this method and as applied to free vibration (Section 4.4.1) is that, the external force term is added to the effective force term in Newmark Method and beside all variables stored in free vibration case (4.4.1), external force is also extracted at the end of each cycle (Refer Flowchart 7).

4.5.2 Forced Damped Vibration: Negative Velocity FBC (Sensor And Actuator)

The difference between this method applied to forced vibration case and that applied to free vibration (Section 4.4.2) is that, the external force term is added to the effective force term in Newmark Method and beside all variables stored in free

vibration case (4.4.1), external force is also extracted at the end of each cycle (Refer Flowchart 8).

4.5.3 Forced Damped Vibration: IMSC

As previous method, the difference between this method and as applied to free vibration (Section 4.4.3) is that, the external force term is added to the effective force term in Newmark Method and beside all variables stored in free vibration case (4.4.3), external force is also extracted at the end of each cycle (Refer Flowchart 9).

How? Explain

4.5.4 Forced Damped Vibration: MIMSC

As previous method, the difference between this method and as applied to free vibration (Section 4.4.4) is that, the external force term is added to the effective force term in Newmark Method and beside all variables stored in free vibration case (4.4.4), external force is also extracted at the end of each cycle (Refer Flowchart 10).

4.6 VIBRATION CONTROL USING CONTROLLED AXIAL STIFFNESS VARIATION

In section 3.9, description of axial stiffness variation, due to actuation of piezo-patches has been given. This concept can be used to control vibration i.e. to reduce the amplitude of forced vibration. If tensile force is exerted on the beam, by using patches, then the stiffness of the beam increases, causing increase in the natural frequency of the beam.

Explain physically how this happens?

Suppose, a beam is required to vibrate with varying frequency like ramp input, in which case the excitation frequency varies from zero to some definite frequency. In such a case the resonance may occur at which, the excitation frequency matches natural frequency. This concept can be used as, let the beam vibrate with increased natural frequency till the first resonance (i.e. resonance with normal natural frequency) will pass. Then again deactivate the patches so that the beam will have original natural frequency and the second resonance i.e. resonance with increased natural frequency will also pass. This will cause the reduction in the maximum amplitude of vibration (Figure 4.1). Parameters of the beam used for this model are as below in Table 4.1, an Aluminum beam with PZT patches is considered here.

Explain?

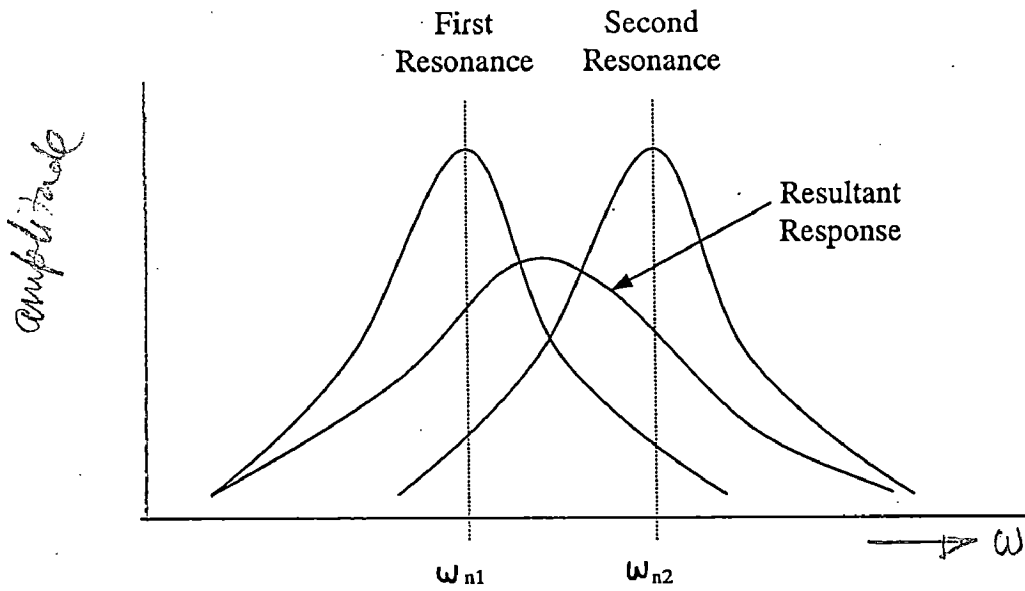


Figure 4.1 Effect of Axial Stiffness Variation on Vibration Response

Table 4.1 Properties of Beam and Patches

Property	Beam	Piezoelectric Patches
Material	Aluminum	PZT
E (GPa)	70	63
ρ (kg/m ³)	2700	7600
Length (cm)	25	8.5
Width (cm)	3	2
Thickness (cm)	0.2	0.03
d_{31} (m/V)	-	210×10^{-12}

With this configuration the natural frequency results are

$$\text{Natural Frequency without Axial Stiffness} = 31.856 \text{ Hz}$$

$$\text{Natural Frequency with Axial Stiffness} = 36.260 \text{ Hz} \quad (4.17)$$

Now the voltage that could be applied on the patch has ranges specified by the manufacturer. The patches used by National Instrumentation have limitation on voltage as -500 V to +1500 V. So applying -500 V on the patches, and using

$$\xi_1 = 0.01, \xi_2 = 0.03, \Delta t = 0.003 \text{ sec and}$$

$$\omega = \omega_0 + \alpha \Delta t \quad (\omega_0 = 0, \alpha = (50-0)/\text{Iterations}).$$

$$F = f_0 \sin(\omega t) \quad (f_0 = 0.1) \quad (4.18)$$

The patch is activated at the beginning of the iterations, and deactivated after $n^*(\omega_1 + \omega_2)$, where n ranges from 0 to 1. The results were obtained and the maximum amplitude is calculated (Section 5.3).

CHAPTER 5

RESULTS AND DISCUSSION

Introduction to the various control techniques such as Negative Velocity FBC, IMSC and MIMSC has been briefed in the previous chapter. This chapter deals with the implementation of these techniques in controlling the free and forced vibrations of the beam. The results obtained from the codes (programmes) developed in Matlab 5.3 using Newmark Method of direct numerical integration technique; to find the free and forced vibration responses with and without control are presented in the subsequent sections. A lot of simulations have been carried out for every type of control method, to find ^{the} effect of various parameters such as weighting factor R, Gain, etc on vibration control. Only one type of response is taken from each category to show the nature of the response using that particular control method. After this, in each category, the effect on the resultant vibration response (i.e. amplitude, damping ratio, settling time, etc.) of various control parameters like R, Gain has been studied.

For all the programmes, ~~the values~~ the following values are common,

Number of Finite Elements = 12

$\xi_1 = 0.01$ and

$\xi_2 = 0.03$

$\Delta t = 0.005$ sec except MIMSC

= 0.00025 sec for MIMSC

Iterations = 500 to 10000 (\approx Time / Δt)

Threshold Value = ± 0.005 mm ($< \pm 0.05\%$ of maximum amplitude in case of free vibration without any control)

The results are divided into three sections, free vibration with and without control, forced vibration with and without control and vibration control using axial stiffness variation.

5.1 FREE DAMPED VIBRATION

The free damped vibration response, implies uncontrolled free vibration response of the beam using inherent (proportional) damping of the system and is shown in Figure 5.1. The Figure 5.1 shows that the peak amplitude is exponentially decaying due to natural inherent damping of the system. The graph shows the response for 5 seconds. As stated earlier, the settling time is the time required to attain the response by structure within threshold value, which is ± 0.005 mm.

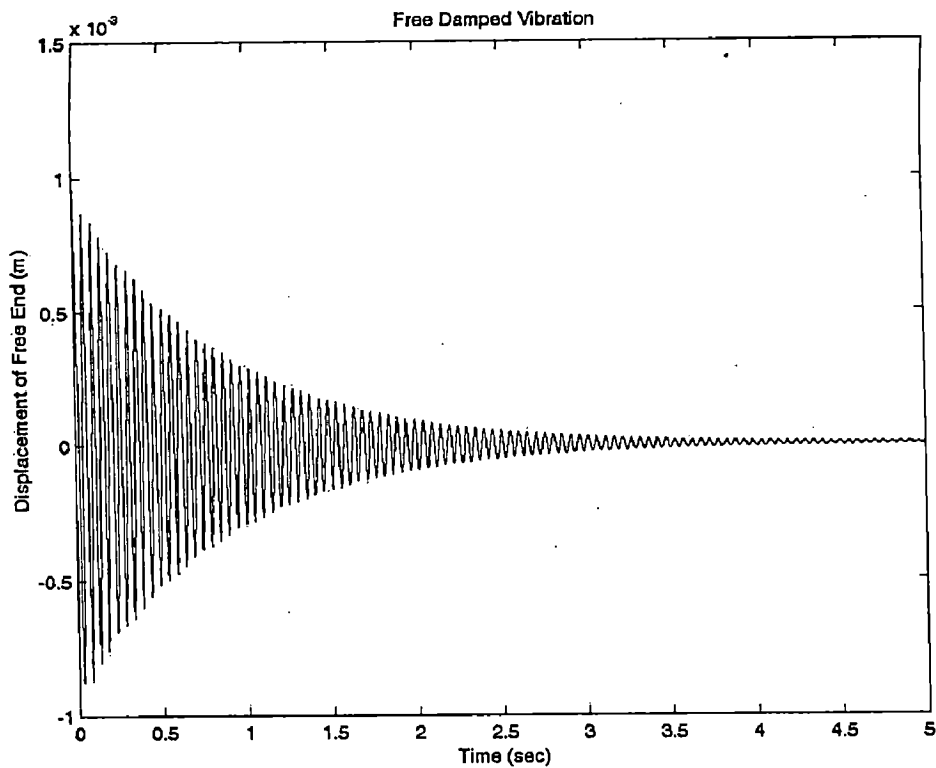


Figure 5.1 Variation of displacement with time (uncontrolled Free Vibration)

For the case of the beam studied here, and for the given damping values, and patches used, the results obtained are as below (refer Figure 5.1).

$$\xi_{10} = 0.01101 \text{ (Damping Ratio based on first 10 cycles)}$$

$$\text{Settling Time} = 4.500 \text{ sec}$$

$$\text{Amplitude} = 0.04388 \text{ mm (at the end of 2.5 sec)}$$

$$= 0.00194 \text{ mm (at the end of 5.0 sec)}$$

5.1.1 Free Damped Vibration: Negative Velocity FBC (First Approach)

The free damped vibration response with negative velocity control by first approach with Gain value as 0.1 is shown in Figure 5.2.

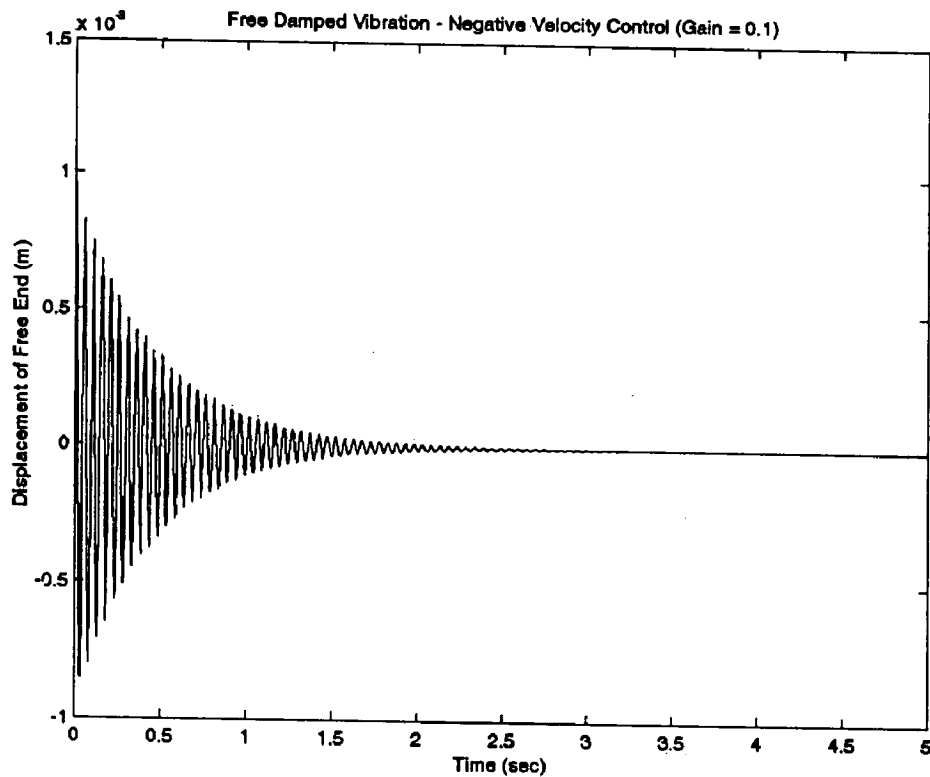


Figure 5.2 Variation of displacement with time (NVFBC) (Gain = 0.1)

The effect on amplitude at end of 5 sec, damping ratio and settling time due to variation in gain is tabulated in Table 5.1 and depicted in Figures 5.3 to 5.5.

From the figures and Table, it is seen that damping ratio almost linearly increases with gain. Amplitude at end of 5.0 seconds is decreasing with gain, it starts increasing again after gain value 0.115 and response became unstable, after gain value of 0.175. Settling time first decreases till the gain becomes 0.12 and then again increases with gain. Figure 5.6 shows the vibration response with negative velocity feedback control for gain 0.2, for which the response becomes unstable.

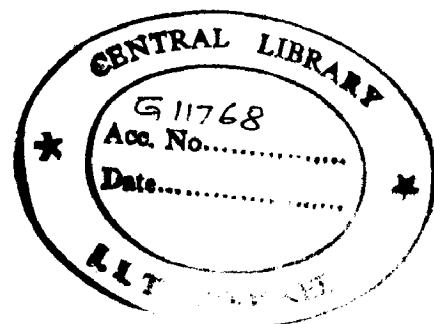


Table 5.1 Free Damped Vibration with Negative Velocity FBC (Simple)

Gain	ξ_{10}	ξ_{10} (compared to uncontrolled)	Amplitude at 5 sec (mm)	Settling Time (sec)	Settling Time (compared to uncontrolled)
0.000	0.011010	100.00	1.9400×10^{-3}	4.500	100.00
0.010	0.011950	108.54	1.5580×10^{-3}	4.140	092.00
0.050	0.014930	135.60	1.4700×10^{-4}	3.165	070.33
0.075	0.016566	150.46	1.7236×10^{-5}	2.730	060.67
0.100	0.018298	166.19	1.6665×10^{-5}	2.445	054.33
0.110	0.019030	172.84	7.1918×10^{-6}	2.365	052.56
0.115	0.019408	176.28	3.2726×10^{-5}	2.265	050.33
0.120	0.019794	179.78	7.2315×10^{-5}	2.265	050.33
0.150	0.022338	202.89	2.7850×10^{-3}	2.895	064.33
0.175	0.024463	222.19	2.2995×10^{-2}	Unbounded	-
0.200	0.027726	251.83	5.4817×10^{-1}	Unbounded	-

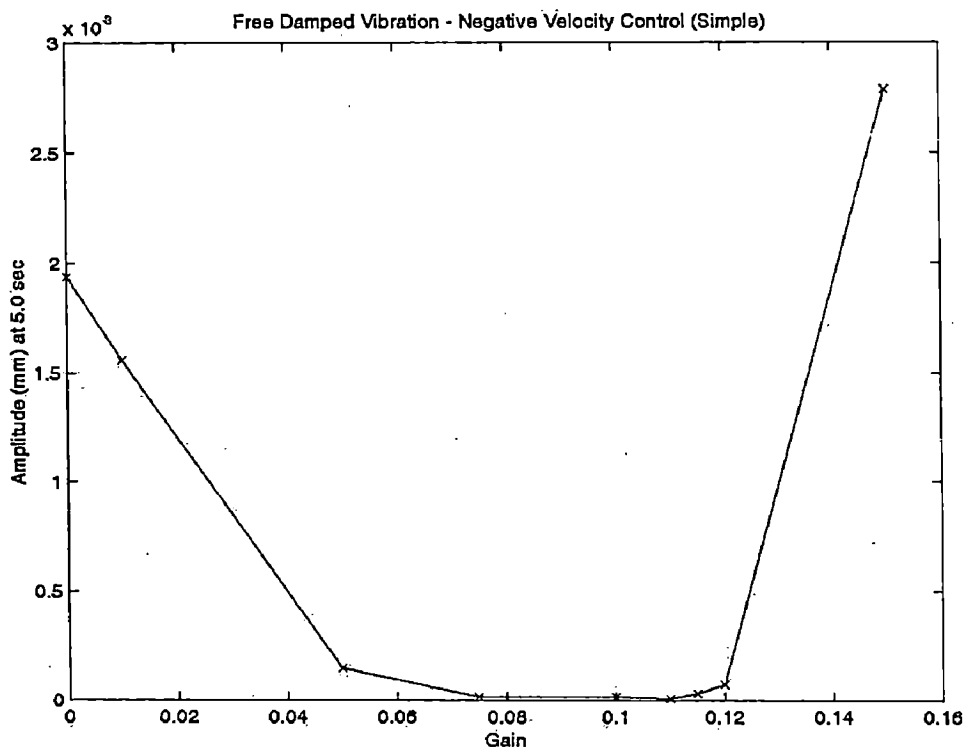


Figure 5.3 Variation of amplitude (at the end of 5 sec) with Gain (NVFBC)

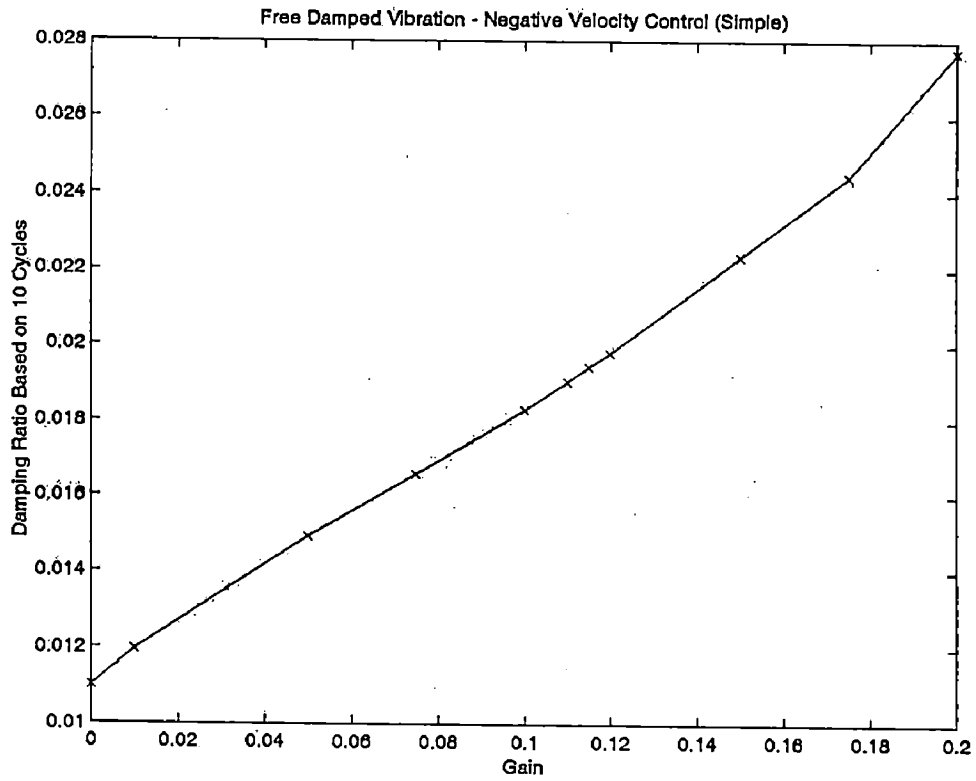


Figure 5.4 Variation of damping ratio with gain (Negative Velocity FBC)

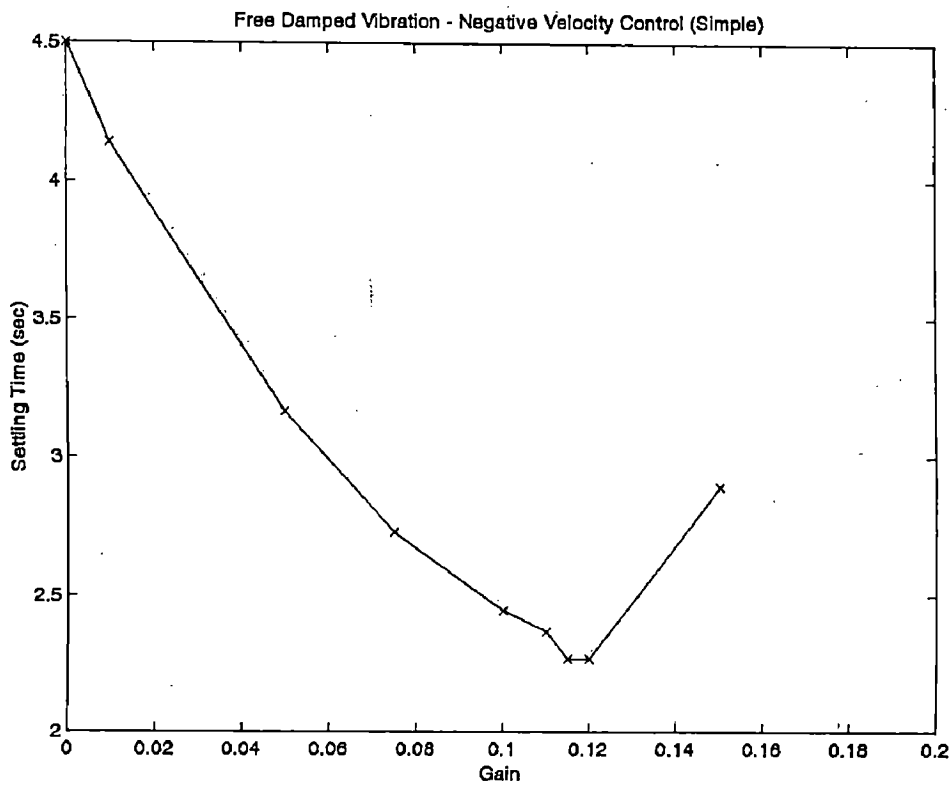


Figure 5.5 Variation of settling time with gain (Negative Velocity FBC)

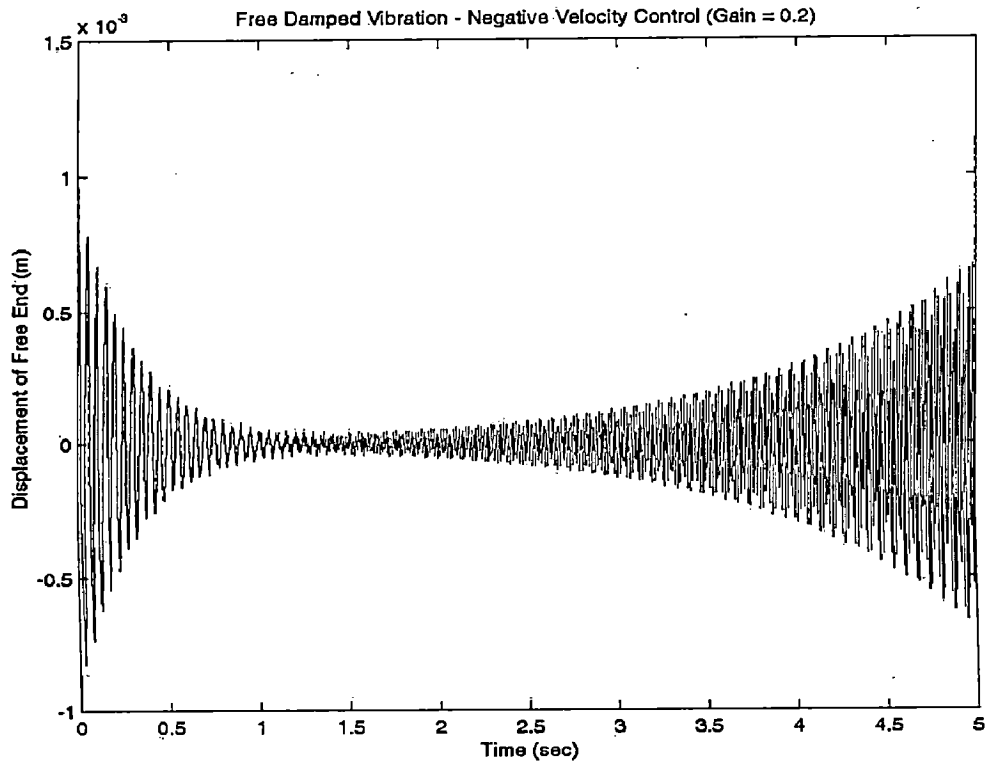


Figure 5.6 Variation of displacement with time (NVFBC) (Unstable Response)

5.1.2 Free Damped Vibration: Negative Velocity FBC (Second Approach)

The free damped vibration response with negative velocity feedback control by actually modelling sensors and actuators in Newmark Method (second approach) is shown in Figures 5.7 and 5.8 with Gain 0.01. Figure 5.7 shows the variation of displacement of the tip of the cantilever beam with time, while Figure 5.8 shows the variation of actuator voltage with time. The displacement is decaying logarithmically with time, but due to increased damping owing to added active damping, compared to free uncontrolled case (Figure 5.1), the decay is fast. The actuator voltage also shows almost similar type of nature as that of displacement.

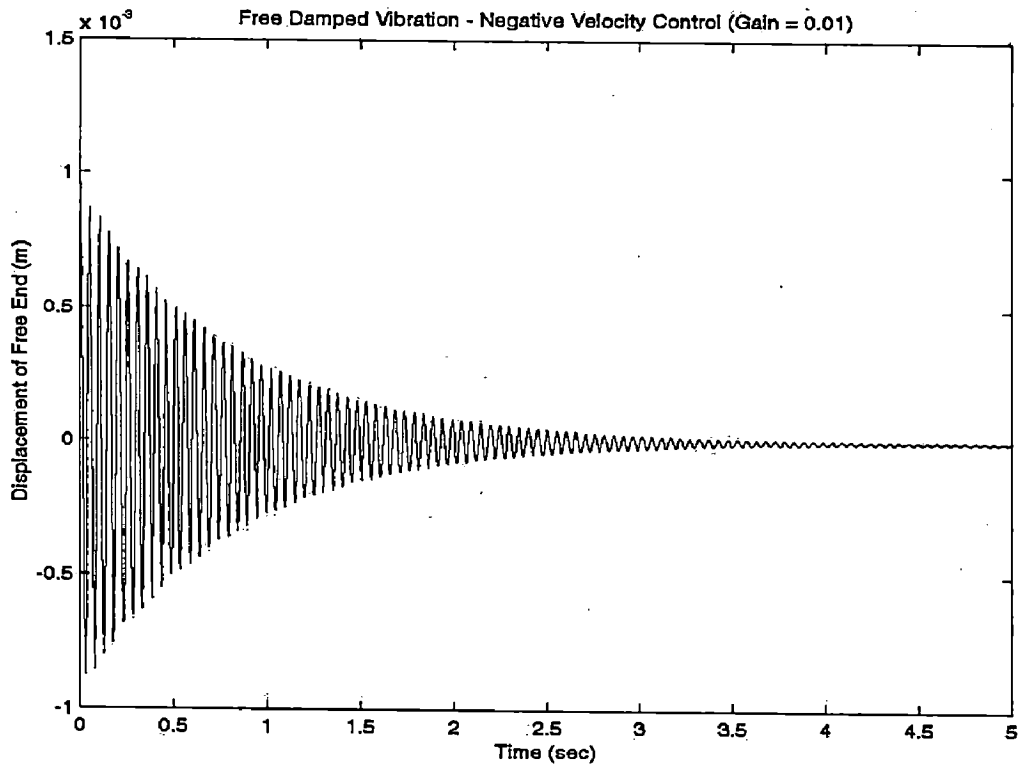


Figure 5.7 Variation of displacement with time (Negative Velocity FBC)

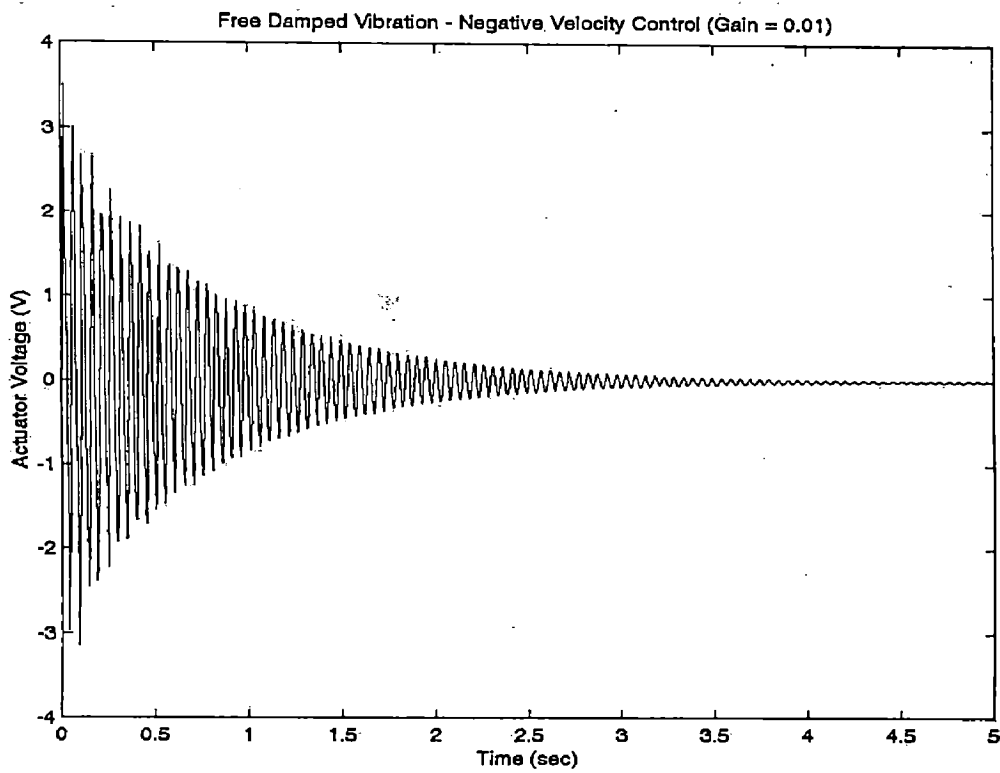


Figure 5.8 Variation of actuator voltage with time (Negative Velocity FBC)

The effect on amplitude at 5 sec, damping ratio and settling time due to variation in gain value is tabulated in Table 5.2 and shown in Figures 5.9 to 5.11, respectively. Variation of actuator voltage with gain is shown in Figure 5.12.

From the figures it is seen that amplitude at end of 5.0 seconds and settling time decreases with gain till gain value becomes 0.12 and the response becomes unstable after that. The damping ratio shows the linear increase with gain. The actuator voltage also found to linearly increasing with gain till gain value becomes 0.12, and as after that the response becomes unstable, so obviously the voltage increases suddenly.

Table 5.2 Free Damped Vibration with Negative Velocity FBC (Sensor)

Gain	ξ_{10}	ξ_{10} % of free vibrations without control	Amplitude at end of 5.0 sec (mm)	Settling Time	Settling Time % of free vib. without control	Voltage (V)	
						Max	Min
0.00	0.01101	100.00	1.9400×10^{-3}	4.500	100.00	0	0
0.01	0.01152	104.63	1.7650×10^{-3}	4.320	096.00	3.506	-3.148
0.05	0.01350	122.62	7.4700×10^{-4}	3.655	081.22	17.28	-15.66
0.10	0.01521	138.15	9.1685×10^{-5}	3.060	068.00	33.94	-30.96
0.11	0.01557	141.42	4.3282×10^{-5}	2.985	066.33	518.52	-518.57
0.12	0.01601	145.41	1.5989×10^{-5}	2.880	064.00	32029	-31057
0.20	0.01891	171.75	2.850×10^{28}	-	-	-	-

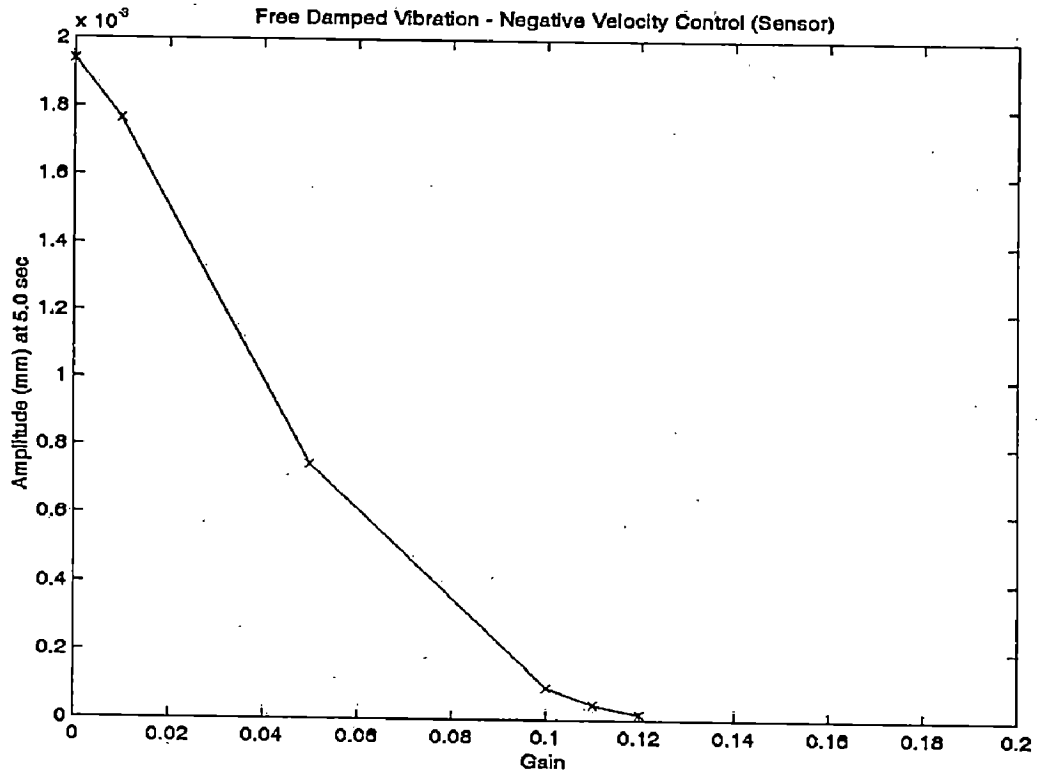


Figure 5.9 Variation of amplitude (at the end of 5 sec) with gain (NVFBC)

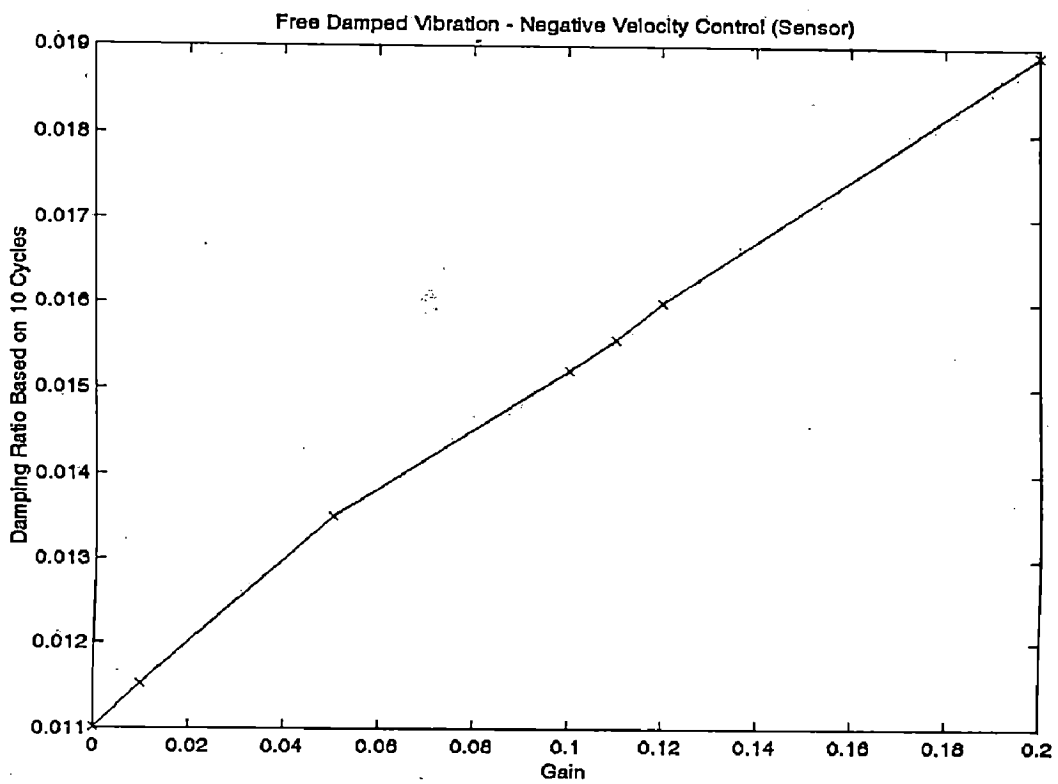


Figure 5.10 Variation of damping ratio with gain (Negative Velocity FBC)

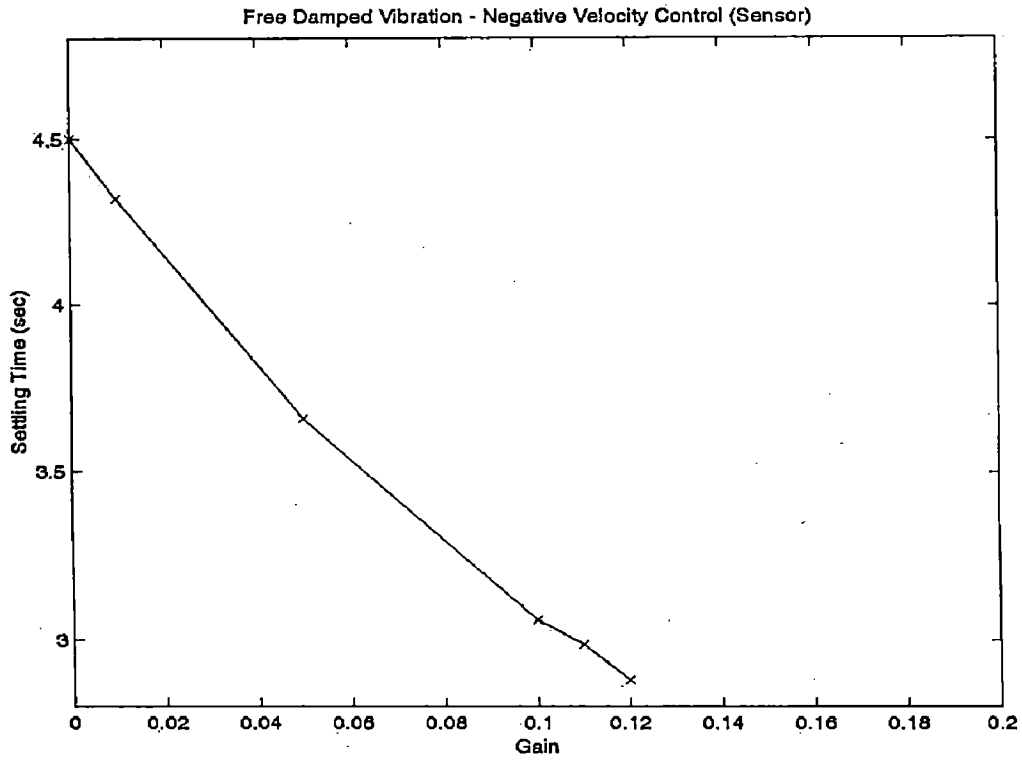


Figure 5.11 Variation of settling time with gain (Negative Velocity FBC)

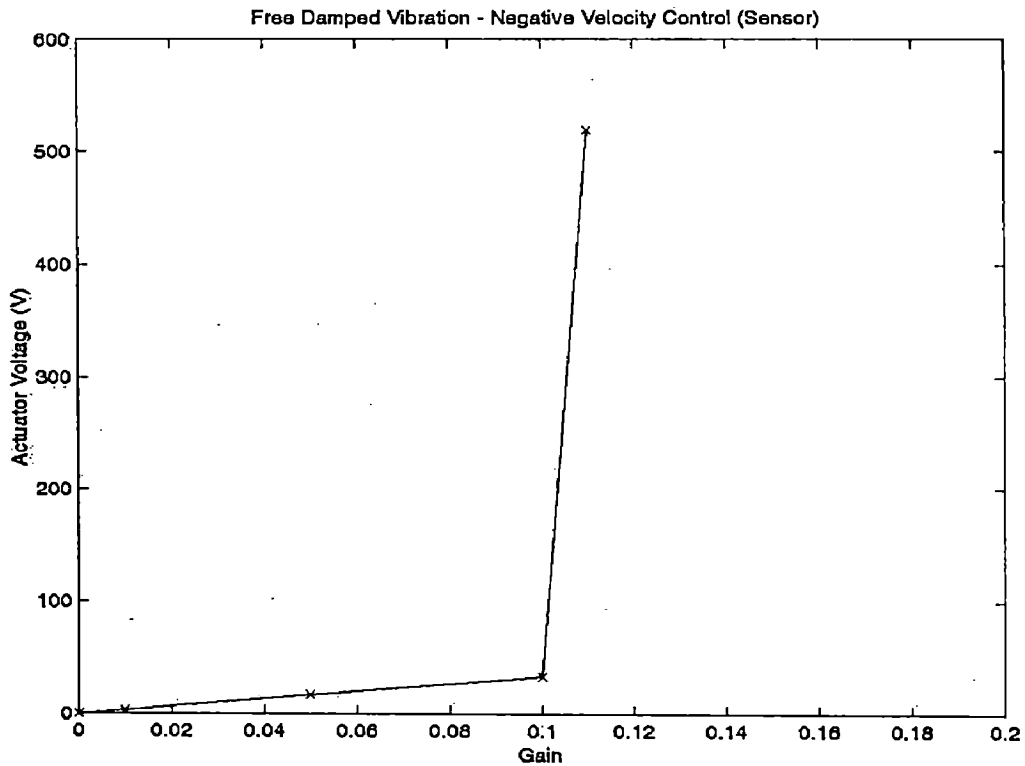


Figure 5.12 Variation of actuator voltage with gain (Negative Velocity FBC)

5.1.3 Free Damped Vibration with IMSC

How you choose the value of R? Arbitrarily or there is some basis to choose?

The free damped vibration response with IMSC is shown in Figures 5.13 and 5.14. Using the weighting factor (R) as 1.0, the time domain response of the beam is shown in Figure 5.13, while variation of actuator voltage with time is shown in Figure 5.14. The effect of variation of R on the values of maximum amplitude and steady state amplitude is given separately in Section 5.1.5. The effect of R on damping ratio, amplitude at 1.0 seconds and settling time is tabulated in Table 5.3 (given after the Section 5.1.5).

From Table 5.3 it is seen that, damping is considerably high in case of IMSC, as compared to free uncontrolled as well as free vibration with negative velocity feedback control, maximum damping is about 1.45 times than free uncontrolled case, settling time is 2.88 seconds for the gain = 0.12 (Table 5.2). While for IMSC, damping is 8.42 times, and the settling time is 0.22 seconds at R = 9. Thus, settling time has reduced drastically in case of IMSC than NVFBC. For the same amount of control, voltage requirement is less in case of IMSC.

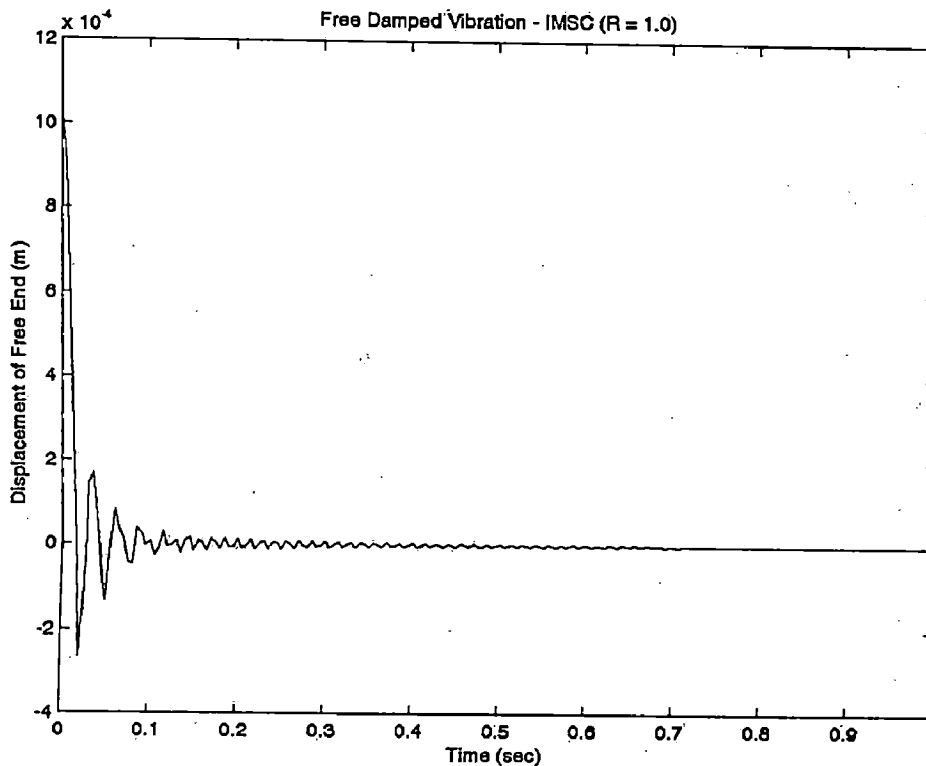


Figure 5.13 Variation of displacement with time (IMSC)

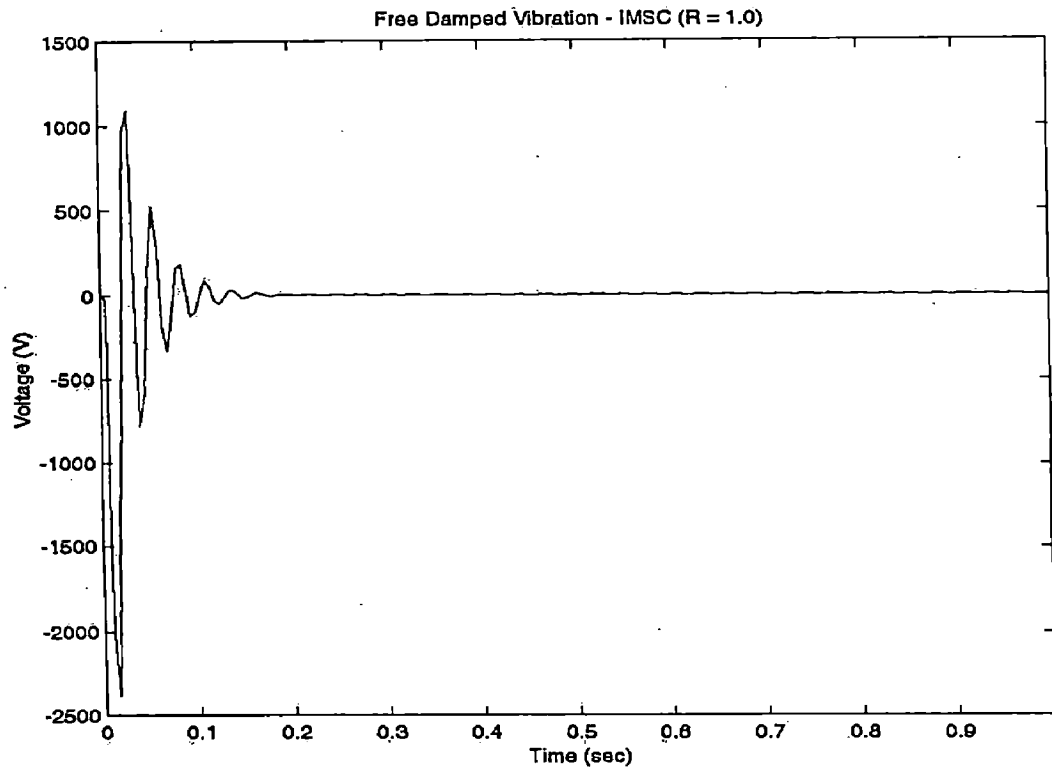


Figure 5.14 Variation of voltage with time (IMSC)

5.1.4 Free Damped Vibration with MIMSC

Using the weighting factor (R) as 1.0, the time domain response of the beam is shown in Figure 5.15, while variation of applied voltage with time is shown in Figure 5.16. The effect of variation of R on the values of maximum amplitude and steady state amplitude is given separately in Section 5.1.5. While its effect on damping ratio, amplitude at 1.0 seconds and settling time is tabulated in Table 5.4 (given after the Section 5.1.5).

Peak voltage in case of MIMSC is 1022.1 V. For NVFBC, maximum damping is about 1.45 times than free uncontrolled case, setting time is 2.88 seconds for the gain = 0.12 (Table 5.2), for IMSC, damping is 8.42 times, and the settling time is 0.22 seconds at $R = 9$, and for MIMSC damping is about 9 times, settling time is 0.30 seconds at $R = 35$. For the same amount of control, voltage requirement is less in case of IMSC than NVFBC, while least for MIMSC.

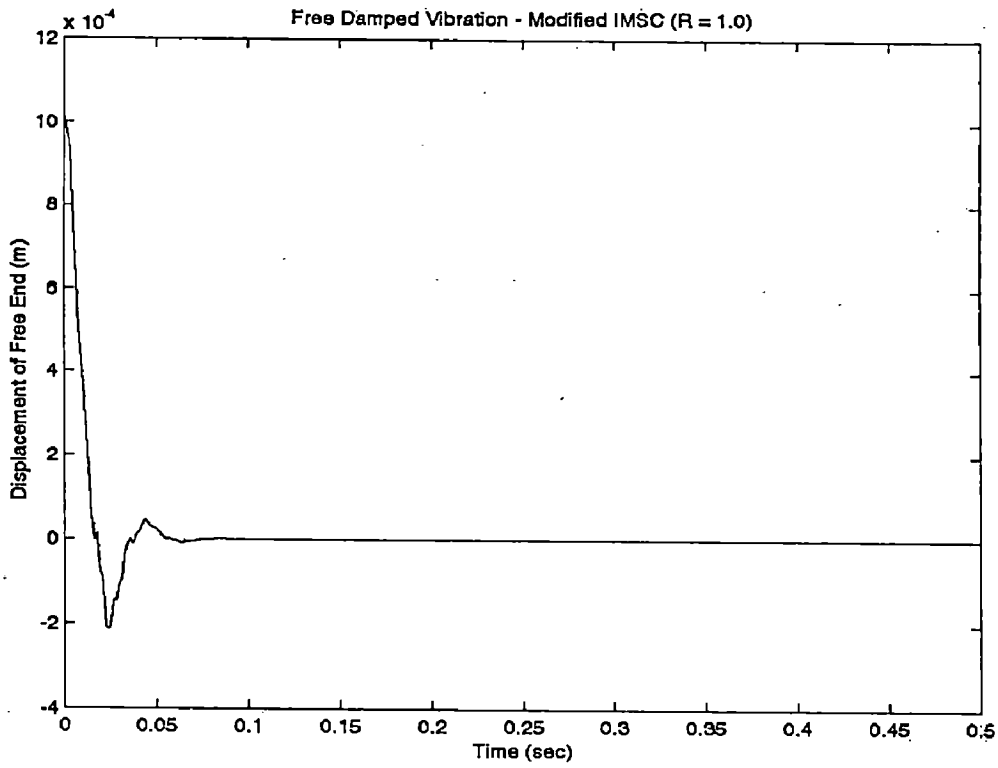


Figure 5.15 Variation of displacement with time (MIMSC)

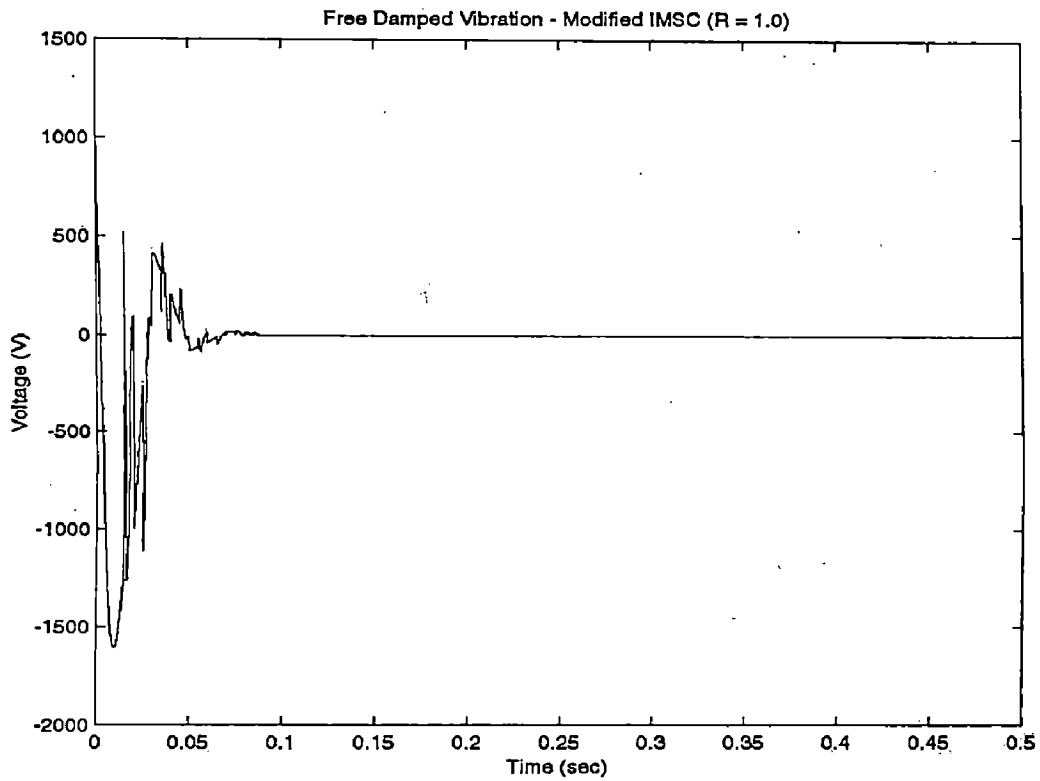


Figure 5.16 Variation of voltage with time (MIMSC)

5.1.5 Comparison of Controlled Vibration using IMSC and MIMSC

The comparison between IMSC and MIMSC to find effect of weighting factor (R) on active vibration control is given here. The common ground for comparison is the weighting factor (R). The results are tabulated in Table 5.5 and shown in Figures 5.17 to 5.20.

Figure 5.17 shows the variation of amplitude at the end of 5 seconds with weighting factor. The resultant amplitude achieved by MIMSC is smaller than IMSC, and it shows increase with R in case of MIMSC, while it decreases with certain value of R (= 40) and again increases in case of IMSC.

Figure 5.18 shows the variation of damping ratio with R, and as expected, in this case also damping is more in case of MIMSC than IMSC. Figure 5.19 shows the variation of the settling time with R. In case of IMSC it is seen that settling time shows first decrease and then increase with increasing value of R, while for MIMSC, settling time increases with R. Figure 5.20 shows the variation of voltage with R, and as expected, voltage decreases with increasing R, but for MIMSC voltage requirement is lesser than IMSC.

Here one may observe that the peak voltage in case of IMSC is 1088.7 V while in case of MIMSC it is 1022.1 V i.e. a drop of 6.52 % is there in MIMSC (Figures 5.14 and 5.16). This indicates a better effectiveness of MIMSC in place of IMSC. From Tables 5.3 to 5.5 it is seen that, damping is considerably high in case of IMSC, as compared to free uncontrolled as well as free vibration NVFBC, but lesser than that of MIMSC. From Table 5.4 it is clear that, MIMSC controls more than one mode, but as the value of R increased the number of controlled modes decreases. First mode is controlled for every value of R, while second mode is controlled till R=10, and last (24th) mode is controlled till R=6, while IMSC controls only first mode.

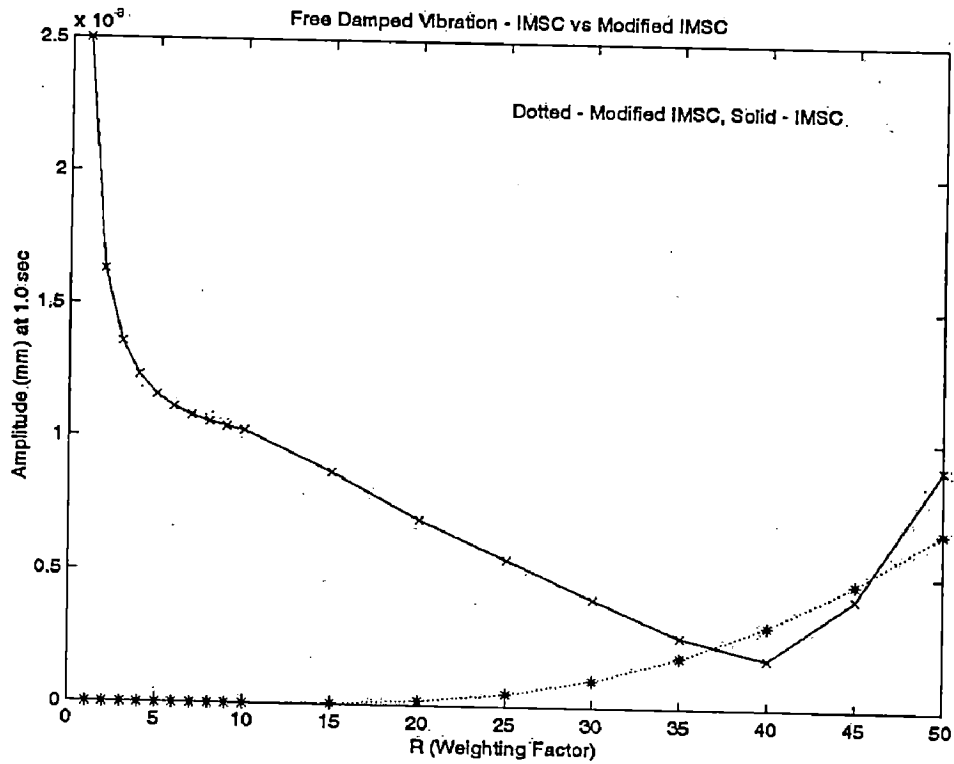


Figure 5.17 Comparison of Free Vibration response with IMSC and MIMSC
(Variation of amplitude with R)

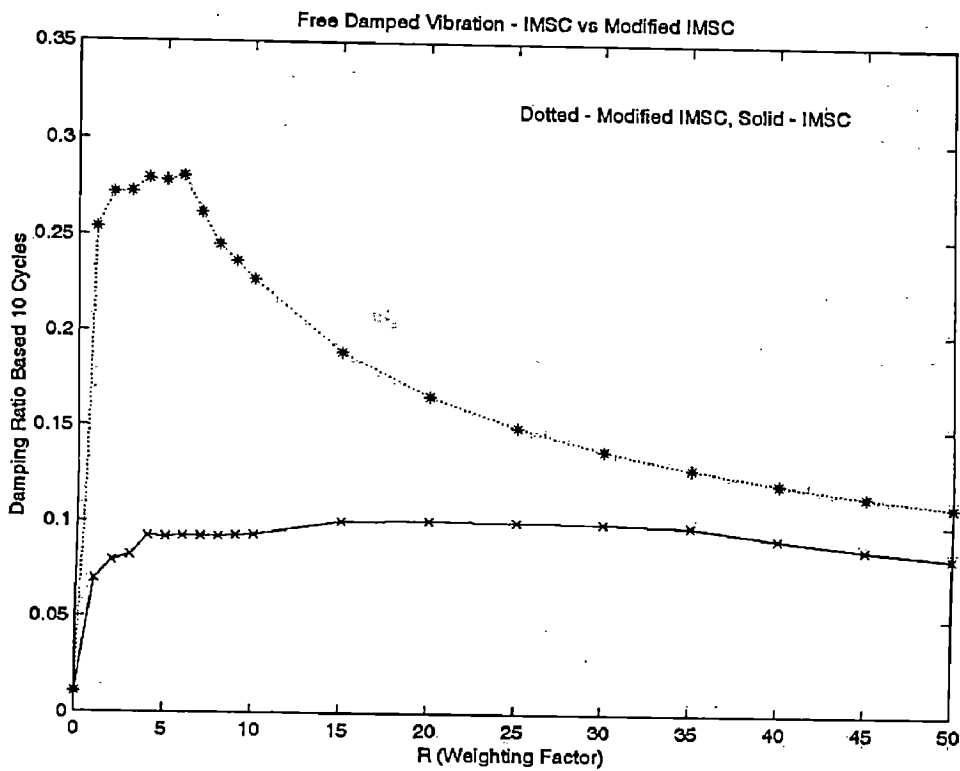


Figure 5.18 Comparison of Free Vibration response with IMSC and MIMSC
(variation damping ratio with R)

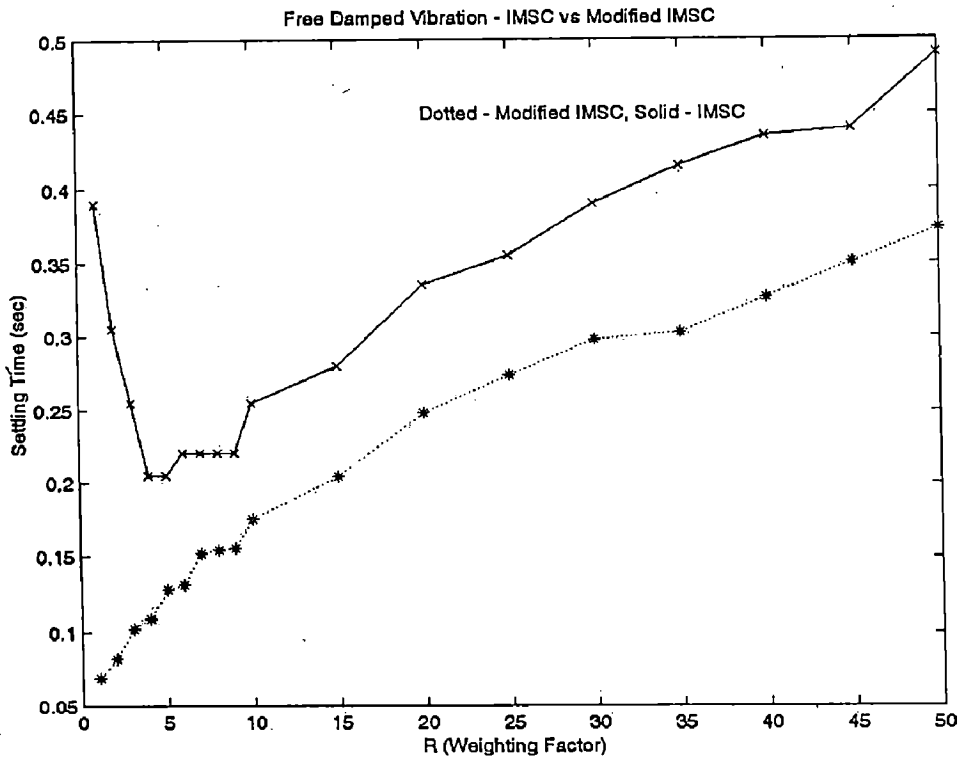


Figure 5.19 Comparison of Free Vibration response with IMSC and MIMSC (variation of Settling Time with R)

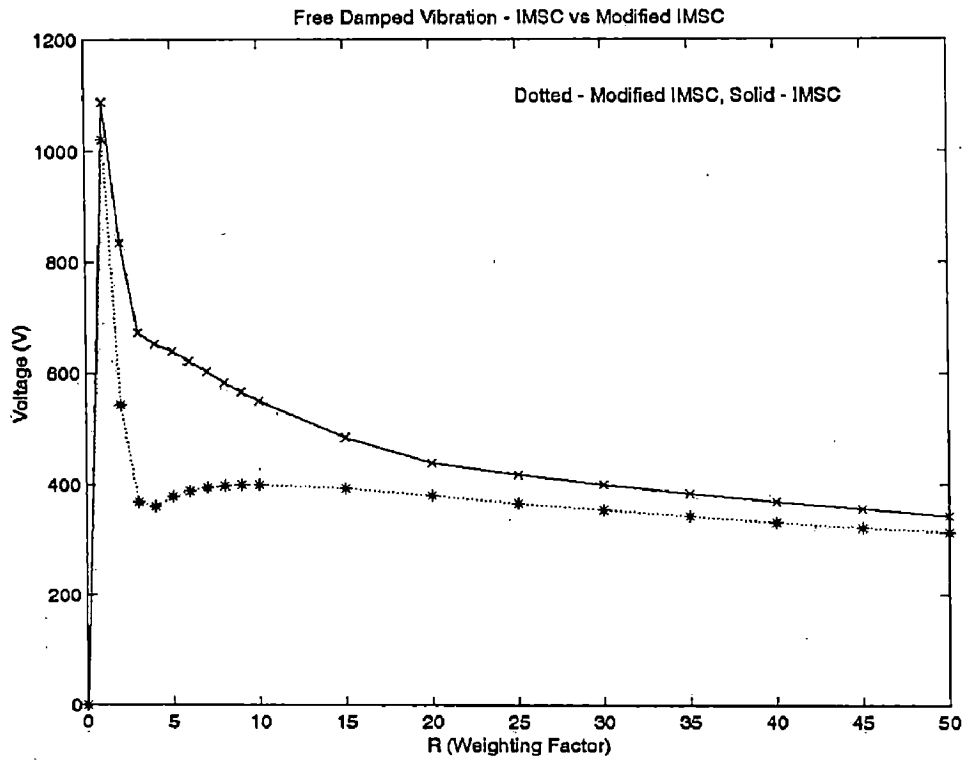


Figure 5.20 Comparison of Free Vibration response with IMSC and MIMSC (Variation of Voltage with R)

Table 5.3 Free Damped Vibration with IMSC

R	ξ_{10}	ξ_{10} % of free vib. without control	Amplitude at the end of 1.0 sec (mm)	Settling Time	Settling Time % of free vib. without control	Actuator Voltage	
						Max	Min
0	0.01101	100.00	193.96×10^{-3}	4.500	100.00	0	0
1	0.06978	633.79	2.9214×10^{-3}	0.390	008.67	1088.70	-2380.5
2	0.07944	721.53	2.7673×10^{-3}	0.305	006.78	0834.21	-1800.2
3	0.08233	747.77	3.2175×10^{-3}	0.255	005.67	0672.66	-1531.2
4	0.09244	839.60	3.6109×10^{-3}	0.205	004.56	0653.13	-1363.7
5	0.09201	835.69	3.9264×10^{-3}	0.205	004.56	0639.93	-1245.1
6	0.09221	837.51	4.1814×10^{-3}	0.220	004.89	0621.63	-1155.0
7	0.09215	836.97	4.3915×10^{-3}	0.220	004.89	0602.48	-1083.2
8	0.09209	836.42	4.5679×10^{-3}	0.220	004.89	583.93	-1024.1
9	0.09271	842.05	4.7186×10^{-3}	0.220	004.89	566.49	-974.22
10	0.09330	847.41	4.8491×10^{-3}	0.255	005.67	550.27	-931.42
15	0.10061	913.81	5.3110×10^{-3}	0.280	006.22	485.22	-781.40
20	0.10075	915.08	5.5950×10^{-3}	0.335	007.44	439.44	-688.13
25	0.10022	910.26	5.7863×10^{-3}	0.355	007.44	418.71	-622.69
30	0.09987	907.08	5.9962×10^{-3}	0.390	008.67	399.96	-573.41
35	0.09832	893.01	6.2848×10^{-3}	0.415	009.22	383.28	-534.51
40	0.09220	837.42	6.5481×10^{-3}	0.435	009.67	368.47	-502.77
45	0.08689	789.19	6.5693×10^{-3}	0.440	009.78	355.25	-476.21
50	0.08284	752.41	6.1366×10^{-3}	0.490	010.89	343.39	-453.55

Table 5.4 Free Damped Vibration with MIMSC

R	ξ_{10}	ξ_{10} % of free vib. without control	Amplitude at the end of 0.2 sec (mm)	Settling Time	Settling Time % of free vib. without control	Actuator Voltage		Modes Controlled
						Max	Min	
0	0.01101	100.00	1.8480×10^{-3}	4.50000	100.00	0	0	-
1	0.25406	598.64	2.7128×10^{-8}	0.06900	010.89	1022.1	-1603.3	1,2,24
2	0.27198	633.79	9.9744×10^{-6}	0.08175	008.67	544.60	-1363.3	1,2,24
3	0.27273	721.53	4.3773×10^{-5}	0.10200	006.78	369.46	-1224.3	1,2,24
4	0.27946	747.77	1.0922×10^{-4}	0.10875	005.67	360.64	-1126.9	1,2,24
5	0.27807	839.60	3.8491×10^{-4}	0.12875	004.56	378.43	-1052.7	1,2,24
6	0.28077	835.69	5.1938×10^{-4}	0.13200	004.56	389.12	-993.47	1,2,24
7	0.26204	837.51	1.0009×10^{-3}	0.15200	004.89	395.42	-944.34	1,2
8	0.24552	836.97	1.4687×10^{-3}	0.15425	004.89	398.95	-902.58	1,2
9	0.23678	836.42	2.0401×10^{-3}	0.15550	004.89	400.54	-866.64	1,2
10	0.22691	842.05	2.7135×10^{-3}	0.17550	004.89	400.81	-835.09	1,2
15	0.18915	847.41	7.3720×10^{-3}	0.20400	005.67	392.85	-719.64	1
20	0.16623	913.81	1.3562×10^{-2}	0.24775	006.22	379.69	-644.26	1
25	0.15024	915.08	2.0624×10^{-2}	0.27375	007.44	366.24	-589.61	1
30	0.13832	910.26	2.8133×10^{-2}	0.29800	007.44	353.55	-547.51	1
35	0.12901	907.08	3.5828×10^{-2}	0.30275	008.67	341.88	-513.78	1
40	0.12147	893.01	4.3584×10^{-2}	0.32675	009.22	331.24	-485.89	1
45	0.11521	837.42	5.1194×10^{-2}	0.35050	009.67	321.54	-462.29	1
50	0.10990	789.19	5.8706×10^{-2}	0.37350	009.78	312.69	-441.97	1

Table 5.5 Free Vibration IMSC Vs. MIMSC

R	Amplitude (mm) at the end of 0.5 sec		Settling Time (sec)		Actuator Voltage (V)				Damping Ratio (Based on first 10 Cycles)	
					IMSC		MIMSC			
	IMSC	MIMSC	IMSC	MIMSC	Max	Min	Max	Min	IMSC	MIMSC
0	0.043880	0.043880	4.500	4.5000	0	0	0	0	0.01101	0.01101
1	0.002500	4.5455 x10 ⁻⁹	0.390	0.0690	1088.70	-2380.5	1022.1	-1603.3	0.06978	0.25406
2	0.001629	9.4452 x10 ⁻⁹	0.305	0.0818	0834.21	-1800.2	544.60	-1363.3	0.07944	0.27198
3	0.001357	2.2286 x10 ⁻⁸	0.255	0.1020	0672.66	-1531.2	369.46	-1224.3	0.08233	0.27273
4	0.001229	1.2926 x10 ⁻⁸	0.205	0.1088	0653.13	-1363.7	360.64	-1126.9	0.09244	0.27946
5	0.001156	9.8931 x10 ⁻⁹	0.205	0.1288	0639.93	-1245.1	378.43	-1052.7	0.09201	0.27807
6	0.001111	5.4030 x10 ⁻⁹	0.220	0.1320	0621.63	-1155.0	389.12	-993.47	0.09221	0.28077
7	0.001079	2.9208 x10 ⁻⁸	0.220	0.1520	0602.48	-1083.2	395.42	-944.34	0.09215	0.26204
8	0.001056	8.3069 x10 ⁻⁸	0.220	0.1543	583.93	-1024.1	398.95	-902.58	0.09209	0.24552
9	0.001037	1.2489 x10 ⁻⁷	0.220	0.1555	566.49	-974.22	400.54	-866.64	0.09271	0.23678
10	0.001024	2.3295 x10 ⁻⁷	0.255	0.1755	550.27	-931.42	400.81	-835.09	0.09330	0.22691
15	0.001052	3.3981 x10 ⁻⁶	0.280	0.2040	485.22	-781.40	392.85	-719.64	0.10061	0.18915
20	0.000997	1.6016 x10 ⁻⁵	0.335	0.2478	439.44	-688.13	379.69	-644.26	0.10075	0.16623
25	0.000651	4.6605 x10 ⁻⁵	0.355	0.2738	418.71	-622.69	366.24	-589.61	0.10022	0.15024
30	0.000406	1.0274 x10 ⁻⁴	0.390	0.2980	399.96	-573.41	353.55	-547.51	0.09987	0.13832
35	0.000268	1.9003 x10 ⁻⁴	0.415	0.3028	383.28	-534.51	341.88	-513.78	0.09832	0.12901
40	0.000188	3.1204 x10 ⁻⁴	0.435	0.3268	368.47	-502.77	331.24	-485.89	0.09220	0.12147
45	0.000418	4.7060 x10 ⁻⁴	0.440	0.3505	355.25	-476.21	321.54	-462.29	0.08689	0.11521
50	0.000904	6.6622 x10 ⁻⁴	0.490	0.3735	343.39	-453.55	312.69	-441.97	0.08284	0.10990

5.2 FORCED DAMPED VIBRATION

The control of forced vibrations is most common problem encountered in industrial life. The main problem is the nature of external force is not definite. The external force may be harmonic, impulse, step and even in worst case random. Most of the times it is not possible to make the response near to zero or within threshold value, but the amplitude of vibration can be reduced to some extent.

The response of the vibrating the beam of Figure 3.2 with a harmonic force input ($F = f_0 \sin(\omega t)$), where $f_0 = 1$ N, $\omega = 15$ Hz (94.2478 rad/s) found using Newmark Method is shown in Figure 5.21.

To compare the response achieved by various control methods in case of forced vibration, the steady state amplitude and maximum amplitude of the vibrating beam are the set parameters.

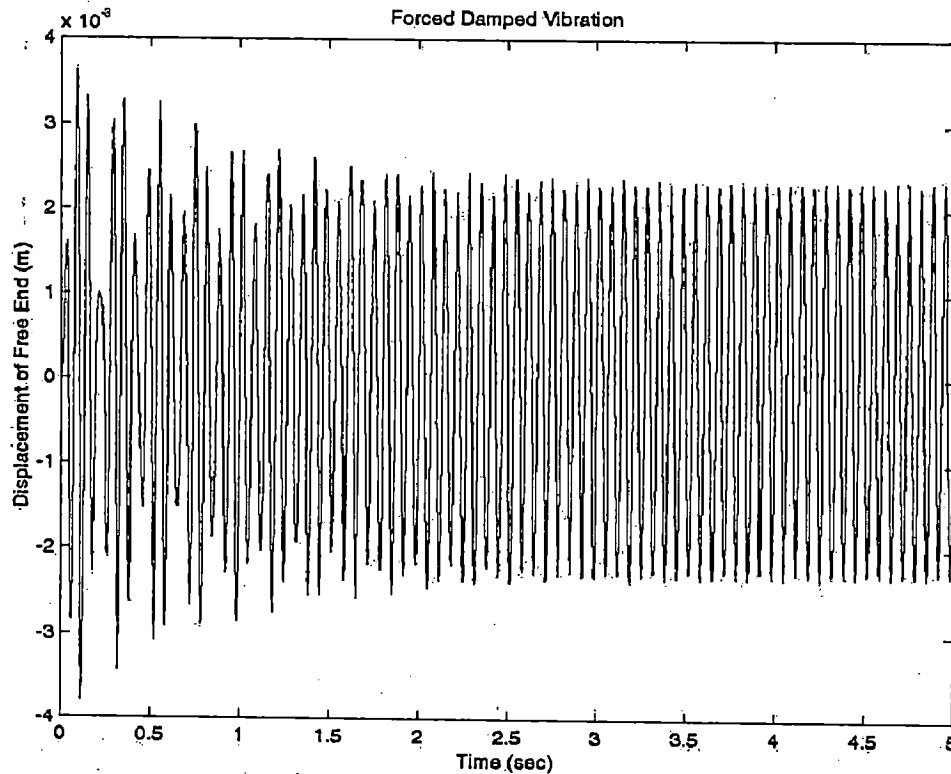


Figure 5.21 Variation of displacement with time (uncontrolled forced vibration)

5.2.1 Forced Damped Vibration with Negative Velocity Feedback Control (First Approach)

The forced vibration response with negative velocity control by first approach with gain value 0.1 is shown in Figure 5.22, while variation of maximum amplitude and steady state amplitude with gain are shown in Figure 5.23 and tabulated in Table 5.6.

Table 5.6 Forced Damped Vibration with Negative Velocity FBC (Simple)

Gain	Amplitude (mm)			Steady State Amplitude (% of forced uncontrolled vibration)
	5.0	Max	Steady	
0.000	-0.07812	3.62220	2.3850	100.00
0.100	-0.14441	3.47320	2.2900	096.02
0.150	-0.17249	3.40290	2.2650	094.97
0.175	-0.18648	3.36870	2.2600	094.76
0.180	-0.16982	3.36200	2.2665	095.03
0.200	-0.38372	3.33520	2.3500	098.53
0.250	18.89000	18.89000	Unbounded	-
0.300	-1.676x10 ¹⁴	1.574x10 ¹⁴	Unbounded	-

From the Figure 5.23, it can be seen that, the maximum as well as steady state amplitude, first decreases with gain, while after some value of gain (0.25) the response gets unstable. The decrease in the amplitude is almost linear with gain value. The maximum reduction in the amplitude is found at the gain value 0.175 and the steady state amplitude is 94.76% of the steady state amplitude in uncontrolled case.

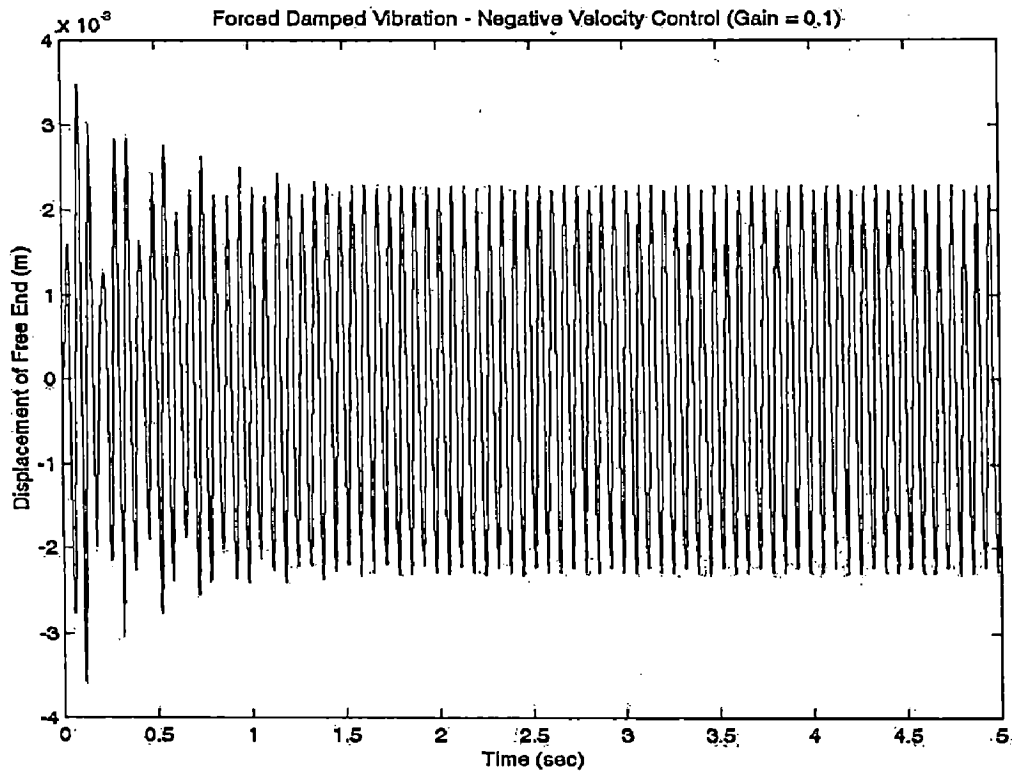


Figure 5.22 Variation of displacement with time (NVFBC) (Gain = 0.1)

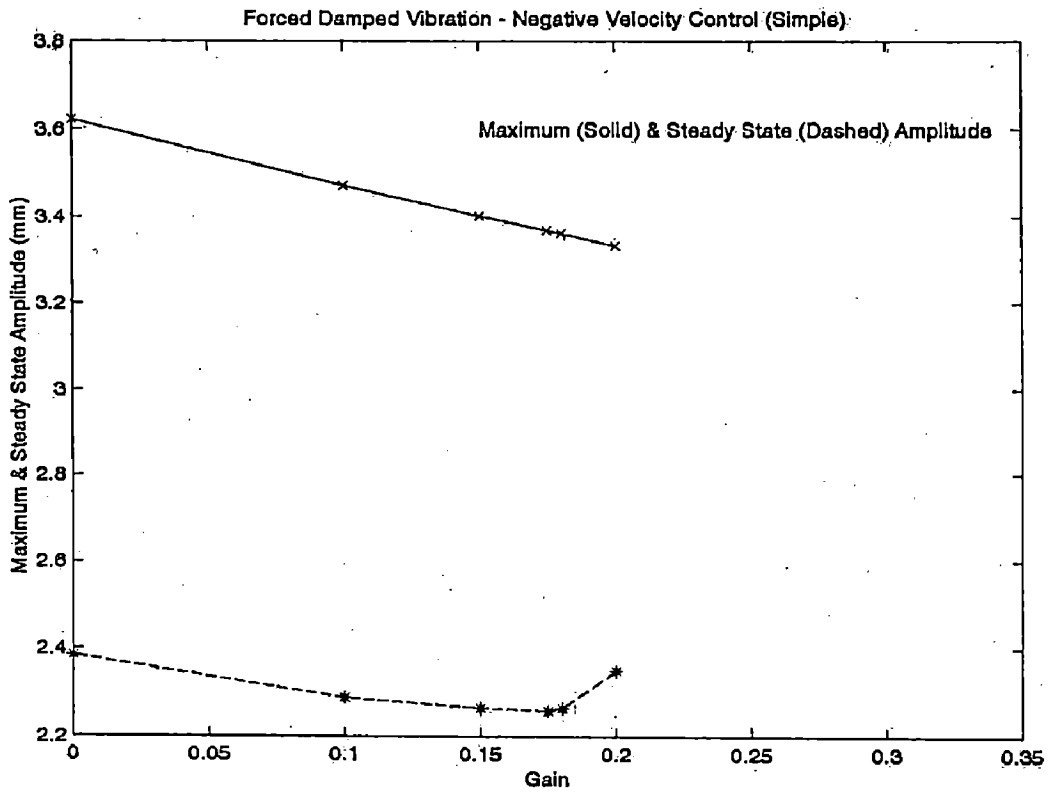


Figure 5.23 Variation of Maximum and Steady state amplitude with gain

5.2.2 Forced Damped Vibration with Negative Velocity Feedback Control (Second Approach)

The forced vibration response with negative velocity control by second approach with 0.1 gain is shown in Figures 5.24 and 5.25.

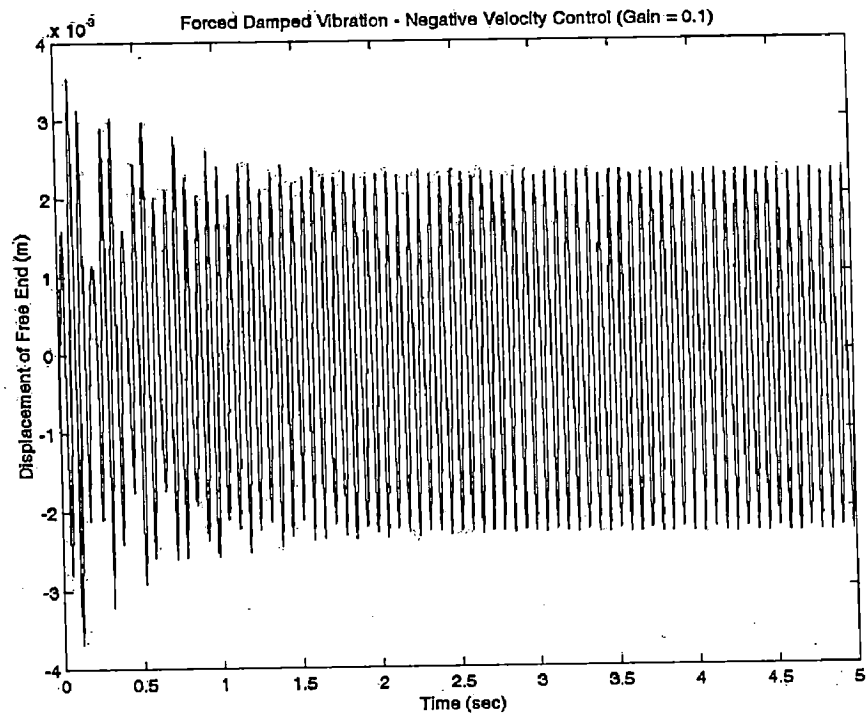


Figure 5.24 Variation of displacement with time (NVFBC) (Gain = 0.1)

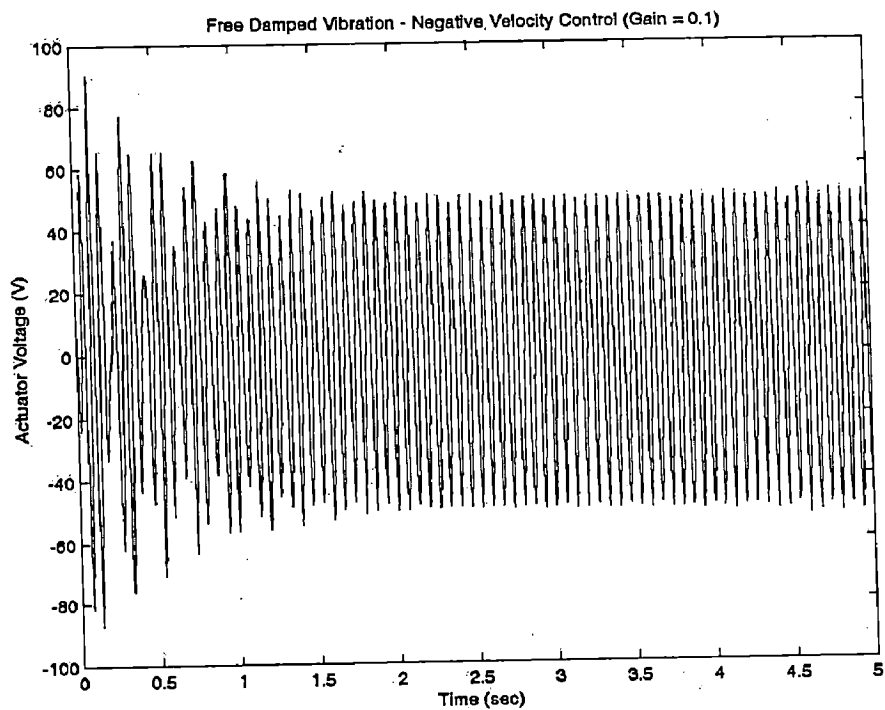


Figure 5.25 Variation of actuator voltage with time (NVFBC) (Gain = 0.1)

Variation of maximum amplitude and steady state amplitude with gain are shown in Figure 5.26, followed by variation in actuator voltage with gain in Figure 5.28 and tabulated in Table 5.7. The maximum amplitude as well as steady state amplitude decreases with gain, while after certain value of gain (0.15) the response gets unstable. Actuator and sensor voltage also increases slowly till the value of gain becomes 0.15, and then increases rapidly. The maximum value of actuator voltage within stable region is found to 180 V.

The least steady state amplitude is found at gain value of 0.11, and this is 96.85 % of the steady state amplitude of uncontrolled case. While in simple mathematical modelling, it was 94.76 % at the gain value of 0.175. The difference may be due to mathematical modelling of sensor and actuator and the values of Piezoelectric Stress Constant and Piezoelectric Strain Constant.

Table 5.7 Forced Vibration Negative Velocity Control (Sensor)

Gain	Amplitude (mm)		Steady state Amplitude (% of forced uncontrolled vibrations)	Actuator Voltage	
	Max	Steady		Max	Min
0.00	3.6222	2.3850	100.00	0	0
0.01	3.6138	2.3800	99.79	9.4172	-9.2465
0.05	3.5804	2.3500	98.53	46.2430	-45.0530
0.075	3.5599	2.3250	97.48	68.5970	-66.4810
0.10	3.5397	2.3155	97.09	90.4611	-87.2134
0.11	3.5317	2.3100	96.85	177.100	-174.580
0.15	1.18×10^{08}	Unbound	-	6.39×10^{17}	-6.72×10^{17}
0.20	6.52×10^{30}	Unbound	-	3.10×10^{39}	-2.81×10^{39}

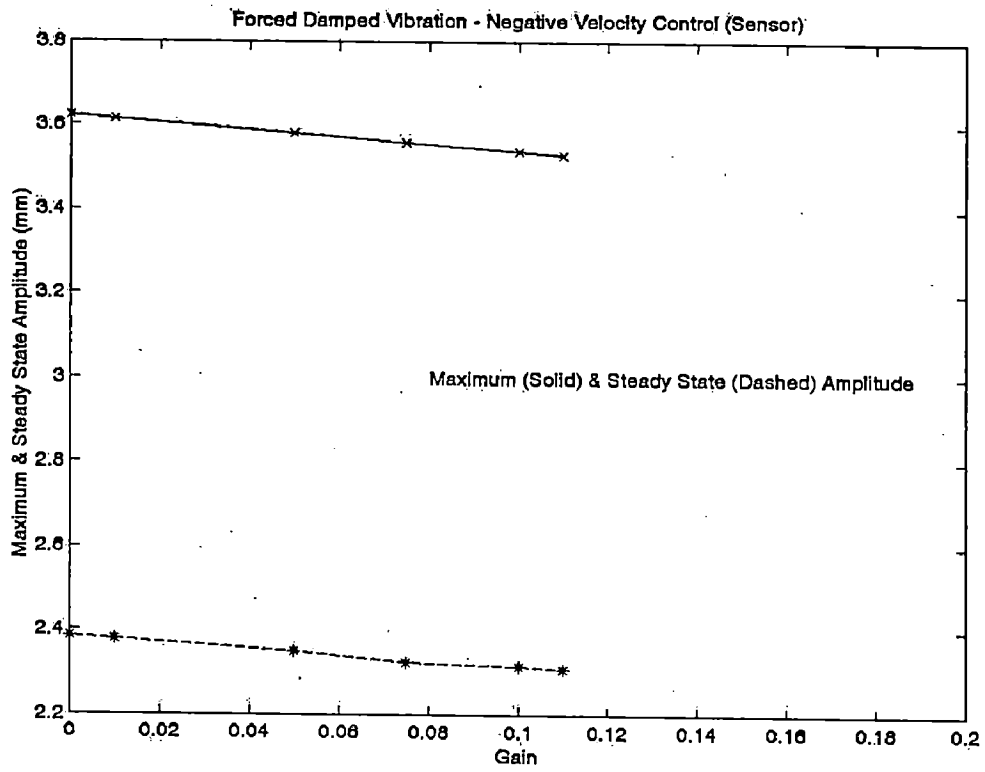


Figure 5.26 Variation of maximum and steady state amplitude with gain

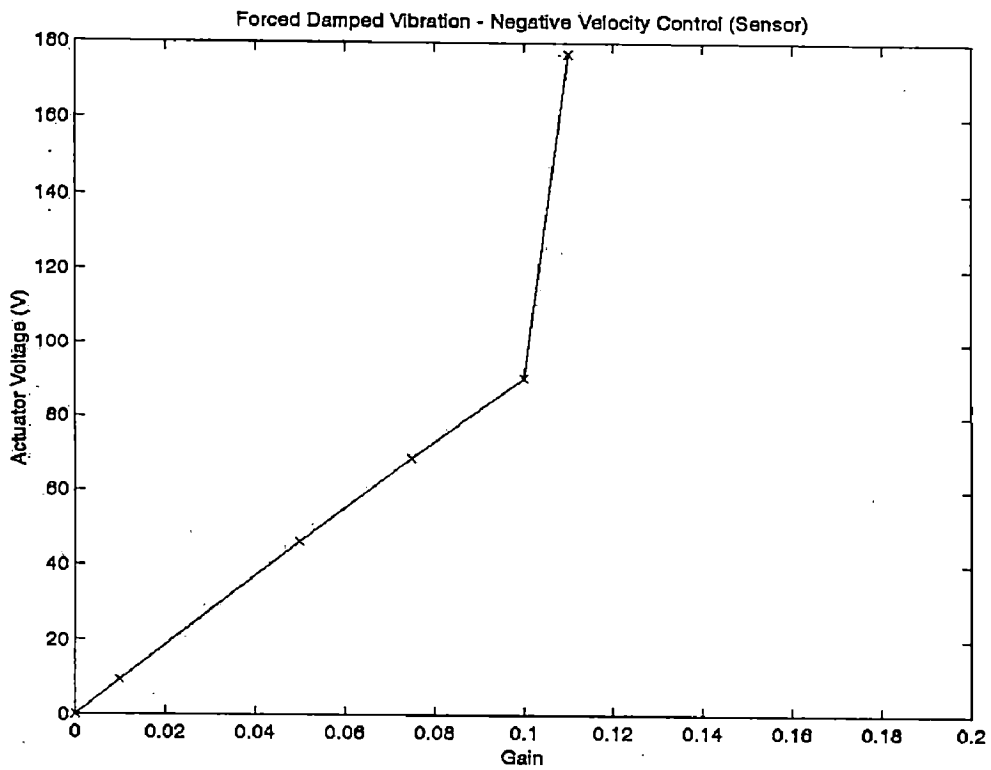


Figure 5.27 Variation of actuator voltage with gain (NVFBC)

5.2.3 Forced Damped Vibration with IMSC

The time domain response of the beam for forced vibration control using IMSC with weighting factor (R) as 1.0 is shown in Figure 5.28, while variation of applied voltage with time is shown in figure 5.29. The effect of variation of R on the values of maximum amplitude and steady state amplitude is included in Section 5.2.5. While its effect on damping ratio, amplitude at 1.0 seconds and settling time is tabulated in Table 5.8. From Table 5.8 it is seen that, voltage decreases with R, but it reduces ^{its} control effect. The steady state amplitude becomes 31.65 % of that of uncontrolled case, with R = 1, but voltage is very high (>2000 V), which is not practically feasible.

Table 5.8 Forced Vibration with IMSC

R	Amplitude (mm)		Steady state Amplitude (% of forced uncontrolled vibrations)	Actuator Voltage	
	Max	Steady		Max	Min
0	3.62220	2.38500	100.00	0	0
1	0.81281	0.75500	31.65	2207.8	-1977.3
2	0.99502	0.95420	40.01	1789.0	-2009.2
3	1.12490	1.08500	45.49	1675.4	-1965.2
4	1.26170	1.17800	49.39	1589.7	-1881.9
5	1.36900	1.25600	52.66	1524.2	-1797.2
6	1.45580	1.31500	55.14	1511.9	-1719.3
7	1.52790	1.36500	57.23	1508.1	-1649.4
8	1.58890	1.40800	59.04	1499.5	-1588.0
9	1.64160	1.44650	60.65	1487.7	-1545.8
10	1.68750	1.47950	62.03	1473.9	-1506.4
15	1.85370	1.60750	67.40	1395.2	-1345.0
20	1.96040	1.69500	71.07	1319.4	-1227.0
25	2.05310	1.76000	73.79	1252.7	-1136.5
30	2.15140	1.79980	75.46	1194.9	-1064.3
35	2.22200	1.84500	77.36	1144.4	-1013.6
40	2.30030	1.87800	78.74	1100.1	-990.53
45	2.35860	1.89550	79.48	1060.8	-968.60
50	2.40950	1.92500	80.71	1025.6	-947.86
60	2.49430	1.95300	81.89	965.22	-909.86
70	2.56270	1.97750	82.91	914.92	-876.06
80	2.61950	2.00550	84.09	872.17	-845.89
90	2.66670	2.01200	84.36	835.24	-818.78
100	2.70920	2.04520	85.72	802.90	-794.27

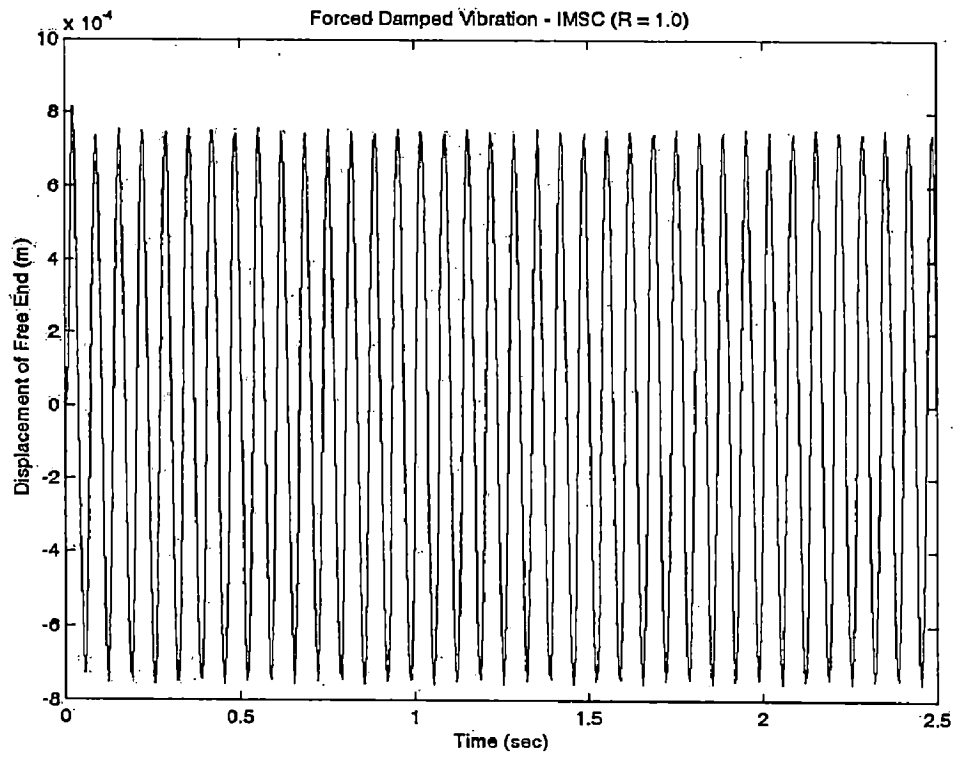


Figure 5.28 Variation of displacement with time (IMSC) (R = 1.0)

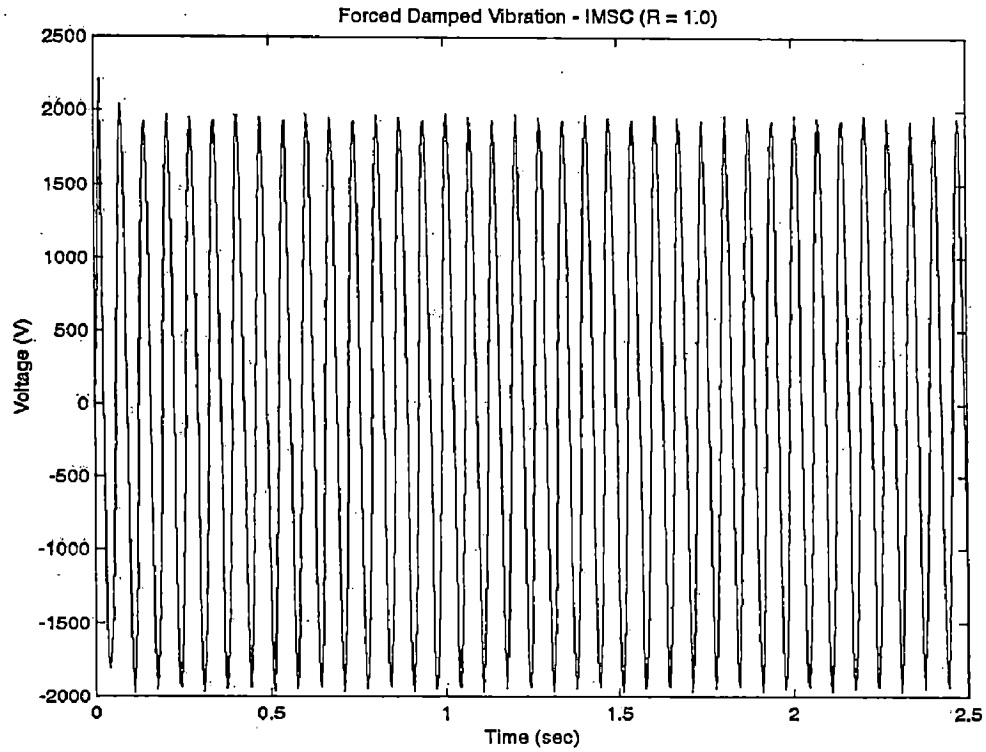


Figure 5.29 Variation of voltage with time (IMSC) (R = 1.0)

5.2.4 Forced Damped Vibration: MIMSC

The response of forced vibration control using MIMSC with weighting factor (R) value 1.0 is shown in Figures 5.30 and 5.31. The time domain response of the beam is shown in Figure 5.30, while variation of applied voltage with time is shown in figure 5.31. The effect of variation of R on the values of maximum amplitude and steady state amplitude is given in Section 5.2.5. While its effect on damping ratio, amplitude at 1.0 seconds and settling time is tabulated in Table 5.9.

Table 5.9 Forced Vibration with IMSC

R	Amplitude (mm)		Steady state Amplitude (% of forced uncontrolled vibrations)	Voltage		Modes Controlled
	Max	Steady		Max	Min	
0	3.6222	2.3850	100.00	0	0	0
1	1.1148	1.0620	44.52	3538.0	-3503.5	1,2
2	1.1676	1.1232	47.09	2069.9	-2658.9	1,2
3	1.2227	1.1830	49.60	1866.2	-1952.6	1,2
4	1.3073	1.2965	54.36	1791.0	-1765.7	1,2
5	1.3984	1.3856	58.09	1731.3	-1695.5	1,2
6	1.4771	1.4569	61.09	1680.9	-1636.0	1,2
7	1.5292	1.5185	63.67	1647.8	-1588.4	1
8	1.6176	1.5675	65.72	1608.9	-1544.0	1
9	1.6721	1.6215	67.99	1573.9	-1504.6	1
10	1.7210	1.6550	69.39	1541.9	-1469.4	1
15	1.9107	1.7780	74.55	1414.4	-1353.1	1
20	2.0445	1.8586	77.93	1320.4	-1242.4	1
25	2.1469	1.9160	80.34	1246.2	-1172.3	1
30	2.2291	1.9560	82.01	1185.2	-1116.2	1
35	2.2974	1.9856	83.25	1133.6	-1069.7	1
40	2.3553	2.0125	84.38	1089.3	-1030.1	1
45	2.4054	2.0298	85.11	1050.4	-995.63	1
50	2.4493	2.0500	85.95	1016.0	-965.19	1
60	2.5234	2.0675	86.69	957.25	-913.47	1
70	2.5839	2.0956	87.87	908.67	-870.68	1
80	2.6346	2.1123	88.57	867.51	-834.37	1
90	2.6778	2.1322	89.40	831.94	-802.93	1
100	2.7157	2.1505	90.17	800.80	-775.28	1

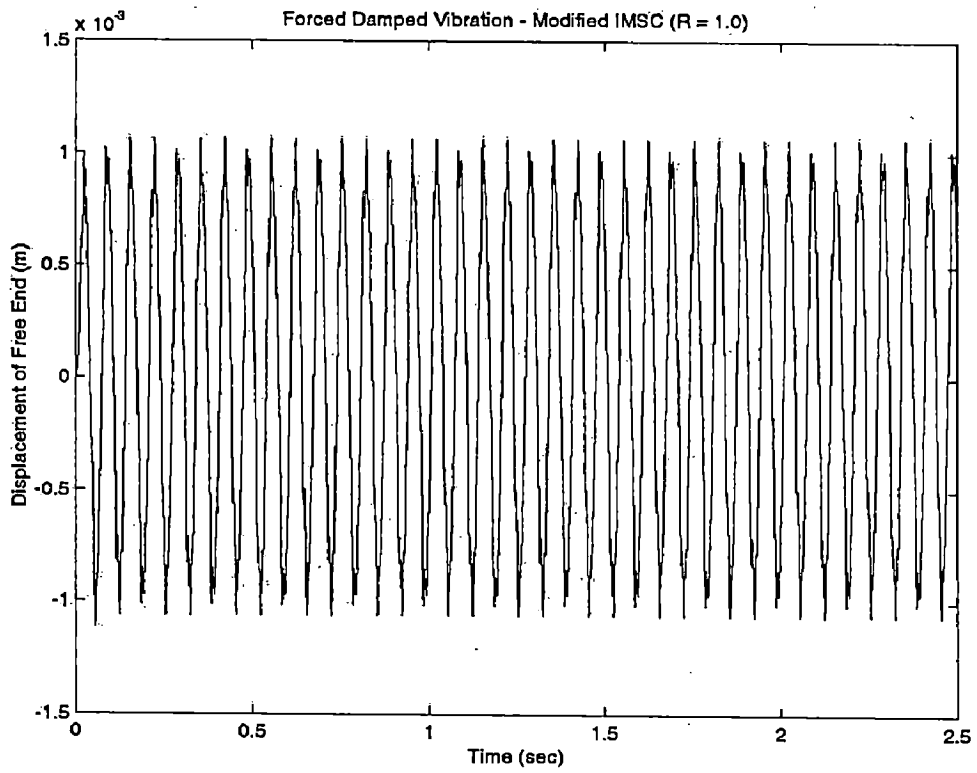


Figure 5.30 Variation of displacement with time (MIMSC) (R = 1.0)

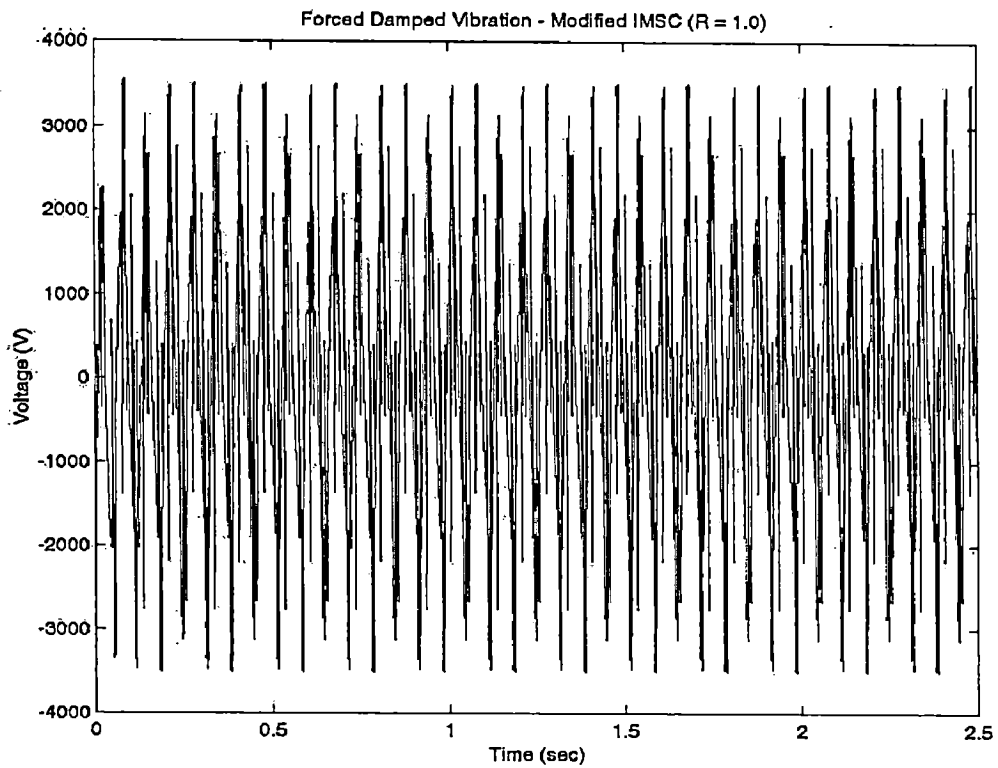


Figure 5.31 Variation of voltage with time (MIMSC) (R = 1.0)

From Table 5.9 it is seen that, voltage decreases with R, but it reduces control effect. The steady state amplitude is 44.52 % of that of uncontrolled case, with R = 1, but voltage is very high (> 3000 V), which is not feasible. It seems for same value of R, IMSC gives better performance than MIMSC, although MIMSC controls more than one mode. First two modes were controlled till R = 6, and after that only first mode is controlled.

5.2.5 Forced Damped Vibration: IMSC Vs MIMSC

Comparison between IMSC and MIMSC is shown in Table 5.10 and Figures 5.32 to 5.38. From figures, it is seen that MIMSC gives lesser control effect in case of forced vibration, while this is otherwise in free vibration.

The amplitude at 2.5 seconds, maximum amplitude and steady state amplitude have higher values for same weighting factor in forced vibration. The amplitude at 2.5 seconds decreases with R, but maximum amplitude and steady state amplitude increases with R; while voltage drops with R. For IMSC, the voltage ranges from 800-2200 V, while for MIMSC range is 800-3540 V, so it may be possible, the control effort by MIMSC may be divided into more than one mode.

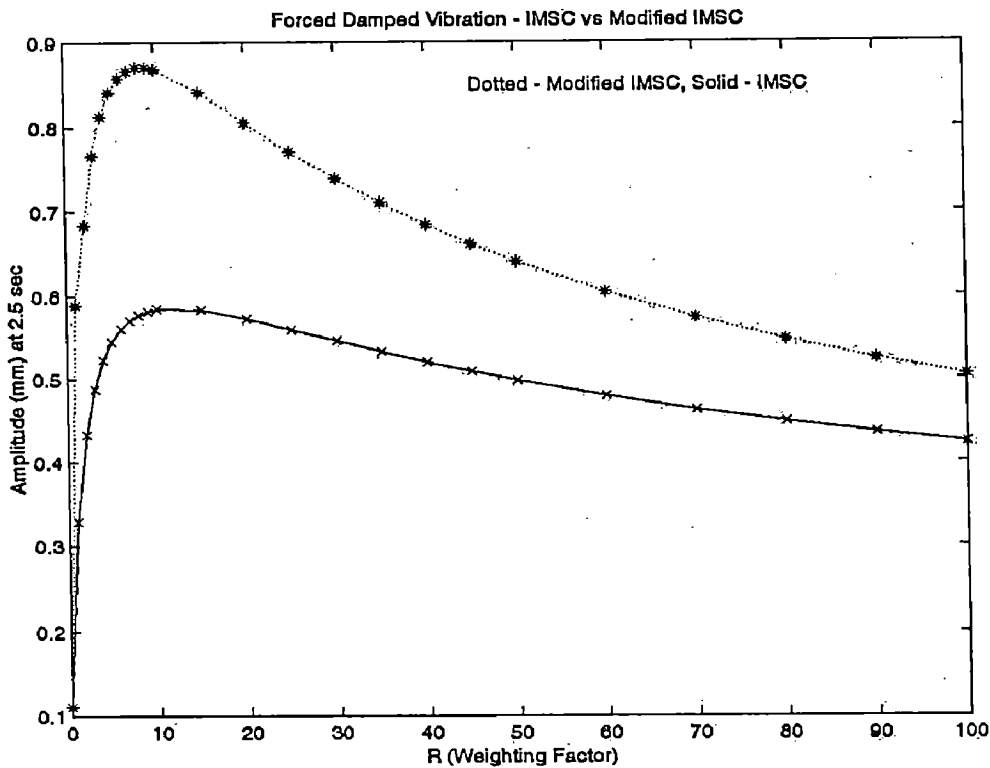


Figure 5.32 Comparison of Forced Vibration response with IMSC and MIMSC (variation of amplitude at end of 2.5 seconds with R)

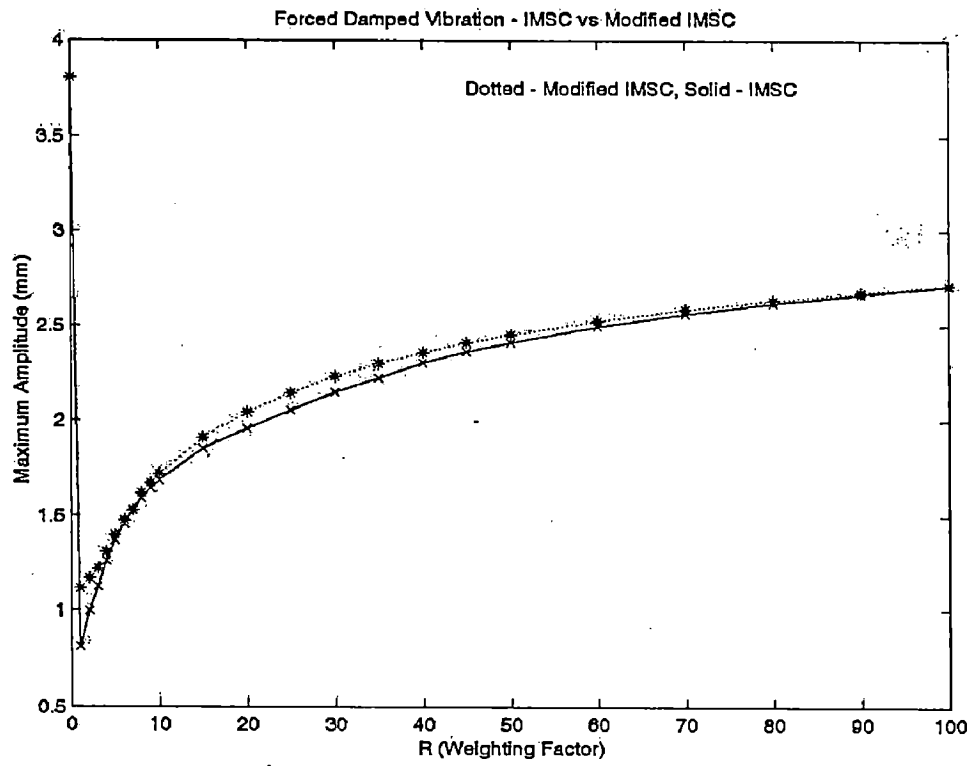


Figure 5.33 Comparison of Forced Vibration response with IMSC and MIMSC (variation of Maximum Amplitude with R)

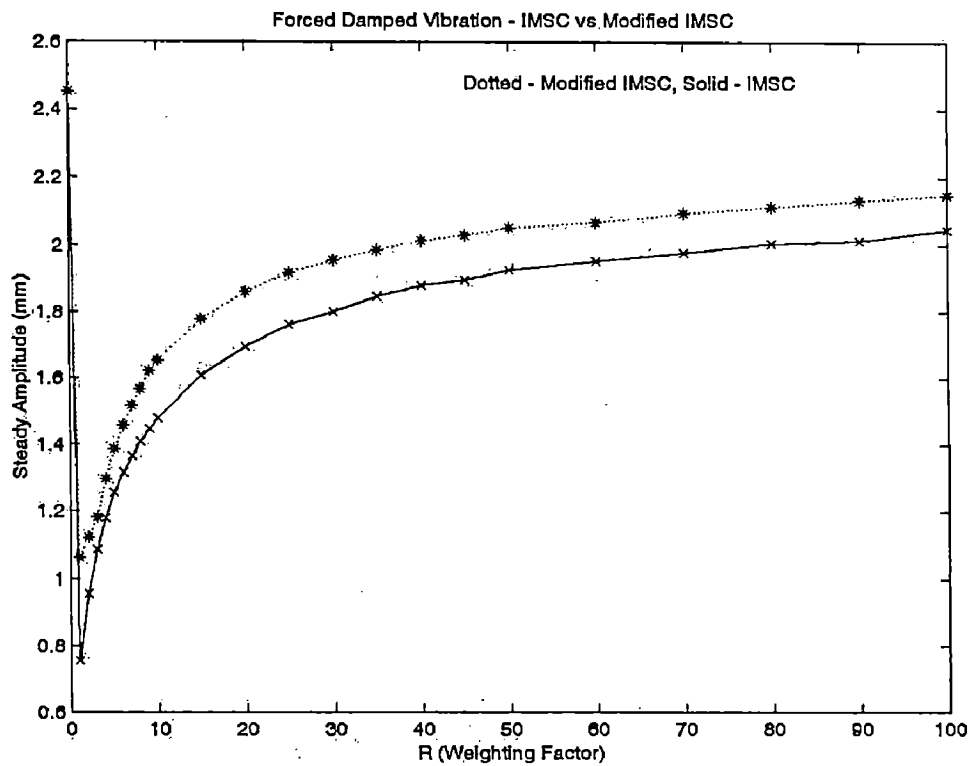


Figure 5.34 Comparison of Forced Vibration response with IMSC and MIMSC (variation of Steady State Amplitude with R)

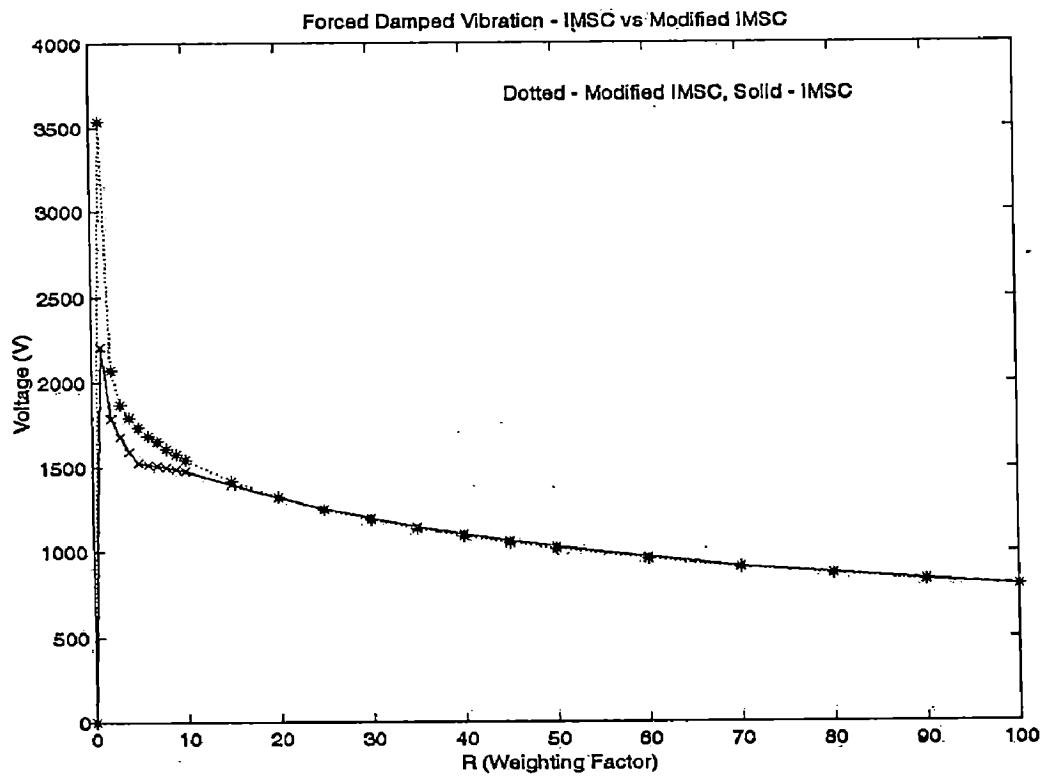


Figure 5.35 Comparison of Forced Vibration response with IMSC and MIMSC
(variation of voltage with R)

Table 5.10 Forced Vibration IMSC vs. Modified IMSC

R	Amplitude (mm)						Actuator Voltage (V)					
	IMSC			MIMSC			IMSC			MIMSC		
	2.5 sec	Maximum	Steady	2.5 sec	Maximum	Steady	Max	Min	Max	Min	Max	Min
0	0.11080	3.80300	2.45200	0.11080	3.8030	2.4520	0	0	0	0	0	0
1	0.32839	0.81281	0.75500	0.58889	1.1148	1.0620	2207.8	-1977.3	3538.0	-3503.5	2069.9	-2658.9
2	0.43205	0.99502	0.95420	0.68362	1.1676	1.1232	1789.0	-2009.2	2069.9	-2658.9	1866.2	-1952.6
3	0.48818	1.12490	1.08500	0.76536	1.2227	1.1830	1675.4	-1965.2	1866.2	-1952.6	1791.0	-1765.7
4	0.52258	1.26170	1.17800	0.81286	1.3073	1.2965	1589.7	-1881.9	1791.0	-1765.7	1731.3	-1695.5
5	0.54493	1.36900	1.25600	0.84115	1.3984	1.3856	1524.2	-1797.2	1731.3	-1695.5	1680.9	-1636.0
6	0.55987	1.45580	1.31500	0.85767	1.4771	1.4569	1511.9	-1719.3	1680.9	-1636.0	1647.8	-1588.4
7	0.56994	1.52790	1.36500	0.86660	1.5292	1.5185	1508.1	-1649.4	1647.8	-1588.4	1608.9	-1544.0
8	0.57667	1.58890	1.40800	0.87045	1.6176	1.5675	1499.5	-1588.0	1608.9	-1544.0	1573.9	-1504.6
9	0.58103	1.64160	1.44650	0.87081	1.6721	1.6215	1487.7	-1545.8	1573.9	-1504.6	1541.9	-1469.4
10	0.58366	1.68750	1.47950	0.86875	1.7210	1.6550	1473.9	-1506.4	1541.9	-1469.4	1414.4	-1353.1
15	0.58273	1.85370	1.60750	0.84108	1.9107	1.7780	1395.2	-1345.0	1414.4	-1353.1	1320.4	-1242.4
20	0.57212	1.96040	1.69500	0.80507	2.0445	1.8586	1319.4	-1227.0	1320.4	-1242.4	1246.2	-1172.3
25	0.55895	2.05310	1.76000	0.77006	2.1469	1.9160	1252.7	-1136.5	1246.2	-1172.3	1185.2	-1116.2
30	0.54545	2.15140	1.79980	0.73817	2.2291	1.9560	1194.9	-1064.3	1185.2	-1116.2	1133.6	-1069.7
35	0.53243	2.22200	1.84500	0.70943	2.2974	1.9856	1144.4	-1013.6	1133.6	-1069.7	1089.3	-1030.1
40	0.52015	2.30030	1.87800	0.68374	2.3553	2.0125	1100.1	-990.53	1089.3	-1030.1	1050.4	-995.63
45	0.50867	2.35860	1.89550	0.66066	2.4054	2.0298	1060.8	-968.60	1050.4	-995.63	1016.0	-965.19
50	0.49797	2.40950	1.92500	0.63983	2.4493	2.0500	1025.6	-947.86	1016.0	-965.19	957.25	-913.47
60	0.47872	2.49430	1.95300	0.60365	2.5234	2.0675	965.22	-909.86	957.25	-913.47	908.67	-870.68
70	0.46193	2.56270	1.97750	0.57321	2.5839	2.0956	914.92	-876.06	908.67	-870.68	867.51	-834.37
80	0.44716	2.61950	2.00550	0.54711	2.6346	2.1123	872.17	-845.89	867.51	-834.37	831.94	-802.93
90	0.43405	2.66670	2.01200	0.52436	2.6778	2.1322	835.24	-818.78	831.94	-802.93	800.80	-775.28
100	0.42232	2.70920	2.04520	0.50426	2.7157	2.1505	802.90	-794.27	800.80	-775.28		

5.3 VIBRATION CONTROL: AXIAL STIFFNESS VARIATION

The sweeping excitation is given to beam at its free end in the form of sinusoidal excitation in the form $0.1\sin(\omega t)$, where ω and t both change continuously from 0 to 15 seconds at the ramp rate of 10 rad/s^2 . Natural Frequency without axial stiffness variation found 31.856 Hz while with axial stiffness variation 36.260 Hz.

The main idea behind controlled switching of the piezoelectric patches is to switch the natural frequency of the beam during sweeping excitation to avoid the resonance phenomenon and the associated large resonant amplitudes. Figure 5.36 shows the response of the beam during sweeping harmonic excitation when the patches are in deactivated state.

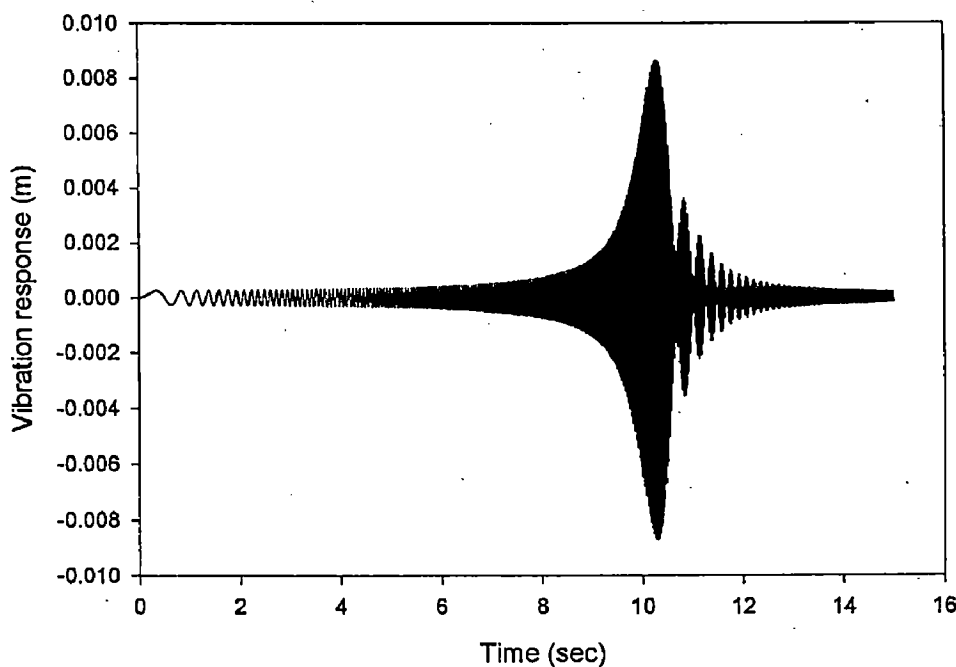


Figure 5.36 Time domain response of the beam (patches in deactivated state)

The expected resonance is showing high resonant amplitude of 8.663 mm and the resonance is encountered at 10.3 sec during sweeping excitation. The beating phenomenon is observed after the resonance is crossed and is expected in such excitation case. The sharp resonance peak is observed indicating a lower damping value. Similar simulation is carried out when both the patches of the beam (applied in collocated fashion) are applied a constant same polarity voltage of -500 Volts. Hence when similar sweeping excitation was applied to the beam, the resulting response of the beam is shown in Figure 5.37. The peak response in this case has been observed at 11.64 sec and the amplitude at resonance is 7.5 mm.

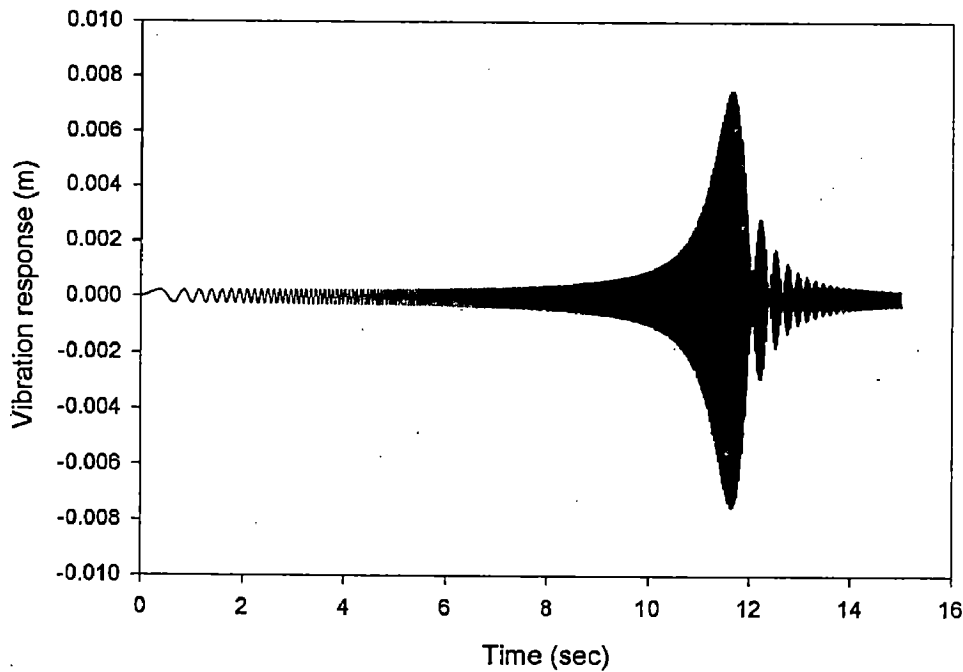


Figure 5.37 Time domain response of the beam (patches in activated state)

The delayed resonance is expected as the stiffness of the beam is more in this case due to activated state of patches and hence the natural frequency is more (36.2Hz), compared to 31.85Hz in case of deactivated state. The peak amplitude (7.5mm) observed is slightly less compared to the peak amplitude of 8.66 mm in case of the deactivated state (Figure 5.36). A gap of 1.34 seconds exists between the time at which peak response occurs in case of activated state (11.64sec) and the time at which peak response occurs in the case of deactivated state (10.3sec). By suitably adjusting the switchover between these two time values, resonance could be avoided. Why?

In this regard, a simulation is carried out with the patches in the activated state initially. This causes the response to start approaching the resonance corresponding to time 11.64 seconds. However, when at time is 10 seconds, the patches are deactivated. This cause the beam to have characteristics corresponding to deactivated state and should encounter resonance at 10.3 seconds. However after the switchover, the beam continues to have a changing sweeping excitation frequency and the resonance at 10.3 sec is not fully realized for lack of time available for the interaction of excitation frequency and natural frequency corresponding to the deactivated state. The ensuing vibration response is shown in Figure 5.38 superimposed over the response for activated and deactivated states. Figure 5.38 shows that when switchover is effected at 10 sec, the peak response of 5.86 mm is observed and the peak response is observed at

time is 10.365. Thus by applying a switchover strategy, of activating and deactivating the patches, a drop in the resonant amplitude is seen. With switchover being effected at 10 sec, the peak resonance amplitude of 8.663 mm (in case of deactivated state) drops to 5.86 mm, a reduction of 33%. Another simulation is carried out, this time by effecting the switchover at roughly the midway between the t_p (activated) i.e.11.64 sec and t_p (deactivated) i.e.10.3 sec. Thus, switchover in the next simulation is effected at 10.6 sec, at which the two response curves corresponding to the activated and deactivated states meet. Figure 5.38 shows the response curve for this case, again superimposed with the other three cases. In this case, the resonance amplitude is the least of all the four cases with peak amplitude value of 3.88 mm observed at 10.77 sec. Thus when stiffness characteristic of the vibrating beam is changed to shift the resonance from 36.2 Hz to 31.86 Hz, the actual resonance is encountered at 10.77 sec after the changeover is effected at 10.6 sec. The drop in the peak amplitude observed in this case is 55.2%. Thus by suitably activating and deactivating the piezoelectric patches, one can get a large drop (of the order of 55.2% in this case) in the peak resonant amplitude. Further simulation could be attempted to optimize the time at which the switchover could be effected to get best reduction in the amplitude.

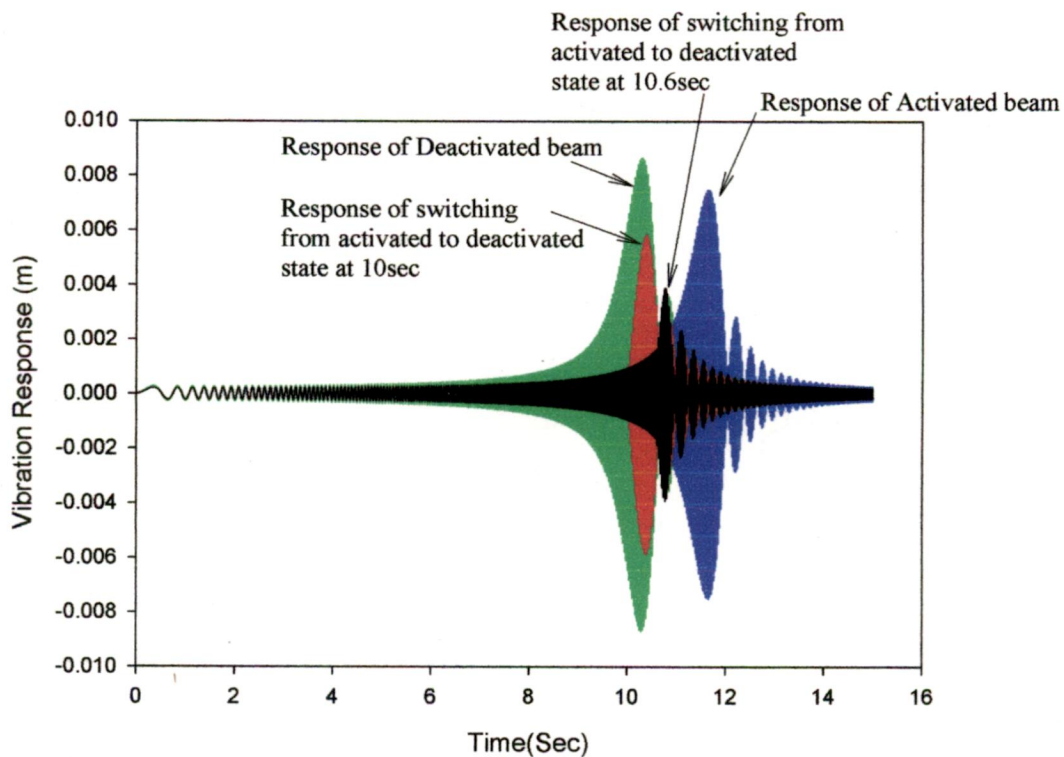


Figure 5.38 Comparison of time domain response of the beam (Patches in activated state, deactivated state and controlled switching cases).

CHAPTER 6

CONCLUSION AND SCOPE FOR FUTURE WORK

The formation of the finite element model, able to handle sandwich beams and the active vibration control of this beam using piezoelectric patches has been carried out. Transient analysis is done by Newmark Method of direct integration techniques. Among various control techniques available, Negative Velocity Feedback Control, Independent Modal Space Control and Modified Independent Modal Space Control were used to control both, free and forced vibrations. Attempt to control vibration (during sweeping excitation) by varying axial stiffness of the beam, with the help of piezoelectric patches excitation has been made.

The following points observed while working on Active Vibration Control of Piezo-Beam using FEM and from the results and discussion presented in previous chapter.

1. The FEM gives almost similar results with the analytical formulae, in case of natural frequency determination, and the error is well below 1 %. The causes of error can be,
 - Matlab does calculation with more than 16 digits after decimal point and the values of constant ' r_i ' (equation 16) available are in 4 digits after decimal point.
 - The analytical formula available is for continuous beam while FEM discretises beam into small elements.
2. The difference between analytical values and result by FEM decreases with increase in number of elements, but it increases iteration time by a little bit. So compromise is needed in both factors, such that error should be within defined limit (say < 1 %).
3. Result of free vibrations with negative velocity feedback control by first approach as well as second approach, shows results of similar nature, except change in gain value for the same amount of control. The difference in these two cases for control effort may be due to actual modelling of sensor and actuator in Newmark method, as Piezoelectric Stress Constant (g_{31}) and Piezoelectric Strain Constant (d_{31}) has different values. The damping almost linearly varies with gain value, but after

some gain value, the control forces dominate the effective forces in the beam, so response get unstable, due to increased control forces.

4. When IMSC applied to control first mode in case of free vibration, it is found that the maximum voltage requirement is very high as compared to that of negative velocity FBC (second approach), but control effect is also more in case of IMSC than NVFBC. The maximum amount of voltage is 518 V and settling time is 2.985 seconds (Table 5.2) for NVFBC, while 1100 V required by IMSC for 0.39 seconds settling time (Table 5.3). When voltage range required to apply to actuator is -453 to $+343$ V, the settling time is 0.49 seconds. Hence IMSC performs better than NVFBC.
5. Results of free vibration with IMSC show that, voltage decreases as the value of R (weighting factor) increased, increasing the amplitude at 1.0 second and settling time. Thus control effort reduces with increasing R, and so R balances the reduction of the vibrational energy with respect to the control voltage required
6. In IMSC only first mode is controlled (in this work), while in MIMSC it is found that, for lower values of R the modes get controlled are first, second and last (24th), while as the value of R increased to 7, the modes that controlled are first and second, and for very high value of R (> 10) only first mode get controlled. As the R increased, voltage decreases i.e. control effort reduced. But it is seen that, for same value of R, damping is more in case of MIMSC than IMSC. The settling time and voltage requirement is less for the same value of R in case of MIMSC (Refer Table 5.5 and Figures 5.17 to 5.20). It has been shown that time-sharing of a small number of actuators to control large number of modes can be achieved by using MIMSC, here one actuator control 3 modes. This control system can be highly effective in large flexible structure, where it is not possible to apply more no of actuators due to restrictions in weight and complexity. In this system, the peak actuator and sensor voltage is crossing some high limits, so control system should be modified so that the, care should be taken, the peak actuator voltage should not exceed the breakdown voltage of the piezoelectric patch, at which, it will loose its piezoelectric properties.
7. Results of free vibration with and without control show that, better performance is obtained by using MIMSC compared to IMSC, and Negative Velocity FBC.
8. The criteria for measurement of amount of control achieved is not settling time or damping in case of forced vibrations. The criteria are the steady state amplitude.

The result of forced vibration with NVFBC (first approach) show that with gain value of 0.175, the steady state amplitude got is 94.76 % of steady state amplitude of forced uncontrolled vibrations (Table 5.6). While by second approach, the minimum amplitude is 96.85 % that of uncontrolled vibrations and actuator voltage is ± 200 V, which is within range (Table 5.7). So, first approach dominates the results of second.

In case of forced vibrations with IMSC, the results show that, very high amount of voltage (± 2000 V) is required, which is not possible in practice, for reduction of steady state amplitude to 40 % of that of uncontrolled case (Table 5.8). Even for $R = 100$, voltage requirement is ± 800 V, and the steady state amplitude is 85.72 % of uncontrolled case. But the linear trend shows that IMSC performs better than NVFBC.

0. In case of forced vibrations, MIMSC controls first two modes till R becomes 7, and after that it controls only first mode. For same value of R , voltage requirement is more in case of MIMSC till $R = 20$, after that it reduces for MIMSC (Table 5.10). But steady state amplitude is more for corresponding values in MIMSC than IMSC. So for forced vibrations, the sequence of performance can be IMSC, MIMSC and then NVFBC.
1. The work with Vibration Control during sweeping excitation using controlled axial stiffness variation has been attempted by developing a program to carry out controlled actuation/deactuation of the patch. As stated earlier, in this case same polarity voltage is applied to patches and both patches work as actuators. The axial stiffness matrix is added to the element stiffness matrix, corresponding to the patched element. The stretching effect of the actuated patch cause increase in the stiffness of the element in the lateral direction. This increase leads to the increase in the natural frequency. The change in the natural frequency of the beam can be utilized in avoiding the large resonant amplitudes by bypassing the resonance phenomenon. The drop in peak amplitude is found to be 55.2%. Further simulation could be attempted to optimize the time at which the switchover could be effected to get best reduction in the amplitude. This method can be useful when the frequency of structure is varying from zero value to some definite value, or Ramp input, e.g. Helicopter Blades while starting the Helicopter or during the speed changes.

6.1 SCOPE FOR FUTURE WORK

The presented work may be extended in any of the following directions

1. Effect of temperature on electrical and mechanical properties of patches as well as beam is assumed to be negligible. The temperature variation could affect the overall performance, which is not considered in this analysis.
2. Bonding is assumed to be thin enough, not to alter the dynamic characteristics of the beam, significantly. But effect of bonding on the overall dynamic characteristics can be done.
3. Bonding between patches and beam is assumed to be perfect. Validation of results largely depends on this assumption of perfect bond. The effect of debonding on the dynamic characteristics of the structure can be done.
4. The combination of axial stiffness variation and active vibration control can give better results, and this method can be applied to any external force, and not only to Ramp input.
5. In IMSC, more than one modes can be controlled by using one actuator, this can be simulated, as MIMSC controls first two and last mode (in this work), so if one actuator is used to control first two modes, then results may be competitive to MIMSC.
6. Viscoelastic material can be used to achieve passive damping along with piezoelectric patches to take advantages of both – AVC and PVC.

REFERENCES

1. Lane, R. and Benjamin, C., 2003, "An Introduction to Smart Materials", The AMPTIAC Quarterly, Vol.7, No.2, 9-14. ✓
2. Flatau, A. B. and Chong, K. P., 2002, "Dynamic Smart Material and Structural Systems", Engineering Structures Vol.24, 261-270 ✓
3. Poulin, K. and Vaicaitis, R., 2003, "Vibrations of Stiffened Composite Panels with Smart Materials", 1-10.
4. Choi, S. B. and Hwang, J. H., 2000, "Structural Vibration Control using Shape Memory Actuators", Journal of Sound and Vibration, Vol.231 (4), 1168-1174.
5. Timothy, M., Bhatia, K., and Archer, G., 2002, "Semi-active Vibration Control for the 3rd Generation Benchmark problem including Spillover Suppression", 15th ASCE Engineering Mechanics Conference, June 2-5, 2002, 1-8
6. Radcliffe, C., Lloyd, J., Andersland, R., and Hargrove, J. B., 1996, "State Feedback Control Of Electrorheological Fluids", 1996 ASME International Congress and Exhibition, November 17-22, 1996, Atlanta, GA, 1-8.
7. Cox, D. E. and Lindner, D. K., 1991, "Active Control for Vibration Suppression in a Flexible Beam using a Modal Domain Optical Fiber Sensor", Journal of Vibration and Acoustics, Vol.113, 369-382.
8. Jinsong, Asundi, A. and Liu, Y., 1998, "Vibration Control of Smart Composite Beams with Embedded Optical Fiber Sensor and ER Fluid", JVA-98-072, 1-4.
9. Nakra, B. C., 1998, "Vibration Control in Machines and Structures using Viscoelastic Damping", Journal of Sound and Vibration, Vol.211 (3), 449-465. ✓
10. Lio, W. H. and Wang, K. W., 1997, "On the Active-Passive Hybrid Control Actions of Structures with Active Constrained Layer Treatments", Journal of Vibration and Acoustics, Vol.119, 563-572.
11. Balamurugan and Narayanan, 2002, "Finite Element Formulation and Active Vibration Control Study on Beams using Smart Constrained Layer Damping (SCLD) Treatment", Journal of Sound and Vibration, Vol.249 (2), 227-250.
12. Incomplete Enrico, C., 2003, "Piezoelectric Technology For Active Vibration Control".
13. Crawley, E. F. and Javier de Luis, 1987, "Use of Piezoelectric Actuators as elements of Intelligent Structures", AIAA Journal, Vol.25, No.10, 1373 -1385.

14. Sze, K. Y. and Yao, L. Q., 2000, "Modelling Smart Structures with segmented Piezoelectric Sensors and Actuators", Journal of Sound and Vibration, Vol.235 (3), 495-520.
15. Aldrainhem, O., Singh, T. and Wetherhold, R. C., 2000, "Optimal Size and Location of Piezoelectric Actuators/Sensors: Practical Considerations", Journal of Guidance, Control and Dynamics, Vol.23, No.3, 509-515.
16. Silva, Ribeiro, Rodrigues, Vaz and Monteiro, 2004, "The Application of Genetic Algorithms for Shape Control with Piezoelectric Patches - an Experimental Comparison", Smart Materials and Structures, Vol. 13, 220-226.
17. Devasia, Tesfay, Brad and Bayo, 1993, "Piezoelectric Actuator Design for Vibration Suppression: Placement and Sizing", Journal of Guidance, Control and Dynamics, Vol.16, No.5, 859-864.
18. Schwinn, A. and Janocha, H., 2004, "Self-Configurable Actuator Sensor Array for Active Vibration Suppression", Laboratory for Process Automation (LPA), Saarland University, Germany, 1-9.
19. Frecker, M., 2004, "Recent Advances in Optimization of Smart Structures and Actuators", accepted for publication by Journal of Intelligent Material Systems and Structures.
20. Trindade, Benjeddou and Ohayon, 2001, "Piezoelectric Active Vibration Control of Damped Sandwich Beams", Journal of Sound and Vibration, Vol.246 (4), 653-677
21. Balamurugan and Narayanan, 2001, "Active Vibration Control of Piezolaminated Smart Beams", Defence Science Journal, Vol.51, No.2, 103-114
22. Narayanan and Balamurugan, 2003, "Finite Element Modelling of Piezolaminated Smart Structures for Active Vibration Control with Distributed Sensors and Actuators", Journal of Sound and Vibration Vol.262, 529-562
23. Chen, S. H., Wang, Z. D. and Liu, X. H., 1997, "Active Vibration Control and Suppression for Intelligent Structures", Journal of Sound and Vibration, Vol.200 (2), 167-177.
24. Nguyen, C. C., 1991, "Implementation of Actuators for the Independent Modal Space Control Scheme", Computers Electrical Engineering, Vol.17, No.2, 75-90.
25. Baz, Poh and Fedor, 1992, "Independent Modal Space Control with Positive Position Feedback", Transactions of ASME - Journal of Dynamic Systems and Measurement Control, Vol.114, 96-103

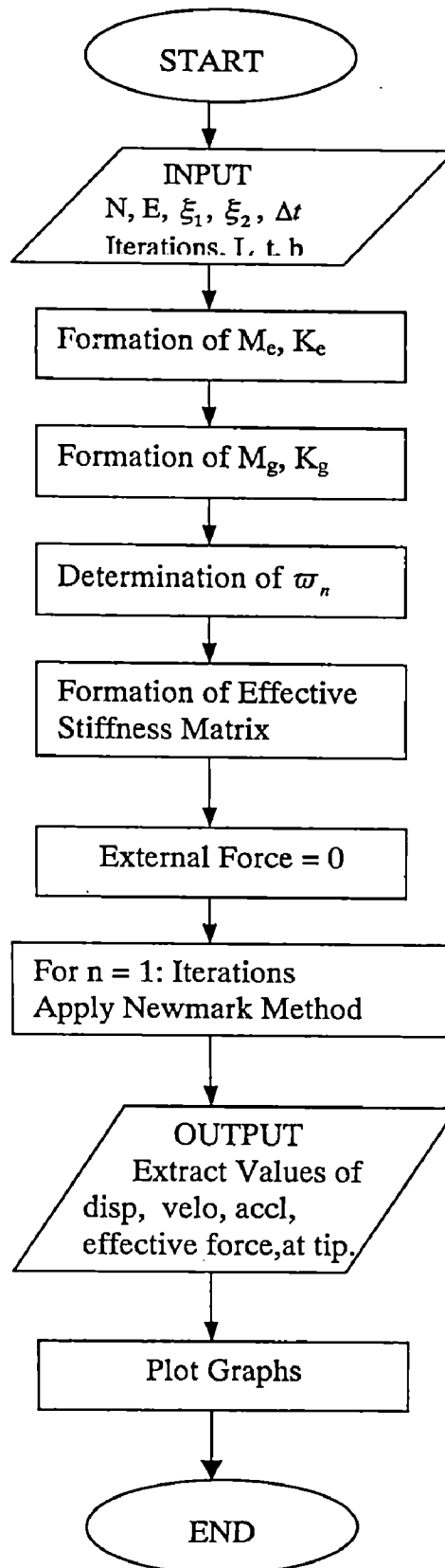
complete

26. Wang and Huang, 2002, "Modal Space Vibration Control of a Beam by using the Feedforward and Feedback Control Loops", *International Journal of Mechanical Sciences*, Vol.44, 1-19.
27. Kamath, G. M., 2002, "Vibration Control using Piezoelectric Materials", *Conference on Smart Materials and Composite Structures*, Feb 19-22, 2002, IIT Kanpur, 1-26.
28. Singh, S. P., Pruthi, H. and Agarwal, V. P., 2003, "Efficient Modal Control Strategies for Active Control of Vibrations", *Journal of Sound and Vibration*, Vol.262, 563-575.
29. Baz, Poh and Studer, 1989, "Modified Independent Modal Space Control Method for active control of Flexible Systems", *Journal of Mechanical Engineering Science*, Part C, Vol. 203, 103-112.
30. Baz and Poh, 1990, "Experimental Implementation of the Modified Independent Modal Space Control Method", *Journal of Sound and Vibration*, Vol. 139 (1), 133-149.
31. Kashani, R., 2003, "Active Vibration Damping using Optimal Control Techniques", 1-8.
32. Clark and Bernstein, 1998, "Hybrid Control: Separation in Design", *Journal of Sound and Vibration*, Vol. 214 (4), 784-791.
33. Salemi, P. and Golnaraghi, M. F., 1997, "Active Control of Forced and Unforced Structural Vibration", *Journal of Sound and Vibration*, Vol. 208 (1), 15-32.
34. Sitti, Campolo, Joseph, Fearing, Tao, Taylor, and Timothy, 2004, "Development of PZT and PZn-PT Based Unimorph Actuators for Micromechanical Flapping Mechanisms", 1-8.
35. Li, Y., Horowitz, R. and Evans, R., 2003, "Vibration Control of a PZT Actuated Suspension Dual-Stage Servo System using a PZT Sensor", *IEEE Transactions on Magnetics*, Vol. 39, No. 2, 932-937.
36. Sun, Tong and Atluri, 2001, "Effects of Piezoelectric Sensor/Actuator Debonding on Vibration Control of Smart Beams", *International Journal of Solids and Structures*, Vol. 38, 9033-9051.
37. Reza Moheimani, 2000, "Experimental Verification of the Corrected Transfer Function of a Piezoelectric Laminate Beam", *IEEE Transactions on Control Systems Technology*, Vol. 8, No. 4, 660-666.

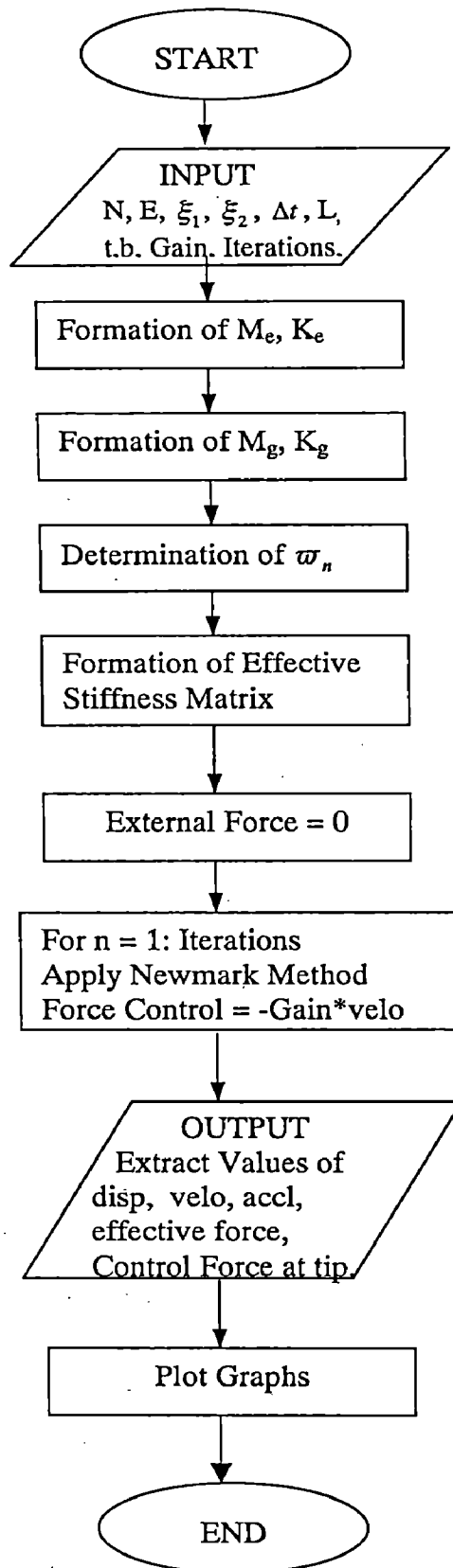
38. Kang, Y., Hyun, P., Kim, J., and Choi, 2002, "Interaction of Active and Passive Vibration Control of Laminated Composite Beams with Piezoceramic Sensors/Actuators", *Materials and Design*, Vol. 23, 277-286.
39. Garga, D. and Anderson, G., 2003, "Structural Vibration Suppression via Active/Passive Techniques", *Journal of Sound and Vibration*, Vol. 262, 739-751
40. James, Smith, Wolford and Whaley, 1989, "Vibration of Mechanical and Structural Systems", Harper & Row Publishers, Singapore, 506.
41. Gere and Timoshenko, 2003, *Mechanics of Materials*, PWS Engineering, Boston, 248-257.
42. Rao, J. S. and Gupta, K., 1995, "Theory and Practice of Mechanical Vibrations", New Age International Publications, 348-349.
43. Klaus- Jurgen Bathe, 1996, "Finite Element Procedures", Prentice Hall of India, 780-829.
44. Srinivasan, A. V. and McFarland D., 2000, "Smart Structures - Analysis and Design", Cambridge University Press, 7-24.
45. Rao, J. S., 1996, "Rotor Dynamics", New Age International Pvt. Limited, 95-98.
46. Inman, D. J., 1989, "Vibration with control, measurement and stability", Prentice Hall Publications.
47. Gandhi, M. V. and Thompson, B. S., 1998, "Smart Materials and Structures", Chapman & Hall Publications.
48. Reddy, J. N., 2003, "An Introduction to the Finite Element Methods", Tata-McGraw Hill Publications Company Limited, New Delhi.
49. Chandrupatala, T. R. and Belegundu, A. D., 2001, "Introduction to Finite Elements in Engineering", Prentice Hall of India Pvt. Ltd., New Delhi.
50. Rudra Pratap, 2003, "Getting Started with Matlab", Oxford University Press
51. Palms, W. J., 2002, "introduction to Matlab for Engineers", McGraw Hill Publications.
52. Chapman, S. J., 2002, "Matlab Programming for Engineers", Bookware Champion Series.
53. www.micromega-dynamics.com
54. www.physics.byu.edu
55. www.scirus.com
56. www.sciencedirect.com

FLOWCHARTS

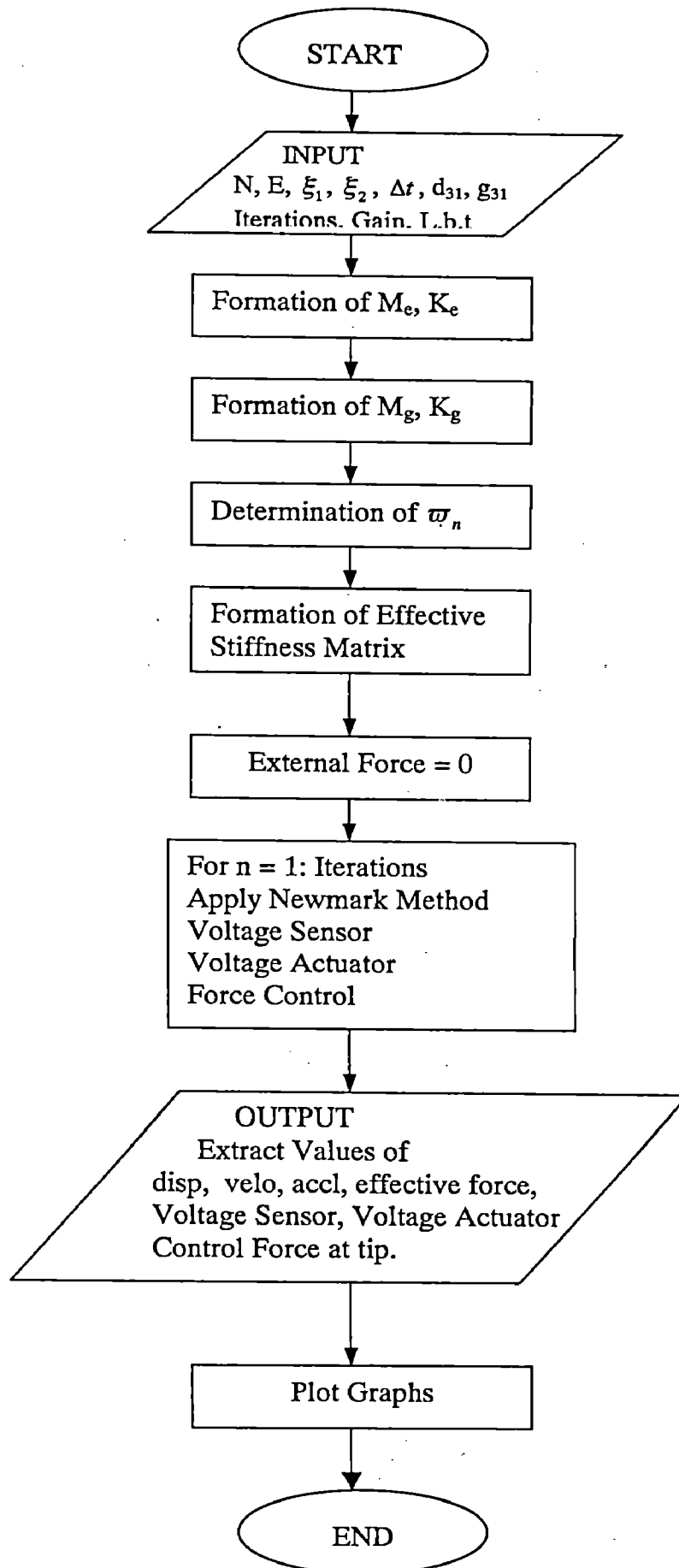
Flowchart 1: Free Damped Vibration Response



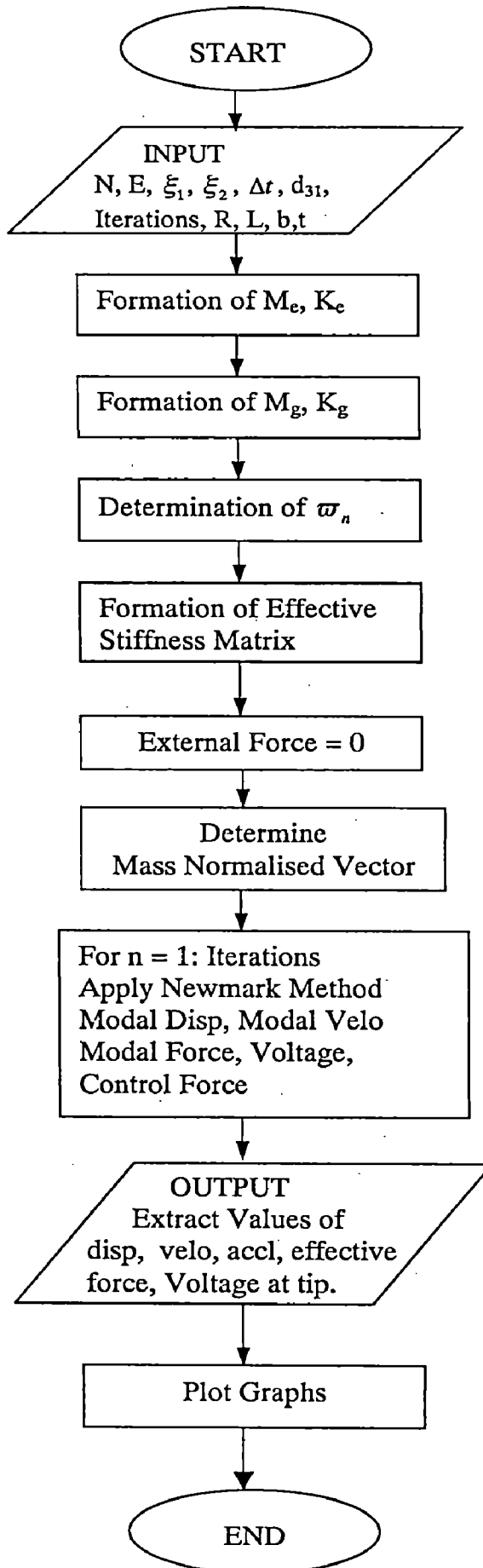
Flowchart 2: Free Damped Vibration with Negative Velocity FBC (Simple)



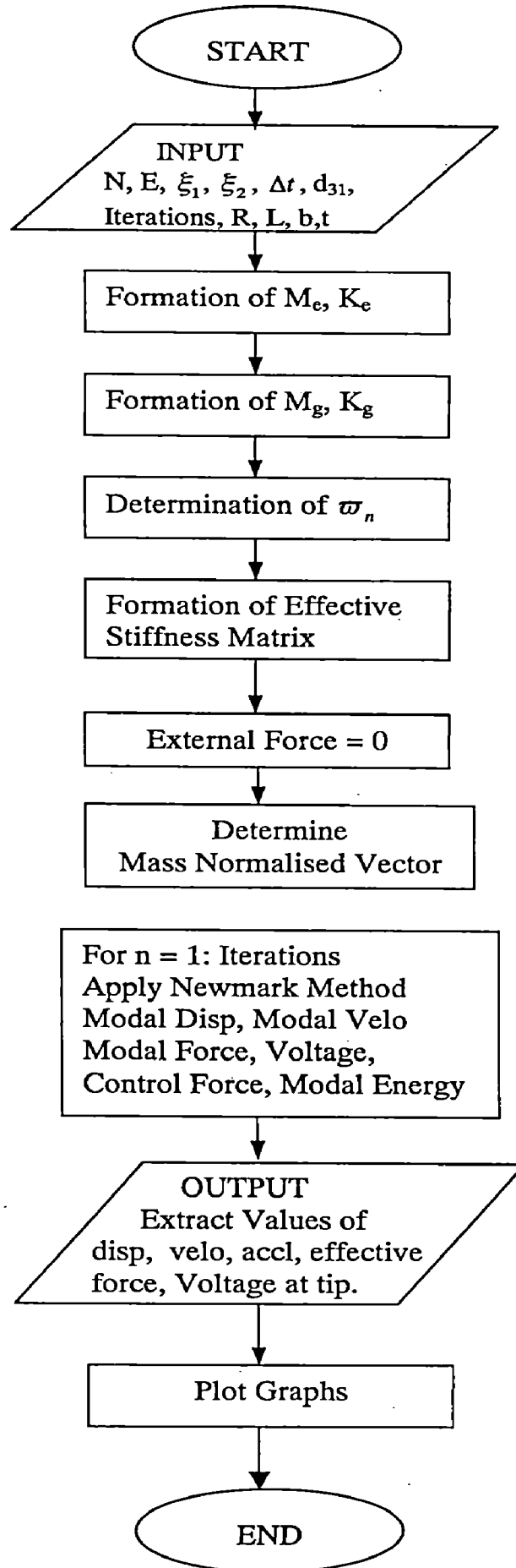
**Flowchart 3: Free Damped Vibration with Negative Velocity FBC
(Sensor & Actuator)**



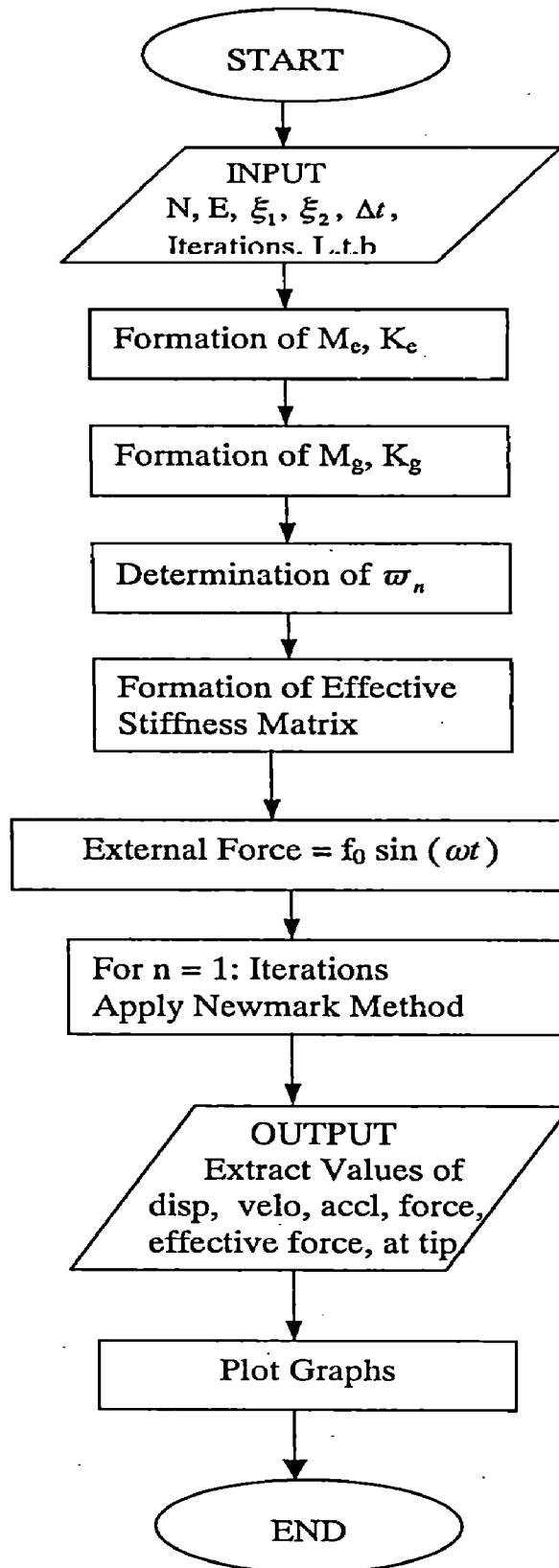
Flowchart 4: Free Damped Vibration with IMSC



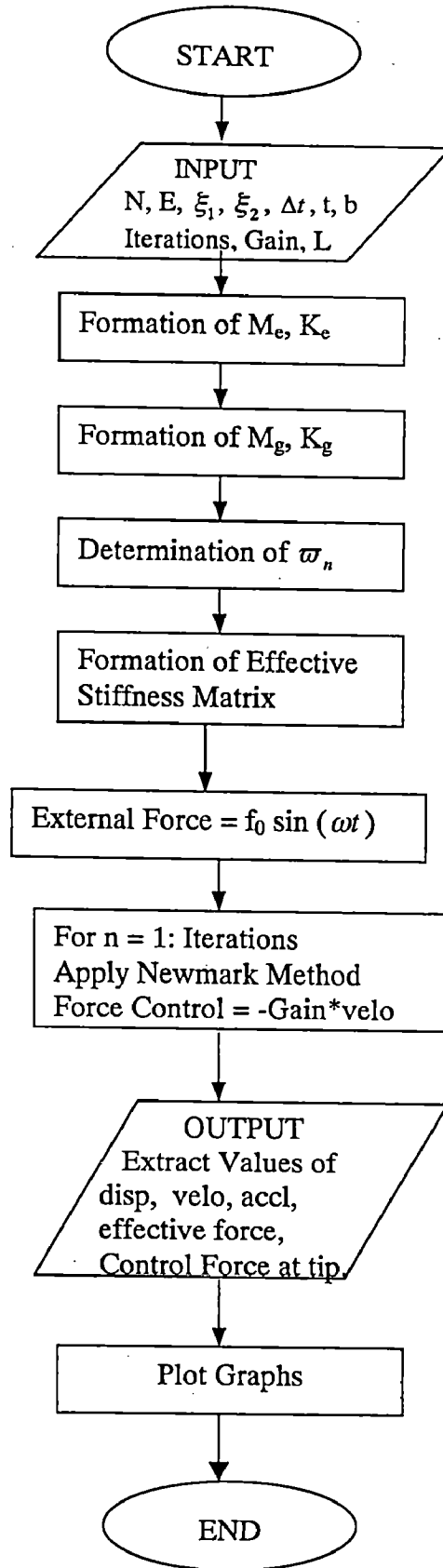
Flowchart 5: Free Damped Vibration with MIMSC



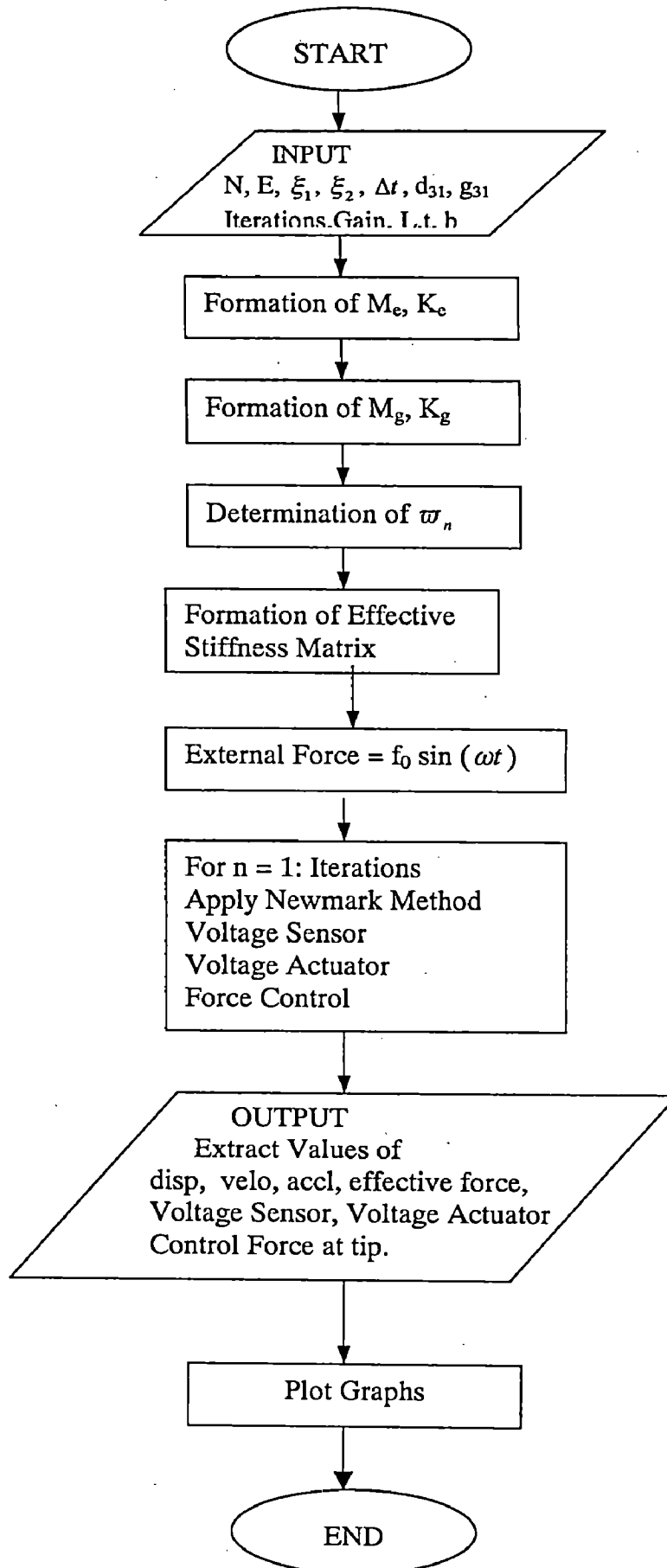
Flowchart 6: Forced Damped Vibration Response



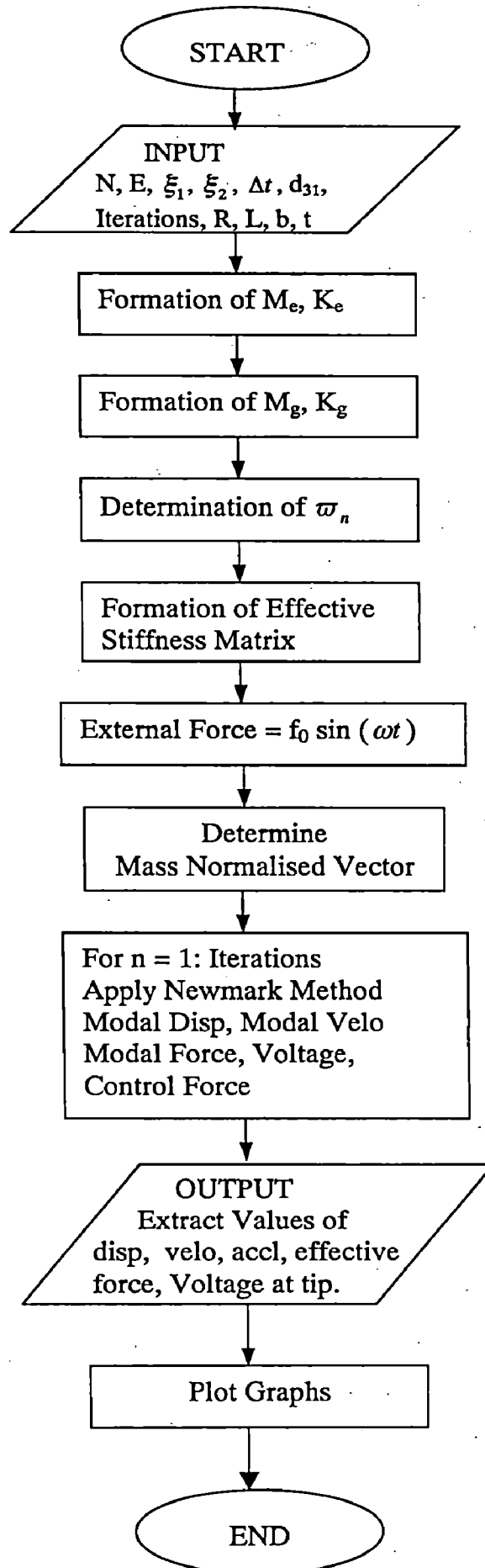
Flowchart 7: Forced Damped Vibration with Negative Velocity FBC (Simple)



**Flowchart 8: Forced Damped Vibration with Negative Velocity FBC
(Sensor & Actuator)**



Flowchart 9: Forced Damped Vibration with IMSC



Flowchart 10: Forced Damped Vibration with MIMSC

